DYNAMICS OF CELL FATE DECISION MAKING BETWEEN SPORULATION AND COMPETENCE IN BACILLUS SUBTILIS

APPROVED BY SUPERVISORY COMMITTEE

Gürol Süel, Ph.D.

Steven Altschuler, Ph.D

Neal Alto, Ph.D.

Jonathan Graff, M.D., Ph.D.

DEDICATION

I dedicate this work to everybody who helped me on my way, current and former Süel lab members: Tolga Çağatay, Alma Alvarado, Mark Kittisopikul, Eric Archer, Andra Robinson, Fang Zhang, Daisy Lee; my current and former Committee Members: Drs. Steven Altschuler, Neal Alto, Jon Graff and Wade Winkler; special thanks to my dear family, my father Yurii Kuchin and my husband Nikolay Burnaevskiy who gave me inspiration and courage. I thank my mentor Dr. Gürol Süel for guidance and support.

DYNAMICS OF CELL FATE DECISION MAKING BETWEEN SPORULATION AND COMPETENCE IN BACILLUS SUBTILIS

by

ANNA KUCHINA

DISSERTATION

Presented to the Faculty of the Graduate School of Biomedical Sciences

The University of Texas Southwestern Medical Center at Dallas

In Partial Fulfillment of the Requirements

For the Degree of

DOCTOR OF PHILOSOPHY

The University of Texas Southwestern Medical Center at Dallas

Dallas, Texas

May, 2013

DYNAMICS OF CELL FATE DECISION MAKING BETWEEN SPORULATION AND COMPETENCE IN BACILLUS SUBTILIS

Anna Kuchina, Ph.D.

The University of Texas Southwestern Medical Center at Dallas, 2013

Gürol Mehmet Süel, Ph.D.

During multipotent differentiation cells must reliably make a cell fate decision under a variety of conditions, yet remain sensitive to changes in extracellular environment. It is unclear how the cells reconcile these seemingly contradictory requirements. To complicate the issue, the cells often face a decision between multiple fates mediated by the respective differentiation programs which could become active at once. How cells make a specific cell fate choice when presented with several possibilities is a fundamental, yet poorly resolved question. To study cell-fate decision-making dynamics, I utilized the soil bacterium *Bacillus subtilis* which under stress can either become competent for DNA uptake or undergo sporulation. The master regulator of

sporulation is the transcription factor Spo0A. Single cell measurements of Spo0A dynamics along with activities of stage-specific sporulation reporters Spo0F, SpoIIE and SpoIIR revealed the reversible and noisy progression of sporulation up until the final irreversible decision point. Mathematical modeling suggested that such strategy might be advantageous for coping with unpredictable environment.

The alternative cell fate of competence is controlled by the transcription factor ComK. Using time-lapse fluorescence microscopy, I quantitatively measured the activities of Spo0A and ComK, along with other cross-regulatory genes, simultaneously in single *B. subtilis* cells. I found that, surprisingly, sporulation and competence progressed independently in the same cell without cross-regulation up to the final decision point. This finding was confirmed by the discovery of cells in a conflicted state that progressed to sporulation despite the expression of ComK. Measurements of gene expression dynamics in these cells revealed key differences in the relative timing of differentiation programs. To investigate the importance of relative timing, I altered it by engineering artificial cross-regulatory links between the sporulation and competence genetic circuits. Results favor a simple model for cellular decision-making that does not require intricate cross-regulation prior to the decision. Rather, cell fate choice appears to be the outcome of a "molecular race" between independently progressing differentiation programs. This temporal competition mechanism provides a simple, yet efficient way to generate mutually exclusive cell fates. Investigation of the benefits and limitations of such strategy opens a promising venue for future studies.

TABLE OF CONTENTS

PRIOR PUBLICATIONS

Kuchina A, Espinar L, Garcia-Ojalvo J, Süel GM (2011) Reversible and Noisy Progression towards a Commitment Point Enables Adaptable and Reliable Cellular Decision-Making. PLoS Comput Biol 7(11): e1002273. doi:10.1371/journal.pcbi.1002273

Kuchina A, Espinar L, Çağatay T, Balbin AO, Zhang F, Alvarado A, Garcia-Ojalvo J, Süel GM (2011) Temporal competition between differentiation programs determines cell fate choice. Mol Syst Biol 7(557) doi:10.1038/msb.2011.88.

LIST OF FIGURES

CHAPTER 1

CHAPTER 3

CHAPTER 4

CHAPTER 5

CHAPTER 6

CHAPTER 7

LIST OF TABLES

LIST OF APPENDICES

LIST OF DEFINITIONS

P_{spo0A} – promoter for Spo0A

P_{spo0F} – promoter for Spo0F

P_{spoIIR} – promoter for SpoIIR

P_{spoIIE} – promoter for SpoIIE

P_{spoIIG} – promoter for SpoIIG

P_{comG} – promoter for ComG

P_{abrB} – promoter for AbrB

P_{sinI} – promoter for SinI

P_{rok} – promoter for Rok

Spo0A~P – phosphorylated Spo0A

YFP – yellow fluorescent protein

CFP – cyan fluorescent protein

DA – "Dual Activity" cell(s)

CHAPTER ONE

INTRODUCTION AND LITERATURE REVIEW

Cell fate decision-making during multipotent differentiation

Multipotent differentiation is a process during which cells adopt a specific cell fate. Cellular decision-making underlying multipotent differentiation appears to be a complex process that proceeds over time and involves many biochemical interactions. Each fate is typically driven by a distinct differentiation program, comprised of multiple genetic regulatory circuits (Bertrand and Traver, 2009; Errington, 1993; Parra, 2009; Perkins and Swain, 2009). Through the dynamics of the activation of these circuits, cellular decision-making can meet the specific requirements imposed by the environment. Some environments are more or less stable, but in many cases the differentiating cells experience fluctuations in the extracellular milieu. Since cells require specific signals for the execution of the genetic differentiation program, they must have evolved distinct dynamic behaviors permitting to react to the withdrawal or change of these signals. For instance, one such strategy is progression of cellular differentiation through reversible intermediate states which permits flexibility and proportional responses to environmental changes at each step. For example, multipotent differentiation of hematopoietic stem cells is a stepwise process with numerous reversible intermediate states that allows cells to gradually adapt to changes in extracellular signals (Bertrand and Traver, 2009; Malhotra and Kincade, 2009; Moldovan, 2005; Parra, 2009; Prindull and Fibach, 2007; Quesenberry and Aliotta, 2008; Sanosaka et al., 2009). On the other hand, in some situations high sensitivity to small changes in the environment can lead to detrimental uncertainty in cell fate outcomes and unproductively delay differentiation. Thus, cell-fate

decision-making must also permit individual cells to reach a decision even in fluctuating extracellular environments (Perkins and Swain, 2009). The property of decisiveness can be reached by the combination of ultra-sensitivity and positive feedback which have been proposed to generate an irreversible and all-or-none cell fate choice such as those observed during *Xenopus* oocyte maturation (Ferrell and Machleder, 1998) and yeast mating decision (Malleshaiah et al., 2010). However, individual cells with such irreversible responses can lack the flexibility to respond proportionally to changing environments. Despite recent insights, how multipotent differentiation systems reach a decisive cell fate choice while maintaining the ability to respond to changes in the environment is largely unknown.

Another level of complexity is added to the problem of reaching a cell fate decision if several differentiation programs are activated in the same cell prior to cell fate choice. In order to choose a cell fate in such situation, the genetic circuits specific for either differentiation program are thought to regulate each other through cross-talk and systems of checkpoints. Numerous studies have suggested that such cross-regulation between competing differentiation programs controls decision-making and ensures that cell fate outcomes are mutually exclusive (Berka et al., 2002; Grossman, 1995; Hahn et al., 1995; Schultz et al., 2009; Veening et al., 2006). In this scenario, multiple interactions between the components of cell-fate specific genetic circuits can progressively favor one cell fate and in turn decrease the probability of the alternative over time. Such regulation could give rise to checkpoints that allow the cell to continue progression towards one cell fate only if the state of the alternative differentiation program permits it (Hosoya et al., 2010). In the opposite case, cross-regulation might not be required for cells to reach a

decision. Indeed, even if potential cross-regulatory interactions have been identified (Bai et al., 1993; Hamoen et al., 2003; Hoa et al., 2002; Smits et al., 2007), when these particular links are active in individual cells and what specific role they play during decision-making is commonly not known. Perhaps these potential links are not active in all cells and at all times, and may not be necessary for decision-making. Cell fate choice could then simply be the outcome of the independent dynamics of competing differentiation programs. For example, recent studies have suggested that the cellular decision-making process in mammalian cells to undergo apoptosis or slippage during cell cycle checkpoint activation may be the result of competition in time among independently operating genetic programs (Huang et al., 2010; Huang et al., 2009). In these systems, the main role of cross-regulation may be to prevent interference among alternative programs after the decision point.

In summary, even though many of the individual components driving differentiation programs may be known, how cells reach a mutually exclusive decision between alternative fates over time remains poorly understood. To understand cellular decision-making, it is critical to determine the single-cell dynamics underlying the progression to cell fate choice. However, these dynamics are poorly characterized in most multipotent differentiation systems ranging from bacteria to mammalian stem cells. Simultaneous measurement of multiple components of a differentiation program in the same cell can reveal the dynamics of cellular decision-making underlying multipotent differentiation. The soil bacterium *Bacillus subtilis* serves as an ideal model system in which the dynamics of multiple genes within a differentiation circuit are simultaneously measurable in single cells (Cagatay et al., 2009; Suel et al., 2006; Suel et al., 2007). In

stressful environments the majority of *B. subtilis* cells form spores that survive environmental extremes, while approximately 3% of cells transiently differentiate into the alternative cell fate of competence allowing uptake of extracellular DNA (Dubnau, 1999; Grossman, 1995). (Errington, 1993; Piggot and Hilbert, 2004). These two processes are mutually exclusive and key components of the genetic circuits regulating each differentiation program have been characterized(Dubnau, 1999; Errington, 1993).

The sporulation program has been extensively studied genetically and multiple stages of sporulation have been described (Fujita et al., 2005; Fujita and Losick, 2005; Hilbert and Piggot, 2004; Schultz et al., 2009; Veening et al., 2006). However, despite these important insights, how individual cells proceed to spore formation and thus the dynamics of the sporulation program in single cells has not been determined. Likewise, even though the overall mechanism of competence initiation has been thoroughly investigated, the relationship between the competing differentiation programs of competence and sporulation and the resulting dynamics of cell fate choice remain unclear. Specifically, it is not known how an individual cell makes a cell fate decision over time and when cross-regulation between competing differentiation programs plays a role.

Therefore, I aim to investigate:

the role of relative timing and cross-regulatory interactions between competing differentiation programs in cell fate decision-making;

how the dynamics of cell fate decision-making in individual cells reconcile the opposing requirements of decisiveness and adaptability during progression to cell fate choice.

Early stages of *B. Subtilis* sporulation

B. subtilis is a gram-positive rod-shaped bacterium commonly found in soil. Under certain conditions, cells of *B. subtilis* differentiate into endospores which are capable of surviving a variety of assaults including extreme heat, dehydration and irradiation. Indeed, spores have been widely cited as being one of the nature's most resilient life forms (Horneck et al., 2012; Kerney and Schuerger, 2011; Setlow, 2006). While both *Bacillus* and *Clostridium* species are known to produce endospores, *B. subtilis* has been used since the beginning of the 20th century as a model organism to study the process of sporulation (Itano and Neill, 1919; Roberts et al., 1938). It is now known that spore formation is a complex, time- and energy-consuming process that upon activation of the sporulation genetic program proceeds through many steps until the spore is finally released into the medium (Hoch, 1976; Phillips and Strauch, 2002; Piggot and Hilbert, 2004). The mature spores are dormant until they sense a signal to germinate, upon which they quickly resume vegetative growth (Moir, 2006). Although the existence in the form of a spore protects the genetic material during harsh conditions, the associated cost of spore formation, among others, is cessation of cell division. For these reasons, the cells faced with environmental challenges such as the transition into stationary phase are believed to first explore other options before committing to sporulation as a last resort. Therefore, the decision to sporulate is regulated at multiple levels.

At the heart of the sporulation initiation lies the so-called phosphorelay comprised of two phosphotransferases, Spo0F and Spo0B, and a transcription factor Spo0A which acts as a global transcriptional regulator activating many downstream genes (Burbulys et al., 1991; Hoch, 1993a, b). The phosphate is first accepted by Spo0F

that receives it from a variety of sources, the major being a histidine kinase KinA (Trach and Hoch, 1993). The exact physiological mechanism that leads to KinA activation is still unknown, although it is somehow triggered by starvation, pH and osmolarity changes, and other environmental cues such as elevated cell density which is sensed through small secreted peptide pheromones (Jiang et al., 2000; Lazazzera, 2000). KinA and KinB overexpression is shown to be sufficient to activate spore formation in cultures even in rich media conditions (Eswaramoorthy et al., 2010). From Spo0F, the phosphate group is subsequently transferred through Spo0B to Spo0A, a master regulator of sporulation (Burbulys et al., 1991; Hoch, 1993a).

At this crucial "zero" stage of sporulation, the cells are leaving the state of pure vegetative growth and entering the "transition state" associated with low levels of Spo0A~P, when they are still presented with possibilities to differentiate into a variety of cell fates other than sporulation, such as matrix production or competence (Lopez et al., 2009). This transition is marked by the Spo0A-mediated inhibition of AbrB, another global regulator acting as a suppressor of transition-state-associated gene expression (Hahn et al., 1995; Strauch et al., 1990; Zuber and Losick, 1987). In this manner, Spo0A~P de-represses the expression of Spo0H which encodes an RNA polymerase sigma factor σ^H (Fujita and Sadaie, 1998; Weir et al., 1991). This sigma factor acts back positively on phosphorelay both directly by promoting expression from Spo0A and Spo0F promoters and indirectly by suppressing the activity of specialized phosphatases (Asai et al., 1995; Britton et al., 2002; Fujita and Sadaie, 1998). Spo0A~P also activates Spo0F transcription more than 10-fold in a positive feedback mechanism (Lewandoski et al., 1986; Strauch et al., 1993). In addition to the positive feedback from kinases, the

phosphate from Spo0F~P is getting removed by some phosphatases, notably the Rap family of phosphatases: RapA, RapB, RapE and RapH (Perego, 2001; Pottathil and Lazazzera, 2003; Veening et al., 2005). Another phosphatase family Spo0E acts on the level of Spo0A~P itself (Ohlsen et al., 1994; Perego and Hoch, 1991).

All this complex regulation on the phosphorelay level ultimately leads to the changes of one main output: the level of Spo0A~P in the cell. For some time, the activation of Spo0A in the cells was considered bistable, that is, the cells at each time were believed to exist as two clearly distinct populations characterized by either low ("OFF") or high ("ON") level of Spo0A (Dubnau and Losick, 2006; Veening et al., 2005). However, latest studies found that the levels of Spo0A in the cells were instead broadly heterogeneous, with many levels of Spo0A expression in between of the extreme values (de Jong et al., 2010; Fujita and Losick, 2005). The asynchronicity in sporulation gene expression and the fluctuations in phosphate flux through the phosphorelay among cells translates into high population-level variability of sporulation outcomes (Chastanet et al., 2010; de Jong et al., 2010). As a result, at each moment in the stationary phase population only a fraction of cells exhibit high Spo0A~P levels and undergo sporulation at each time point.

Spo0A upon phosphorylation directly controls expression of over 120 genes in a concentration-dependent manner: some genes with higher promoter affinities for Spo0A~P are correspondingly known to respond to even low levels of this regulator ("low-threshold" genes), while others are activated only by high levels of Spo0A~P ("high-threshold" genes) (Fujita et al., 2005; Molle et al., 2003). It is generally believed that the earliest-responding genes might be involved in other stationary phase activities or

maybe even in cell fates alternative to sporulation, as well as the most initial stages of spore formation, while the high-threshold genes are thought to be involved in the later stages of spore development. For instance, Spo0F is thought to be low-threshold activated, while other crucial operons like SpoIIA, SpoIIG and SpoIIE are thought to respond to high Spo0A levels (Fujita et al., 2005).

At the stage when Spo0A expression reaches the highest levels, the cell forms a sporulation-specific asymmetric septum at one pole of the cell dividing it into two compartments: a future endospore compartment (called 'forespore') and a so-called 'mother cell' which will eventually engulf the forespore, finish the formation of protective coats surrounding the forespore and then release the mature spore (Errington, 2003; Piggot and Hilbert, 2004). The asymmetric septum is similar to the usual septum formed during the vegetative division, but with several notable differences, such as the recruitment of sporulation-specific proteins that play an important role in the downstream genetic cascade. One of the products of the high-threshold Spo0A~P activated operons, SpoIIE is localized to the septum by direct interaction with the septum component FtsZ and is required for the efficient polar septation (Barak et al., 1996; Khvorova et al., 1998). Importantly, SpoIIE is also a phosphatase whose activity is crucial for establishing the specialized gene expression patterns between the forespore and the mother cell. Specifically, SpoIIE dephosphorylates the anti-anti-sigma factor SpoIIAA on the forespore side that leads to the subsequent activation of the RNA polymerase factor σ^F specifically in the forespore (Arigoni et al., 1996). This step is crucial for the following 'criss-cross' activation of the mother cell and forespore-specific sigma factors, and thus essentially couples the first morphological change with the correct and just-in-time

activation of the downstream signaling that coordinates further differentiation of both cells (Hilbert and Piggot, 2004).

Activated σ^F among others drives the forespore-specific expression of the intercellular signaling protein SpoIIR which is able to cross the first septal membrane and activate SpoIIGA, a *spoIIG*-operon encoded protease, in the intermembrane space (Fujita and Losick, 2002; Hofmeister et al., 1995; Karow et al., 1995; Trempy et al., 1985). This results in the mother cell-specific proteolytic activation of σ^E, synthesized as a precursor under the control of Spo0A~P (Fujita and Losick, 2002). The differential activities of σ^F and σ^E in the forespore and mother cell compartments, respectively, drive the further cascade of gene expression resulting in the mature spore formation (Hilbert and Piggot, 2004).

Commitment to sporulation in *B. subtilis*

One of the hallmarks of any differentiation process in general is the so-called point of cell fate commitment, usually defined as the developmental stage at which the changes induced by the differentiation process become irreversible. In other words, once the cells reach this stage, differentiation becomes unavoidable even if the conditions change and cells receive signals that would previously result in the abortion of differentiation. The identification and characterization of such point has been a major challenge in developmental biology (Keeble and Gilmore, 2007; Klein and Jovanovic, 2011; Welinder et al., 2011). *B. subtilis* sporulation at the later stages has been long known to proceed without interruption even after addition of nutrients and stress release, indicating that at some point the spore formation process becomes irreversible (Sterlini and Mandelstam, 1969). Identification of such point would provide important insights

into the evolutionary meaning of commitment. Indeed, when differentiation becomes irreversible, the cells can no longer respond to changes in the environment even if they can still sense them. This can be either beneficial, or detrimental depending on the circumstances. In the natural soil environment, conditions can change unpredictably with or without a regular pattern. The challenge of the proper placement of the commitment point is to ensure that the cells are not confused with the small and\or fast fluctuations of environmental signals, but still maintain enough responsiveness to be able to alter their decisions in case of a major environmental change.

In *B. subtilis*, the point of irreversible commitment to sporulation has been investigated recently (Dworkin and Losick, 2005; Parker et al., 1996). The irreversible decision to sporulate was shown to coincide with the start of differential activation of σ^F and σ^E in the forespore and mother cell compartments, respectively. Several protein products of σ^F and σ^E –activated operons appear to play a role in the commitment, with the slightly different requirements for the forespore and mother cell compartments. In the forespore, σ^F drives the production of a multifunctional protein SpoIIQ, which is localized to the asymmetric septum and anchors multiple proteins to it on the both sides, while also participating in the cell wall remodeling and coat formation during engulfment (Campo et al., 2008; Londono-Vallejo et al., 1997). Both σ^E and σ^F (the latter through a readthrough mechanism) also drive expression of SpoIIP, a protein involved in limiting growth and preventing the additional rounds of division in both parts of the sporangium (Frandsen and Stragier, 1995). Both of these proteins seem to be required for the forespore commitment to sporulation, while only SpoIIP is needed for the mother cell commitment (Dworkin and Losick, 2005). Accordingly, the deletion of either σ^F or σ^E

results in a 'disporic' phenotype, and while normally the forespore compartments of σ^F mutants are able to resume longitudinal growth on rich agar pads, σ^E mutant forespore compartments are unable to grow after transfer to rich conditions, unless both SpoIIP and SpoIIQ are deleted (Dworkin and Losick, 2005). The exact mechanism of this process is still unknown, although it might be somehow connected to the cell wall remodeling that takes place during stage III of sporulation, namely spore engulfment. Since the exact timing of SpoIIP and SpoIIQ relative to polar septation and cascade of sigma factors activation hasn't been strictly measured in single cells, so far the more reliable definition of the irreversible commitment point for sporulation would be the activation of σ^F and σ^E –driven gene expression in both mother cell and the forespore compartments.

Competence development

During the aforementioned 'transition state', when Spo0A~P levels start to increase and the AbrB-mediated repression of transition state genes is relieved, the cells are primed to explore numerous other options besides sporulation as the first line of defense against the adverse conditions. Such options include, for example, natural antibiotics and toxins production, matrix production for the biofilm development, motility, cannibalism and competence (Lopez et al., 2009). Among others, development of competence has been extensively studied and the mechanism underlying differentiation into the competent state has been understood in remarkable detail (Dubnau, 1999; Maamar et al., 2007; Suel et al., 2006; Suel et al., 2007). Competence represents a specialized physiological state during which the cell temporarily gains ability to bind and uptake free DNA fragments from the environment (Dubnau, 1991a, b; Kruger and Stingl, 2011). Since the DNA is finally integrated into the bacterial chromosome, this

behavior is thought to promote the genetic variability in the population which could be helpful for overcoming detrimental environmental conditions (Cagatay et al., 2009; Suel et al., 2006). Therefore, the development of competence which usually happens in a small fraction of cells is considered a "bet-hedging" strategy for maximizing the survival probability of the population in unpredictable environments (Dubnau, 1999).

Importantly, it has been established that the initiation of competence is spontaneous and driven by noise in the expression of the transcription factor ComK, a master regulator of competence (Maamar et al., 2007; Suel et al., 2006). Upon activation, ComK induces expression of more than 100 genes, some of which, including *ComG* operon, are encoding the molecular machinery that mediates DNA uptake (Chung and Dubnau, 1998). *ComK* transcription during vegetative growth is directly repressed by binding of at least three inhibitory proteins: Rok, CodY, and AbrB (Hamoen et al., 2003; Hoa et al., 2002; Serror and Sonenshein, 1996a, b). In addition, ComK protein is sequestered by interaction with the adapter protein MecA which targets it for degradation by the ubiquitous ClpCP protease (Schlothauer et al., 2003; Turgay et al., 1998). At the onset of the stationary phase, when conditions are deteriorating, both AbrB- and Rok-mediated inhibition is relieved by the expression of Spo0A~P (Hahn et al., 1995), and CodY levels drop as the cell senses the depletion of nutrients (Sonenshein, 2005). Importantly, at the same time due to stress and quorum-sensing the cells express a small peptide ComS which is able to compete with ComK for MecA binding and degradation, therefore promoting higher ComK levels (Ogura et al., 1999; Turgay et al., 1998). As a result, during the stationary phase the intrinsically noisy basal ComK expression rises just below the so-called activation threshold. In a majority of cells, this elevation in basal

ComK expression is not sufficient to trigger a response. But once in a while, as the result of the intrinsic heterogeneity and fluctuations in gene expression, in some cell ComK levels rise above the threshold leading to the activation of the positive feedback acting on ComK expression. Because of this strong positive autocatalytic loop, activation of ComK which governs the entry into competent state was shown to exhibit excitatory dynamics, in other words, even small initial fluctuations of ComK levels above the threshold result in a larger and stereotyped response, much like the action potential in neurons (Maamar et al., 2007; Suel et al., 2006). Once the levels of ComK are elevated and the cell enters the competent state, a slower negative feedback loop is initiated by ComK promoting degradation of ComS, thereby allowing the cell to exit the competence state and return to vegetative division (Suel et al., 2006; Suel et al., 2007). This process is also noisy, resulting in a wide distribution of time spent in competence across all competent cells. This time, when the cells are grown on solid media, can vary from 8 to ~40 hours, further stretching the bets and maximizing the efficiency of DNA uptake in various environmental conditions (Cagatay et al., 2009).

Cross-regulation between competence and sporulation

The competence and sporulation genetic networks share multiple common regulators that are thought to provide the cross-talk between the activities of the respective programs (Figure 1.1). Such cross-talk is expected to ensure that the cell fates of spore formation and competence are mutually exclusive and to avoid the activation of either program at an inappropriate time. As described above, low levels of Spo0A~P expression relieve the inhibition of basal ComK expression. During vegetative growth, the transcriptional regulator AbrB expressed at high levels binds at the ComK promoter directly and inhibits the transcription (Fujita and Sadaie, 1998; Hahn et al., 1995). However, when at the onset of stationary phase the cells start to accumulate Spo0A~P, AbrB levels accordingly drop to intermediate level. At this concentration, AbrB is unable to directly repress *ComK* transcription, but still can efficiently suppress the transcription of Rok, another inhibitor of ComK that can bind to its promoter (Hoa et al., 2002). In this way, intermediate levels of AbrB are thought to be the best permissive for competence development, because once AbrB concentration drops very low as a result of high Spo0A~P accumulation, Rok is no longer repressed and is expected to limit basal ComK expression. This phenomenon is usually regarded as opening of the "competence window" when a fraction of the cells receives the temporary opportunity to experience competence before committing to the terminal sporulation fate (Mirouze et al., 2012; Schultz et al., 2009).

Another multifunctional regulator acting on multiple fates, including competence, sporulation and even matrix production is a DNA-binding protein SinR. The activity of SinR is negatively regulated by its antagonist SinI whose expression depends

on both Spo0A and Spo0H (Bai et al., 1993; Mandic-Mulec et al., 1995). On the other hand, SinR itself is thought to suppress sporulation by inhibiting *Spo0A* along with stage II sporulation genes (Cervin et al., 1998; Mandic-Mulec et al., 1995). Competence initiation, however, requires SinR activity, since SinR, like AbrB, inhibits Rok, thereby positively regulating ComK transcription (Hahn et al., 1996; Hoa et al., 2002). In summary, based on the literature, sporulation activity is thought to indirectly suppress competence through the two-component SinR-SinI switch (Dubnau et al., 1994).

One more two-component system that acts both on competence development and sporulation is DegU-DegS, also playing an important role in regulating other cellular processes such as production of degradative enzymes, motility and multicellular behavior (Amati et al., 2004; Kobayashi, 2007; Kunst et al., 1994; Verhamme et al., 2007). Phosphorylated DegU was shown to promote sporulation, while de-phosphorylated DegU is required for competence development presumably by acting both on ComK and MecA (Dahl et al., 1992; Hamoen et al., 2000).

Another powerful mechanism that regulates *B. subtilis* differentiation is the exchange of signals between cells through extracellular medium, or quorum sensing (Lazazzera, 2000). For instance, ComS expression which is necessary for competence development is activated through the two-component ComPA system, in which phosphate is transferred to ComA through the action of the histidine kinase ComP when the cells reach a certain density to sense the secreted extracellular peptide ComX which binds to ComP at the membrane (Comella and Grossman, 2005; Magnuson et al., 1994). Interestingly, besides ComX, ComA is also activated through the action of another family of quorum-sensing pentapeptides called Phr (Pottathil and Lazazzera, 2003). Each of the

Phr genes lies downstream in the same operon with its cognate *Rap* gene encoding a family of Rap protein phosphatases. All Phr peptides described to date inhibit the action of their corresponding Rap phosphatase. Out of 11 known Rap phosphatases, RapC and RapF specifically inactivate ComA, while PhrC and PhrF, excreted and sensed during the stationary phase, act positively on competence development (Bongiorni et al., 2005; Core and Perego, 2003). Some of the Rap proteins, as mentioned above, have also been shown to act on the sporulation phosphorelay, removing phosphate from Spo0F~P (Perego, 2001). One of them, RapH, was shown to be activated by ComK, thereby constituting an inhibitory link from competence towards sporulation (Smits et al., 2007). The activity of RapH in fact is dual, because is also prevents DNA binding of ComA, but the implications of this negative feedback have not been investigated. The action of RapH has been proposed to contribute to the temporal separation of the sporulation and competence pathways on the basis of the observation that RapH-knockout cultures have a larger proportion of cells expressing both Spo0A and ComK simultaneously (Smits et al., 2007). However, this fact can be interpreted in a variety of ways since competence is a transient fate and those observed cells with dual expression of Spo0A and ComK may represent the fraction of cells at any stage of competence, including early initiation and exit. The actual timing of RapH activation, like that of many other cross-regulators including SinI-SinR and DegU-DegS switches, in single cells relative to either differentiation program has not been established.

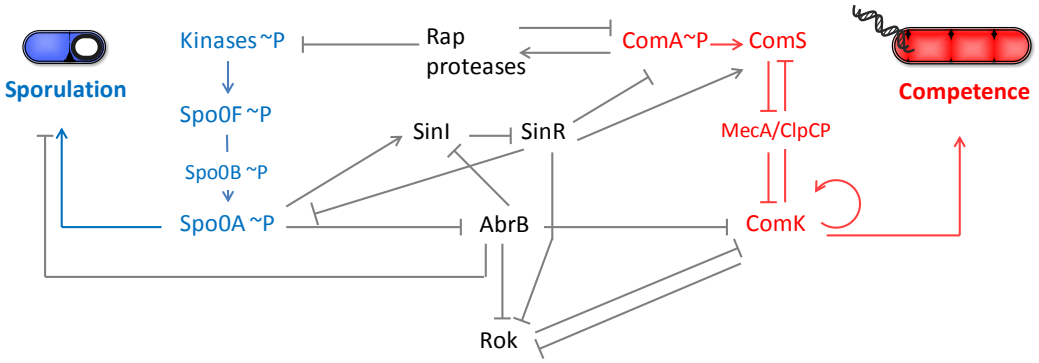

Figure 1.1. Simplified schematic representation of the core competence (in red) and sporulation (in blue) genetic circuits with some of the most prominent cross-regulatory links shown in black and grey.

In summary, a variety of regulatory proteins have been found in *B. subtilis* that seem to have effect both on competence and sporulation and may also act as cross-regulatory links between the corresponding genetic circuits of both programs (see Figure 1.1). Most of the knowledge about the actions of these cross-regulators has been gained by utilizing gene knockouts and overexpression, then measuring the population-level outcomes. In such experiments, the single-cell dynamics of cellular behavior during decision-making is usually ignored. Only the final outcomes are considered, with no knowledge of the exact way they were generated. However, in light of the heterogeneous and variable cellular behavior of *B. subtilis* cells during stationary phase, the role of these cross-regulatory interactions in cell-fate decision-making may depend on the exact timing of their activation relative to the activities of differentiation programs components. Such relative temporal profiles of these regulators are yet to be measured.

Scientific aim and experimental approach

Despite the important recent insights into the processes of *B. subtilis* differentiation, the dynamics of the sporulation program in single cells is still largely unknown. Furthermore, the role of cross-regulatory links and relative timing in the relationship between the competing differentiation programs of competence and sporulation remains unclear. I aim to analyze cell fate decision-making dynamics in single cells of *B. subtilis*, focusing on the role of interactions between competing differentiation programs of sporulation and competence in generating cell fate decisions. Since these processes are not synchronized across the naturally differentiating bacterial population (de Jong et al., 2010), average population measurements are little informative. Therefore, in order to explore the mutual interactions between alternative cell fates, I analyze single cell measurements of multiple gene activities involved in the decision-making, including master regulators of sporulation and competence. A bacterial system is ideal for this purpose due to ease of genetic manipulation and availability of powerful techniques for quantitative measurement of gene and protein activity inside single cells.

Specifically, I measure multiple gene activities during differentiation simultaneously in the same cells over many generations using time-lapse microscopy. I next use this data to determine the relative timing and activities of competing differentiation programs. I also utilize mathematical modeling to understand and interpret my results. In order to perturb the dynamics of competence and sporulation programs relative to each other, I engineer artificial cross-regulatory links between the corresponding circuits. This approach allows me to understand how interactions between differentiation circuits translate into cell fate decisions. The results are expected to be applicable to other cellular decision-making

systems such as stem cells and might provide a foundation for studying and controlling the differentiation processes in such systems.

CHAPTER TWO

GENERAL EXPERIMENTAL PROCEDURES

Strain Construction

Bacillus subtilis strains used in the study are isogenic to wild-type *B. subtilis* PY79 strain and are listed in Table 2.1. Promoter – protein fusions were generated using fusion polymerase chain reaction (PCR) and cloned into *B. subtilis* chromosomal integration vectors following standard protocols. The following *B. subtilis* chromosomal integration vectors were used: pSac-Cm, integrating into the *sacA* locus (constructed by R. Middleton and obtained from the Bacillus Genetic Stock Center); pLD30 designed to integrate into the *amyE* locus (kind gift from Jonathan Dworkin, Columbia University); pGlt-Kan, designed to integrate into the *gltA* locus(Middleton and Hofmeister, 2004) (constructed by R. Middleton and obtained from the Bacillus Genetic Stock Center); per449, a generic integration vector constructed for integration into the gene of interest (kind gift from Wade Winkler, UT Southwestern); and the bifunctional cloning plasmid pHP13 carrying the replication origin of the cryptic *B. subtilis* plasmid pTA1060 (5 copies per genome)(Haima et al., 1987). Standard one-step *B. subtilis* transformation protocol was followed to transform *B. subtilis* strain PY79 with these constructs.

B. subtilis strains isogenic to P*Y79*	Genotype
0A-IIR	*AmyE*::P_{spo0A}-*yfp*, P_{comG}-*mCherry* (Sp^R) *SacA*::P_{spoIIR}-*cfp* (Cm^R)
0F-IIR	*AmyE*::P_{spo0F}-*yfp* (Sp^R) *SacA*::P_{spoIIR}-*cfp* (Cm^R)
IIE-IIR	*AmyE*::P_{spoIIE}-*spoIIE-yfp* (Sp^R) *SacA*::P_{spoIIR}-*cfp* (Cm^R) ΔSpoIIE::Neo
0A (5x)-IIR	*SacA*::P_{spoIIR}-*yfp* (Cm^R)

	pHP13-P_{spo0A}-cfp (Erm^R)
0A-0F	*AmyE*:: P_{spo0F}-*yfp* (Sp^R) *SacA*:: P_{spo0A}-*cfp*, P_{comG}-*mCherry* (Cm^R)
0F-comG	*AmyE*:: P_{spo0F}-*yfp* (Sp^R) *SacA*:: P_{comG}-*cfp* (Cm^R)
0A-comG	*SacA*:: P_{spo0A}-*yfp*, P_{comG}-*cfp* (Cm^R)
IIG-comG	*AmyE*::P_{spoIIG}-*yfp*, P_{comG}-*cfp* (Sp^R)
IIR-comG	*SacA*:: P_{spoIIR}-*yfp*, P_{comG}-*cfp* (Cm^R)
IIE-comG	*AmyE*::P_{spoIIE}-*spoIIE-yfp* (Sp^R) *SacA*::P_{comG}-*cfp* (Cm^R) *spoIIE::neo* (Neo^R)
0A-comG-abrB	*SacA*:: P_{spo0A}-*cfp*, P_{comG}-*mCherry* (Cm^R) *AmyE*::P_{spoIIG}-*comK*/P_{abrB}-*yfp* (Sp^R)
0A-comG-sinI	*SacA*:: P_{spo0A}-*cfp*, P_{comG}-*mCherry* (Cm^R) *AmyE*::P_{spoIIG}-*comK*/P_{sinI}-*yfp* (Sp^R)
0A-comG-rok	*SacA*:: P_{spo0A}-*cfp*, P_{comG}-*mCherry* (Cm^R) *AmyE*::P_{spoIIG}-*comK*/P_{rok}-*yfp* (Sp^R)
[0A-comG] $^{0A\text{-}K}$	*AmyE*::P_{spo0A}-*yfp*, P_{comG}-*cfp* (Sp^R) *SacA*:: P_{spo0A}-*comK* (Cm^R)
[IIG-comG] $^{0A\text{-}K}$	*AmyE*::P_{spoIIG}-*yfp*, P_{comG}-*cfp* (Sp^R) *SacA*:: P_{spo0A}-*comK* (Cm^R)
[IIR-comG] $^{0A\text{-}K}$	*AmyE*::P_{spo0A}-*comK* (Sp^R) *SacA*::P_{spoIIR}-*yfp*, P_{comG}-*cfp* (Cm^R)
[IIE-comG] $^{0A\text{-}K}$	*AmyE*::P_{spoIIE}-*spoIIE-yfp* (Sp^R) *SacA*:: P_{spo0A}-*comK* (Cm^R) *spoIIE::* P_{comG}-*cfp* (Neo^R)
[0A-comG] $^{IIG\text{-}K}$	*AmyE*::P_{spoIIG}-*comK* (Sp^R) *SacA*:: P_{spo0A}-*yfp*, P_{comG}-*cfp* (Cm^R)
[IIG-comG] $^{IIG\text{-}K}$	*AmyE*::P_{spoIIG}-*yfp*, P_{comG}-*cfp* (Sp^R) *SacA*:: P_{spoIIG}-*comK* (Cm^R)
[IIR-comG] $^{IIG\text{-}K}$	*AmyE*::P_{spoIIG}-*comK*, P_{comG}-*cfp* (Sp^R) *SacA*:: P_{spoIIR}-*yfp* (Cm^R)
[IIE-comG] $^{IIG\text{-}K}$	*AmyE*::P_{spoIIE}-*spoIIE-yfp* (Sp^R) *SacA*:: P_{spoIIG}-*comK*, P_{comG}-*cfp* (Cm^R) *spoIIE::neo* (Neo^R)
[0A-comG] $^{IIR\text{-}K}$	*AmyE*:: P_{spo0A}-*yfp*, P_{comG}-*cfp* (Sp^R) *SacA*:: P_{spoIIR}-*comK* (Cm^R)
[comG-comGA] $^{IIG\text{-}K}$	*AmyE::* P_{spoIIG}-*comK*, P_{comG}-*cfp* (Sp^R) *SacA*:: P_{comG}-*comGA-yfp* (Cm^R)
[comG] $^{2xIIG\text{-}K}$	*AmyE*::P_{spoIIG}-*comK* (Sp^R) *SacA*:: P_{spoIIG}-*comK*, P_{comG}-*cfp* (Cm^R)
[comG] $^{2x0A\text{-}K}$	*AmyE*::P_{spo0A}-*comK* (Sp^R) *SacA*:: P_{spo0A}-*comK*, (Cm^R) *GltA::* P_{comG}-*mCherry (*Neo^R*)*

NoE	*SacA*::P_{spo0A}-*yfp*, P_{comG}-*cfp* (Cm^R) *AmyE*::P_{spoIIG}-*comK*, P_{comG}-*sspB*^{EC}-*XP* (Sp^R) *spoIIE::neo* (Neo^R) *GltA*::P_{spoIIE}-*spoIIE-ssrA*^{EC} (Erm^R)
[comG] $^{0A\text{-}yneA}$	*AmyE*::P_{comG}-*cfp* (Sp^R) *SacA*:: P_{spo0A}-*yneA*, (Cm^R)
[comG] $^{0A\text{-}K/0A\text{-}yneA}$	*AmyE*::P_{spo0A}-*comK* (Sp^R) *SacA*:: P_{spo0A}-*yneA*, P_{comG}-*cfp* (Cm^R)
[comG] $^{IIG\text{-}yneA}$	*AmyE*:: P_{spoIIG}-*yfp*, P_{comG}-*cfp* (Sp^R) *SacA*:: P_{spoIIG}-*yneA* (Cm^R)
[IIG] $^{IIG\text{-}yneA}$	*AmyE*:: P_{spoIIG}-*yfp*, P_{spo0A}-*cfp* (Sp^R) *SacA*:: P_{spoIIG}-*yneA* (Cm^R)
[comG] $^{IIG\text{-}K/IIG\text{-}yneA}$	*AmyE*:: P_{spoIIG}-*comK*, P_{comG}-*cfp* (Sp^R) *SacA*:: P_{spoIIG}-*yneA* (Cm^R)

Table 2.1. Strain definitions and genetic background.
In the first column, promoters expressing fluorescent proteins are shown as plain text and/or in square brackets, while additional ectopic expression of comK (abbreviated as "K") and/or yneA from various promoters is indicated in subscript. "0A", P_{spo0A}. "0F", P_{spo0F}. IIE, spoIIE. "IIG", P_{spoIIG}. "IIR", P_{spoIIR}.

Promoter Definitions

All promoter sequences were polymerase chain reaction (PCR) amplified from *B. subtilis* PY79 chromosomal DNA with reverse primer carrying an optimized ribosomal binding sequence (RBS) and spacer sequence (SS) AAGGAGGAA. Promoter sequences were defined as follows:

P_{spo0A}: chromosomal sequence 2518060 to 2518350 (minus-strand);

P_{spo0F}: chromosomal sequence 3809924 to 3810089 (minus-strand);

P_{spoIIG}: chromosomal sequence 1602809 to 1603061 (plus-strand);

P_{spoIIE}: chromosomal sequence 70327 to 70523 (plus-strand);

P_{spoIIR}: chromosomal sequence 3794404 to 3794543 (minus-strand);

P_{comG}: chromosomal sequence 2559328 to 2559937 (minus-strand);

P_{AbrB}: chromosomal sequence 45137 to 45422 (minus-strand);

P_{sinI}: chromosomal sequence 2551439 to 2551663 (plus-strand).

P_{rok}: chromosomal sequence 1492731 to 1493093 (plus-strand).

Growth and Imaging Conditions

Preparation for Microscopy

For imaging, *B. subtilis* cells were grown at 37^0C in LB medium with shaking under appropriate selection. Antibiotics for selection were added to the following final concentrations: 5 μg/ml chloramphenicol, 5 μg/ml neomycin, 5μg/ml erythromycin and 100 μg/ml spectinomycin. Cells grown to OD 1.8 were resuspended in 0.5 volume of Resuspension Media (RM; composition [per 1 liter]: 0.046 mg $FeCl_2$, 4.8 g $MgSO_4$, 12.6 mg $MnCl_2$, 535 mg NH_4Cl, 106 mg Na_2SO_4, 68 mg KH_2PO_4, 96.5 mg NH_4NO_3, 219 mg $CaCl_2$, 2 g L-glutamic acid)(Sterlini and Mandelstam, 1969) supplemented with 0.02% glucose. RM reduces the growth rate of microcolonies on agarose and leads to sporulation. The resuspended cells were grown at 37^0C for 1 hour, then diluted 15-fold in RM and applied onto a 1.5% low-melting agarose pad placed into a coverslip-bottom Willco dish for imaging. This protocol is optimized for time-lapse microscopy.

Time-Lapse Microscopy

Growth of microcolonies on an agarose pad was observed with fluorescence time-lapse microscopy at 37^0C with an Olympus IX-81 inverted microscope with a motorized stage (ASI) and an incubation chamber. Image sets were acquired either every 40 min, or every 20 min with a Hamamatsu ORCA-ER camera. The imaging time has

been optimized in order to prevent phototoxicity (Suel et al., 2006). Custom Visual Basic software in combination with the Image Pro Plus (Media Cybernetics) was used to automate image acquisition and microscope control.

Image Analysis

Time-lapse movie data analysis was performed by Schnitzcells software (http://cell.caltech.edu/schnitzcells/) in combination with custom written MATLAB programs. Schnitzcells software allows to segment images obtained with time-lapse microscopy, track cell lineages frame-by-frame and quantitatively extract fluorescence data (Rosenfeld et al., 2005; Young et al., 2012). In current work, segmentation was performed on phase contrast images and mean fluorescence values over the cell area were used. In case the cell was forming a spore, the whole cell was still being segmented until the mother cell lysed and released the spore, with the exception of measurement of SpoIIE localization at the cell pole where only the area of the cell pole was measured (see Figure 3.3C). Where noted in the figure legend, the fluorescence traces were smoothed using a standard MATLAB method.

CHAPTER THREE

SPORULATION COMBINES REVERSIBLE AND IRREVERSIBLE DYNAMIC BEHAVIORS TO FACILITATE DECISION-MAKING

Introduction

Sporulation in *Bacillus subtilis* has been extensively studied revealing the concerted action of many genes and proteins involved in this process (Grossman, 1995; Hoch, 1976; Phillips and Strauch, 2002; Piggot and Hilbert, 2004; Stragier and Losick, 1996). Sporulating cells have been shown to proceed through specific developmental stages characterized by the expression of multiple regulators (see Chapter 2). Yet, the relative single cell dynamics of these regulators at key stages of sporulation have not been exactly determined. Likewise, the overall dynamics of the sporulation process in single cells remains somewhat unclear, since spore formation in the cells growing on solid media is highly asynchronous, thereby complicating population measurements (Chastanet et al., 2010; de Jong et al., 2010). In contrast, measurements of the activity of several sporulation program components acting at different stages together in the same cell could establish a relative temporal profile of sporulation gene activities in single cells and point towards the source of the observed heterogeneity of sporulation times. Our laboratory has established that such simultaneous measurement of multiple gene activities within a differentiation circuit over time in *B. subtilis* model system is possible and may lead to important insights about the dynamics of cell-fate decision making (Cagatay et al., 2009; Suel et al., 2006; Suel et al., 2007). These measurements could also shed light onto how a specific cell-fate decision-making strategy translates into the important properties of adaptability and reliability of the differentiation process. Sporulation therefore

provides a convenient model differentiation pathway to investigate the dynamics of cell-fate decision-making and its implications.

Results

Early progression to spore formation in single cells of Bacillus subtilis is bursty and reversible

I began to investigate the single-cell dynamics of sporulation progression by measuring the temporal profile of four sporulation components (Figure 3.1). I utilized fusions of spectrally distinct fluorescent proteins (CFP and YFP) to Spo0A (P_{spo0A}), Spo0F (P_{spo0F}) and SpoIIR (P_{spoIIR}) promoters, each of which was integrated into a specific locus on *B. subtilis* chromosome at one copy per cell. The expression from most of the resulting fluorescent reporters was tested to be not location-specific, with the exception of P_{spoIIR} reporter. The native SpoIIR gene is known to be subject to positional regulation (Khvorova et al., 2000). It is located close to the origin of replication, with the expression normally confined to the forespore compartment, where a copy of the chromosome gets translocated during the septation process. I found that upon integration into the *AmyE* locus (327.20kb) P_{spoIIR} expression starts to exhibit unusual bleed through effects, possibly due to mis-expression in the mother cell. Therefore, for the current study I have only used the P_{spoIIR} reporter integrated into the *SacA* gene (3902.70kb) which is close to the native SpoIIR location (3794.40kb) and does not result in fluorescence mis-expression. I also constructed a functional translational fusion of YFP and CFP to SpoIIE protein which replaced the native SpoIIE protein. The resulting construct expression did not lead to a loss of sporulation efficiency.

Because CFP and YFP maturation time and dynamics have been established to be very similar in our system (Suel et al., 2006), their quantitative measurements of fluorescence intensity could be directly compared. Hence, the strains were designed to contain overlapping pair-wise combinations of either P_{spo0A}-YFP, P_{spo0F}-YFP or SpoIIE-YFP together with P_{spoIIR}-CFP. Figure 3.1A shows the overlays of phase and fluorescence images of these strains grown on a solid sporulation medium (RM, see Chapter 2, General Experimental Procedures) and captured by fluorescence time-lapse microscopy. Since completing sporulation on this medium takes on average 1-2 full days, the images captured either every 40, or 20 minutes provided enough temporal resolution to obtain the dynamics of fluorescent reporters activation during sporulation (Figure 3.2). The averaged curves of reporter activation from each strain (Figure 3.2A-C) were combined using the common P_{spoIIR}-CFP reporter as a temporal anchor to produce a relative temporal profile for the measured sporulation steps with single-cell resolution (Figure 3.2D). This profile schematically summarized in Figure 3.2E is consistent with the genetically established hierarchy within the sporulation circuit (Stragier and Losick, 1996).

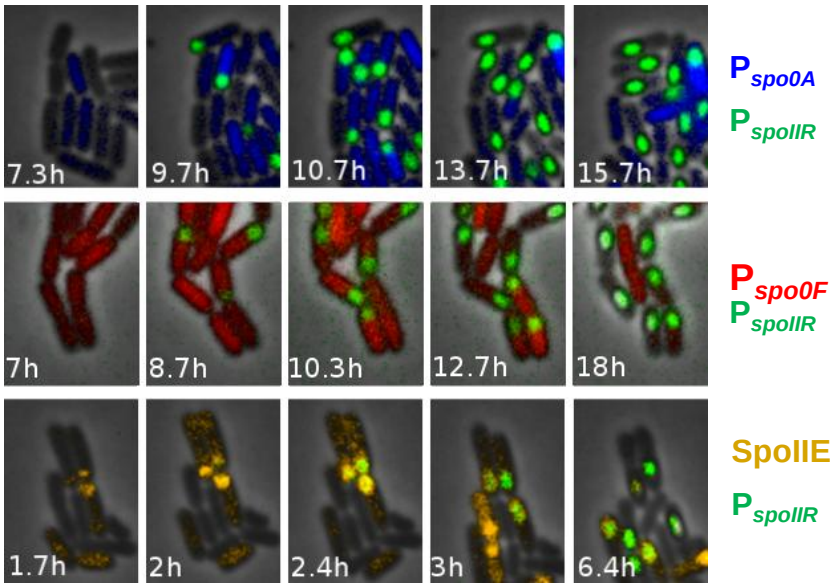

Figure 3.1 Filmstrips of phase and fluorescence image overlays of sporulating *B. subtilis* cells expressing pair-wise combinations of fluorescent proteins. For all panels, CFP fluorescence expressed from the P_{spoIIR} promoter is colored in green. In the same cells, YFP is expressed from the P_{spo0A} promoter (upper panel, blue), from the P_{spo0F} promoter (middle panel, red), and as a translational fusion to SpoIIE protein (lower panel, orange). Time is indicated in hours.

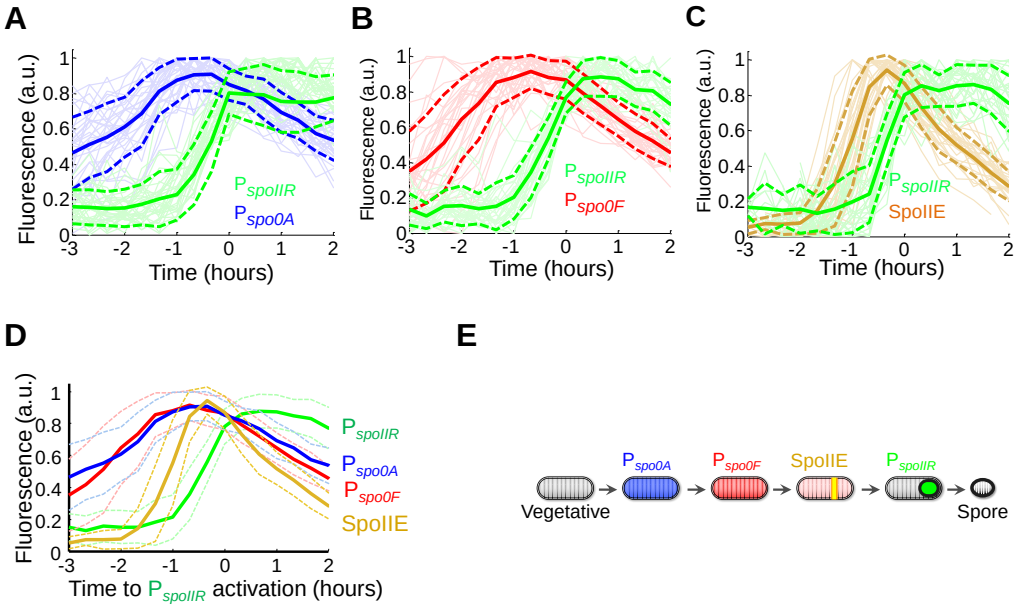

Figure 3.2 Mean quantitative time traces of sporulation reporters during typical sporulation events. In panels (A) through (C), individual time traces of sporulation reporters are shown in lighter colors, with mean trace shown on top in bright color. Dynamics of the reporters in each panel were obtained from strains expressing pair-wise combinations of indicated sporulation reporters: (A) strain 0A-IIR, n = 33, (B) strain 0F-IIR, n = 30, (C) strain IIE-IIR, n = 28. All traces were aligned with respect to P_{spoIIR} activation (in green) defined by P_{spoIIR} fluorescence higher than 70% of maximum P_{spoIIR} fluorescence at sporulation. (D) Combined data from panels (A) through (C) showing mean traces. (E) Scheme representing the temporal sequence of cellular states during the progression to sporulation, summarizing data from the plot shown in (D). Activities of all reporters were measured as mean fluorescence intensities in single cells. All traces have been normalized for amplitude. Dashed lines above and below the mean curves indicate standard deviation (SD).

While the averaged curves did not add major novel insights, the examination of individual single-cell trajectories revealed surprising behavior. During the early progression to spore formation, some cells exhibited bursts of P_{spo0A} gene expression that did not result in spore formation (Figure 3.3A). Such spontaneous bursts of gene expression at a single-cell level during *B. subtilis* sporulation have not been previously described, although it has been long known that during this process Spo0A is activated in a heterogeneous manner (Chastanet et al., 2010). It is important to note that while some cells did exhibit one or more bursts of P_{spo0A} activity, the majority of cells were able to proceed to spore formation directly with no bursts (Figure 3.3D-E). No defined pattern of non-productive bursts relative to the P_{spo0A} peaks that resulted in spore formation could be identified, suggesting that in this case the bursts were not a part of pre-defined response, but a stochastic phenomenon. They also did not seem to correlate with cell division, occurring on a longer temporal scale (Figure 3.3A).

Such bursts in gene expression were not limited to P_{spo0A}, but were also observed for P_{spo0F} (Figure 3.3B). Since P_{spo0F} is transcriptionally activated by dimerized phosphorylated Spo0A many-fold over unphosphorylated Spo0A (Asayama et al., 1995), the dynamics of that promoter might be a better reporter for the activity of Spo0A~P than the activity of P_{spo0A}. Consequently, the observed bursts in P_{spo0F} indicate that not only the expression, but also the activity of Spo0A exhibits bursts in single cells. Both P_{spo0F} and P_{spo0A} expression is activated at the level of the phosphorelay, while SpoIIE protein localization is triggered downstream and serves as a morphological hallmark of sporulation (Barak et al., 1996). Even at this later stage I observed reversible protein localization of SpoIIE in approximately 2 ± 1% (SEM) of cells (Figure 3.3C).

Specifically, SpoIIE-YFP fusion protein transiently localized to the asymmetric septum which nevertheless did not give rise to spore formation. In some of these cells, SpoIIE switched its localization between opposite poles, and in others it completely disappeared and cells continued with cell division (Figure 3.3C). It has been known that at the beginning of the septation process two septa start to form at the both poles, but soon afterwards one of them dissolves (Lewis et al., 1998; Wu et al., 1998). However, the stochastic reversibility of the asymmetric septation process altogether has not been described previously.

SpoIIE also plays a major role in turning on the compartmentalized σ^E and σ^F cascade, which results in SpoIIR expression in the forespore compartment (Arigoni et al., 1996). However, in contrast to other analyzed reporters described above, bursts of gene expression were not observed for P_{spoIIR} (Figure 3.3), with the spore always forming after the observed sharp signal increase. P_{spoIIR} signal also did not fade away after mother cell lysis and spore release. Taken together, I was able to observe variability and reversibility during the early stages of the progression to spore formation introduced by gene expression bursts, whereas the later stages (P_{spoIIR} expression stage) do not appear to be subject to such stochasticity.

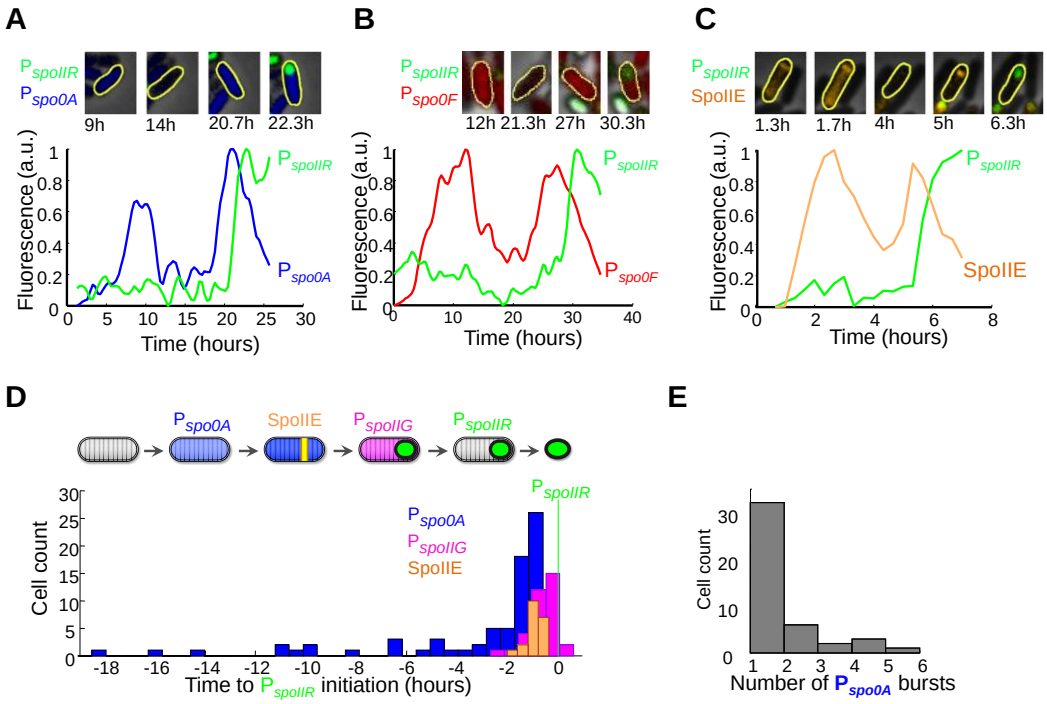

Figure 3.3 Panels (A) through (C): smoothed quantitative time traces of normalized fluorescence signals reporting sporulation component activities in single cells. On top of each panel, cell images are shown at sample time points. The measured cell is outlined. (A) 0A(5x)-IIR strain with P_{spo0A}-CFP (blue) and P_{spoIIR}-YFP (green). (B) 0F-IIR strain with P_{spo0F}-YFP (red) and P_{spoIIR}-CFP (green). (C) IIE-IIR strain showing localization of fusion protein SpoIIE-YFP (orange) and P_{spoIIR}-CFP (green). For SpoIIE-YFP, local fluorescence measurements near the cell poles are shown. (D) Histogram of time between initiation of P_{spo0A}, P_{spoIIG}, SpoIIE activities (40% of maximum activity) and initiation of P_{spoIIR} activity (60% of maximum activity) in sporulating cells. Time of P_{spoIIR} initiation was aligned at zero (green line). (E) The distribution of P_{spo0A} bursts (40% of maximum activity and higher P_{spo0A} peaks) observed per cell.

Commitment to sporulation in B. subtilis is switch-like and precise

As mentioned previously, P_{spoIIR} expression bursts were not observed during spore formation (Figure 3.3). SpoIIR expression in the forespore is controlled by σ^F, the same sigma factor which drives SpoIIQ expression (Karow et al., 1995; Londono-Vallejo et al., 1997). SpoIIQ in the forespore along with SpoIIP in the mother cell has been shown to be necessary for the irreversible commitment to sporulation (Dworkin and Losick, 2005). After this stage, even if the conditions are changed to favorable (e.g. with addition of nutrients), the differentiation process will be completed. At this step, consistent with the literature, we found that the irreversible commitment for spore formation is executed within a narrow time window. I quantified this timing by using the morphological appearance of an actual spore (a phase-bright spot in our single-cell movies) as a reference time point from which to measure commitment time (Figure 3.4A). Single-cell data analysis shows that the temporal distance between P_{spoIIR} activation in the future forespore compartment and the visible phase-bright forespore formation is fast compared to the typical cell cycle duration under our conditions and tightly distributed (CV= 0.2, and 15% of median cell cycle duration) (Figure 3.4A and B). Thus, P_{spoIIR} activation (which as mentioned above, denotes the sporulation commitment point) and the following sporulation completion are precise and deterministic compared to the earlier stages of progression to spore formation. Therefore, single cell measurements of sporulation dynamics exposed a cell intrinsic decision point in time, the temporal precision of which was previously concealed in population measurements (see Figure 3.1) by the cell-to-cell variability in the reversible progression to spore formation.

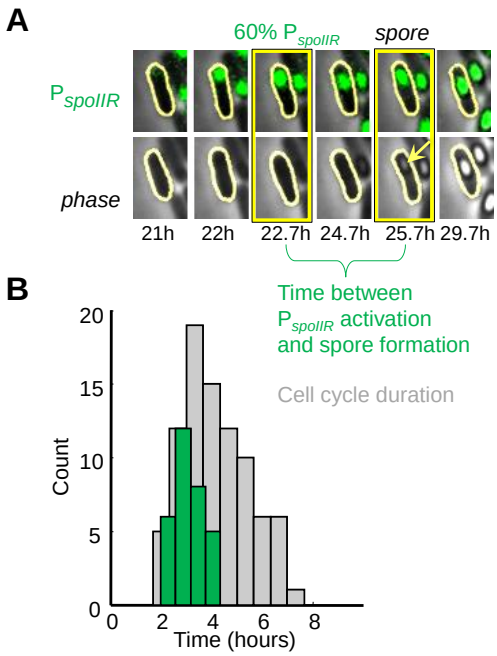

Figure 3.4 Precise timing of P_{spoIIR} activation prior to spore formation. (A) Filmstrips showing fluorescence (top) and phase (bottom) images of a sample sporulating cell (highlighted; strain 0A-IIR) activating P_{spoIIR} expression in the forespore (green). Phase bright spore appearance is indicated by an arrow. (B) Histogram presenting, in green, the distribution of time between P_{spoIIR} activation and phase bright spore formation (n=31, sample events highlighted by yellow boxes in the filmstrips in panel (A)), compared to sample cell cycle durations, in light grey, measured in the same cells under movie-making conditions. P_{spoIIR} activation is measured as >60% of maximum P_{spoIIR} fluorescence at sporulation.

Gradual progression towards irreversible decision point maximizes adaptable and reliable decision-making

The data suggests that following the reversible and gradual progression through many initial steps, *B. subtilis* cells finally commit to sporulation in a switch-like all-or-none fashion. Therefore, sporulation seems to combine two seemingly opposed dynamic mechanisms: reversible and irreversible. In order to examine the potential advantages of this hybrid mechanism, I sought the help of Jordi Garcia-Ojalvo and Lorena Espinar, graduate student in his laboratory. We constructed three simplified mathematical models of cellular decision-making, schematically shown in Figure 3.5, each representing a distinct decision-making strategy: either purely reversible, purely irreversible or 'hybrid', the latter suggested by the data. These models describe the dynamics of a population of cells progressing toward sporulation under stress, in terms of the number of cells existing at any given time in a given state along the progression, from initial vegetative state to the final spore state. The dynamics of cell populations in all these states is given by a set of coupled ordinary differential equations that are linear, and thus can be solved exactly (Appendix A). In the irreversible-only scheme, cells decide whether or not to sporulate in a single irreversible step. The reversible-only model takes cells gradually toward sporulation through multiple reversible intermediate states, without any irreversible commitment step taking place along the process. Only the ultimate transition to the spore state, taking place *after* the decision, is irreversible. Finally, the third "hybrid" model features the actual sporulation dynamics identified for *B. subtilis* that combines a gradual progression through reversible intermediate states with an irreversible all-or-none decision prior to the spore transition.

For all described models, we coupled the rates of progression toward/back from sporulation, growth and death rates to the level of environmental stress (see Appendix A). Next, we introduced a random variation of the environment, with alternation of a high and a low level of stress (insets in Figure 3.6A and Appendix A). Specifically, we systematically varied the ratio of high stress to the constant total cycle duration. To compare the relative fitness of the three described models under the introduced stress profiles, we measured the ratio of total cells in the population produced by the hybrid model to the total cells produced by the irreversible-only and reversible-only models (Figure 3.6A, blue and red lines respectively).

Results of this analysis show that the survival rate of the different models depends on the stress profile and none of the models dominates over the entire range of environmental stress conditions. However, overall the hybrid model performs best. For short phases of high stress, it outgrows the irreversible-only model (left half of main plot in Figure 3.6A, blue line), since the latter is driven irreversibly to sporulation even for short stress periods. Under these conditions, the hybrid and reversible-only models perform similarly (red line) since in both models reversible progression delays sporulation. However, in the opposite limit where high stress durations approach the total duration (right half of main plot in Figure 3.6A), the irreversible-only model outgrows the hybrid model, since responsiveness is a disadvantage. Since non-spore cells have a higher death than growth rate under stress, for such prolonged high stress durations, spores are at an advantage. In this limit, the hybrid model is in turn more reliable than the reversible-only model, since the reversible-only model is driven away from sporulation even by short intervals of rich phase. Parameter sensitivity analysis showed that these

results hold over a range of parameter values (Figure 3.6A, light blue and light red regions). Taken together, the results presented in Figure 3.6A show that the hybrid model outperforms both the irreversible-only and reversible-only schemes over a broader range of randomly alternating stress profiles, given its flexibility to both respond to the long-term recovery from stress and allow reliable decision-making during short-term release of stress conditions.

Next, we put all three models to the direct test of relative fitness by subjecting them to random changes in the fraction of time spent in high stress. In these extended simulations cells were exposed to 100 random samplings of environmental stress ratios (part of an environmental profile is shown in the inset in Figure 3.6B). We then calculated the relative fitness of each model as the ratio of the total cell population of the hybrid model to that of the irreversible-only and reversible-only models averaged over the entire simulation (Figure 3.6B). Our data demonstrate that the hybrid model has an overall higher fitness over both the irreversible-only and reversible-only models when populations are subjected to a randomly changing range of environmental conditions. Therefore, the combination of gradual progression toward an all-or-none decision in *B. subtilis*, as represented in the hybrid model and observed experimentally, enables the system to cope with a broader range of unpredictable stress conditions.

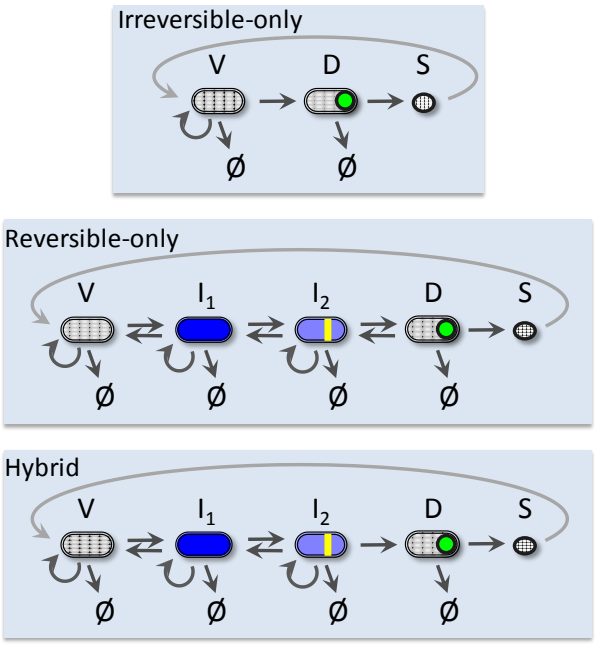

Figure 3.5 Schematic representation of the three models.

Irreversible-only, top panel: Decision to sporulate is made by cells in a single step. The model comprises three cellular states: vegetative (V), decided (D) and spores (S).

Reversible-only, middle panel: In this model vegetative cells (V) proceed toward sporulation through two intermediate states I1 and I2. All transitions, including the transition to the decided state (D), are reversible.

Hybrid, lower panel: This model combines characteristics from the two mechanisms described above. In this scenario, cells initially progress toward sporulation through intermediate states I1 and I2 with reversible transitions, with the irreversible final transition to the decided state (D). For all models the transition rates between sporulation stages, as well as growth and death (Ø) rates, are coupled to the stress level. For details, see Appendix A.

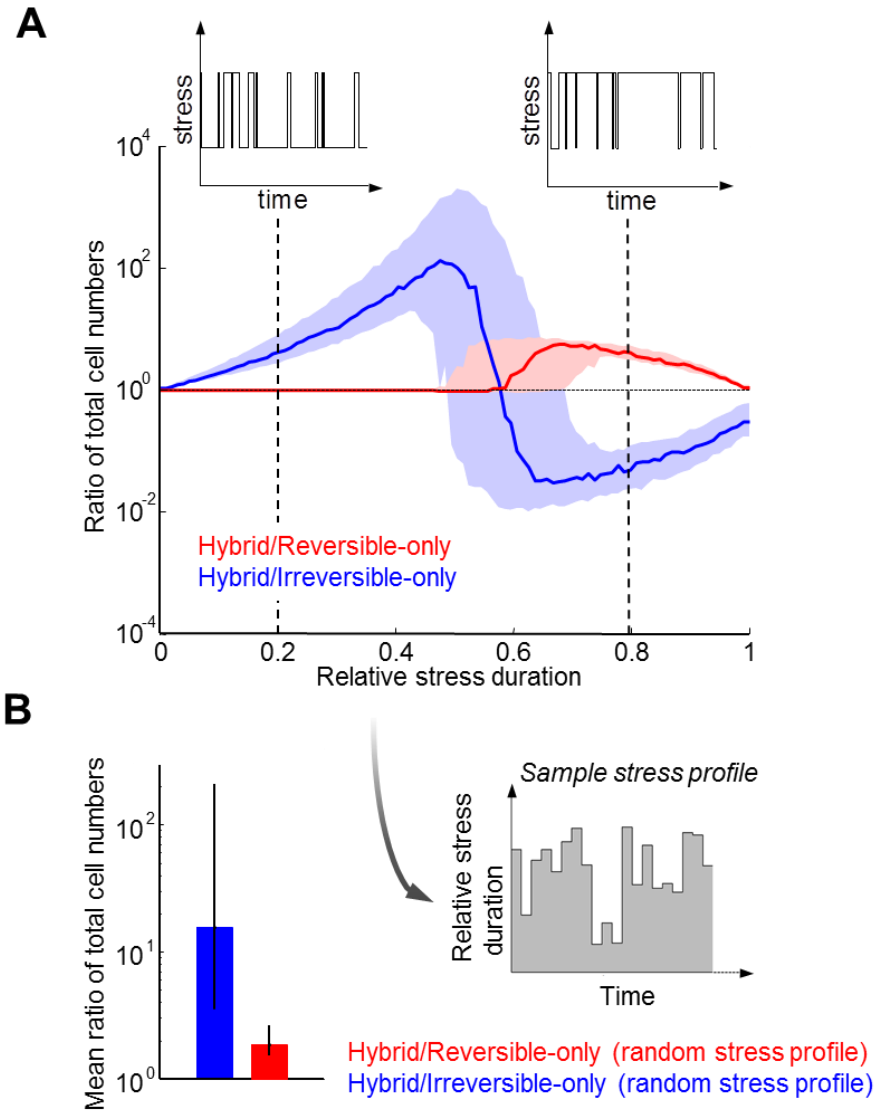

Figure 3.6 Mathematical comparison of distinct cell-fate choice dynamics under alternating environmental conditions. (A) Relative fitness of the hybrid model with respect to the irreversible-only and reversible-only models described in Figure 3.5. The blue and red lines correspond to the ratio of the total cell populations (summed over all cell states) of the hybrid model and the irreversible-only and reversible-only models, respectively. A random dichotomic variation of the environment is applied to all models, with the relative average duration of high versus low stress phases increasing in the x axis. The two insets depict sample profiles of stress for relative average durations of high stress phase equal to 0.2 and 0.8. The shaded areas in light blue and light red represent the maximum variation resulting from simultaneous random changes in all non-zero

parameters of up to 20% around their baseline values given in Table A2, Appendix A. (B) Average fitness of the hybrid model with respect to the irreversible-only and reversible-only models obtained from a random sampling of environmental conditions. The inset shows short sample series of the average stress levels used to study the response of the three models to random stress conditions. Relative stress durations where chosen from a uniform random distribution in the range [0, 1]. The blue and red bars represent the ratio of the total cell population of the hybrid model to that of irreversible-only and reversible-only, respectively, averaged over 100 values of the relative average duration of high versus low stress scanned in (A). For each stress level, the models were integrated over 30 hours, in the same conditions as in (A). The error bars represent the maximum variation resulting from parameter changes up to 20% their baseline values, as in (A).

Discussion

The dynamics of activation of various sporulation-specific promoters marking different stages of spore formation have been measured extensively in well shaken liquid cultures. Such conditions are convenient for the laboratory research because they permit free diffusion of nutrients and allow for fast and more synchronized bacterial growth. However, the properties of *B. subtilis* growth and differentiation in such cultures may markedly differ from their natural counterparts, since this bacterium's natural habitat is soil in which the cells are not motile and exist in a specific microenvironment. Such conditions are better imitated by the bacteria growing on an agarose pad and forming microcolonies. In contrast to the faster growth and differentiation in bulk liquid cultures, *B. subtilis* cells on an agarose pad containing the same sporulation medium grow slower and thus are allowed to explore much more possibilities in terms of choosing cell fates. Although the ultimate final outcome for all cells under relentless stress conditions is still either sporulation or death, the cells form spores much less synchronously in time and exhibit high heterogeneity in sporulation regulators activities. Therefore, population

measurements in such conditions are unable to provide precise information about the dynamics of sporulation.

In contrast, time-lapse microscopy utilized as my main experimental method to study cell-fate decision making in *B. subtilis* growing on agarose pads, allows me to quantitatively measure the timing of sporulation components activation in single cells. Using spectrally distinct fluorescence proteins reporting the activities of several sporulation specific promoters, I discovered the single-cell reversibility in the earliest sporulation steps in the form of 'non-productive' gene expression bursts, sometimes even exceeding in absolute amplitude the final activation peak that did result in spore formation. This observation indicates that there might be no strictly set "absolute threshold" to the expression of Spo0A~P above which the cells automatically commit to sporulation, as prior suggested (Chung et al., 1994; Eswaramoorthy et al., 2010). Rather, the accumulation of Spo0A~P increases the overall probability of sporulation (measured in Chapter 4), while individual cell fate outcomes still remain to a large degree subject to high variability and noise.

Importantly, no change in extracellular conditions was required to observe this reversibility at the initial stages of sporulation. These gene expression bursts therefore represent a random cell autonomous behavior that is distinct from what has been reported in previous studies that showed the reversibility of sporulation process upon stress relief by adding back nutrients (Dworkin and Losick, 2005). Such cell autonomous random sampling of various expression states in single cells has also been observed in other systems where it may provide a fitness advantage, such as the generation of antibiotic resistant *Escherichia coli* persister cells (Balaban et al., 2004) and the survival of

Saccharomyces cerevisiae to cellular stress (Blake et al., 2006). The single-cell approach utilized here also allowed me to discover the switch-like dynamics of the later commitment point. The temporal precision of this decision point coinciding with the P_{spoIIR} expression in the forespore would have been concealed in population measurements that describe average behaviors of cells. Similarly, a recent study of the post-infection decision in bacteriophage lambda to undergo lysis or lysogeny showed how cell-cell variability obscured the precision of cell fate choice (Zeng et al., 2010). Therefore, the temporal precision of numerous cellular processes can be masked by stochastic fluctuations and noise in the single cells. Measuring multiple components of genetic circuits simultaneously in the same cell allows bypassing this problem by identifying cell intrinsic reference points that can establish the accurate relative timing of cellular processes.

The identified reversibility of the initial stages of the sporulation process exaggerates the variability in time required for cells to reach spore formation. The resulting broad distribution of wait times prior to differentiation extends the window during which *B. subtilis* cells can be responsive to changes in the extracellular milieu. Since sporulation is considered the "last resort" for the cells both because of the energetic cost associated with making a spore and the cessation of cell division, creating a prolonged period during which the cells could sense the positive change in the environment and respond to it can be biologically beneficial. My findings thus follow in the line of previous studies highlighting the advantageous role of stochasticity in enhancing survival in uncertain environments (Blake et al., 2006; Cagatay et al., 2009; Kussell and Leibler, 2005; Thattai and van Oudenaarden, 2004; Wolf et al., 2005a, b).

The final decision to differentiate into a spore seems to require much more than simply crossing the threshold for Spo0A~P accumulation. What are the additional requirements to proceed with stage II of sporulation is not clear. However, I established that this decision, in contrast to the initial noisy sporulation steps, exhibits markedly distinct properties. The irreversible and switch-like dynamics of the actual decision point appears to contribute to the reliable execution of the sporulation program. Traditionally, the point of cell-fate commitment has been defined as the point of no return for differentiation even if the conditions change in favor of a different fate (i.e. receiving a conflicting signal or coming across nutrients after starvation). However, my findings re-define the commitment point without the need for the change in environmental cues. As per an alternative definition, the point of commitment could also indicate that the system loses the capability to stochastically reverse the differentiation program and instead starts to follow a strict deterministic path towards the chosen fate. In other words, this point would indicate the switch between different dynamical regimes rather than the loss of responsiveness towards environmental cues.

This new definition also reflects the observation that *B. subtilis* differentiation process seems to combine the two opposite dynamic behaviors: a reversible and gradual progression towards an irreversible and all-or-none switch. Mathematical modeling suggests that this combination of gradual and all-or-none dynamics could reconcile the seemingly contradictory requirements of adaptability and reliability during cellular decision-making. Such strategy would therefore allow *B. subtilis* to successfully survive under a broad range of alternating environmental stress conditions. A similar strategy has been suggested for other systems as well. For example, in mammalian cells undergoing

apoptosis the process has been described as slow progression towards a fast decision (Choi et al., 2007). Furthermore, during cell cycle mammalian cells are often reversibly arrested in G phase until deciding to irreversibly commit to division (Pfeuty, 2012). Therefore, this strategy of combining opposing dynamic behaviors may be common to various other biological processes, and may represent a general mechanism for decision-making in unpredictably changing environments. Models for decision-making under uncertain conditions have been developed and applied to numerous unrelated complex systems, such as finance (Black and Myron, 1973). Perhaps a stochastically reversible progression to an irreversible all-or-none switch as observed here in cells, may also serve as a strategy for adaptable and reliable decision-making in other complex systems that are subject to unpredictable conditions.

CHAPTER FOUR

COMPETENCE INITIATION IS INDEPENDENT OF SPORULATION PROGRESSION

Introduction

A critical determinant of cell fate choice is the activity of key molecules, often referred to as master regulators, that are expected to be the target of cross-regulation between mutually exclusive alternative cell fates (Fujita and Losick, 2005; Grossman, 1995; Kalmar et al., 2009; van Sinderen et al., 1995). In *Bacillus subtilis*, such master regulators have been identified and well characterized for the competing processes of sporulation and competence (Fujita and Losick, 2005; van Sinderen et al., 1995). The master regulator of sporulation is the phosphorylated transcription factor Spo0A, while competence is controlled by the master transcription factor ComK. Recent single cell measurements revealed cell-to-cell variability in ComK and Spo0A expression that generated heterogeneity at the population level (Chastanet et al., 2010; de Jong et al., 2010; Suel et al., 2006). Despite these recent advances, it is not well understood how the activities of ComK and Spo0A govern cellular decision-making as a function of time in individual cells. It is generally assumed that competence initiation is only possible during the so-called "competence window" that is opened by low levels of Spo0A~P and closed by higher levels of Spo0A~P that lead to the sporulation cell fate (Mirouze et al., 2012). However, I have established that Spo0A activity is reversible and sometimes even high levels of *Spo0A* expression do not result in spore formation (Chapter 3). Therefore, high concentration of Spo0A~P in the cells does not necessarily indicate that cells have chosen sporulation as the only cell fate outcome. Perhaps competence is still possible during these unproductive peaks of sporulation components activation. Simultaneous

measurements of sporulation and competence master regulators in the same cell during cell-fate decision making can shed light on the relationship between alternative cell fates during cell fate choice.

Results

Average P_{spo0A} activity is increasing during sporulation

Since sporulation is a gradual process, I needed to establish a suitable reporter in order to reliably track early sporulation activity. The master regulator of entry into sporulation is the phosphorylated form of Spo0A, which has a high affinity for its own promoter and positively regulates its own expression (Asayama and Kobayashi, 1993; Molle et al., 2003; Strauch et al., 1992). I utilized the promoter for Spo0A (P_{spo0A}) fused to YFP to visualize the progression towards spore formation in single cells using fluorescence time-lapse microscopy of microcolonies differentiating on agarose pads made with stress medium as described before (see Chapters 2 and 3). In the previous chapter, I found that the final commitment to sporulation coincides with the expression of the SpoIIR promoter (P_{spoIIR}) which always occurs in the forespore (Dworkin and Losick, 2005; Karow et al., 1995). Therefore, to establish a reference point for spore formation I also simultaneously measured P_{spoIIR} expression in the same cells by fusing the SpoIIR promoter to CFP. The measurements showed that in individual cells P_{spo0A} expression was highly bursty and heterogeneous as expected (see Chapter 3). However, when the individual traces are aligned in time with respect to P_{spoIIR} activation as the reference point for spore formation and averaged, the average trace of P_{spo0A} expression steadily increased and reached its maximum near forespore formation (Figure 4.1). Therefore, average P_{spo0A} expression could potentially serve as a marker for sporulation progression.

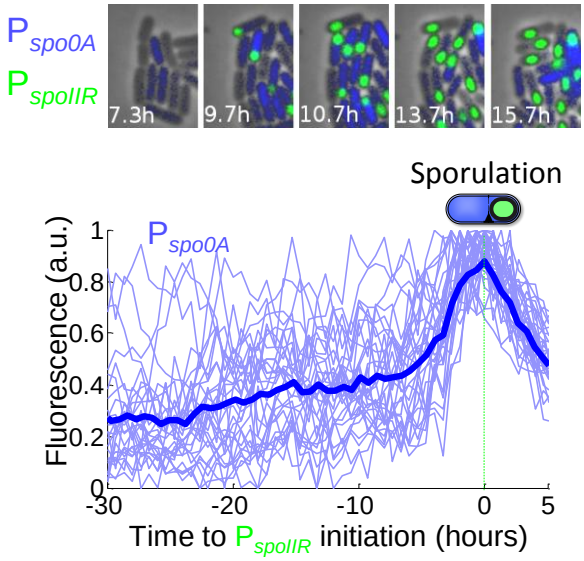

Figure 4.1 Average fluorescence time trace (bright blue) of sporulating cells from 0A-IIR strain with P_{spo0A}-YFP (blue) and P_{spoIIR}-CFP (green). Individual traces (n=32) shown in light blue are normalized in amplitude and aligned in time with respect to P_{spoIIR} initiation (60% of peak activity) prior to averaging. A representative filmstrip of sporulating microcolony of 0A-IIR strain is shown above. For strain definitions see Chapter 2, General Experimental Procedures. The drop of fluorescence signal after the maximum is due to lysis of the mother cell during the spore formation process**.**

In order to further test the suitability of average P_{spo0A} expression to report sporulation progress, I measured the conditional probability of sporulation for each level of P_{spo0A} expression. The probability of making a morphologically visible phase-bright spore (referred to as probability of sporulation) in a cell expressing a specific level of P_{spo0A} activity (denoted as x) can be calculated from the Bayes' theorem:

$$P(\text{sporulation}|P_{spo0A} = x) = P(P_{spo0A}=x|\text{sporulation})P(\text{sporulation})/P(P_{spo0A} = x);$$

where:

P(sporulation|P_{spo0A} = x) is the probability of sporulation given that the cell has a specific level of P_{spo0A} activity (denoted as x),

P(P_{spo0A}=x| sporulation) is the probability of observing a specific value of P_{spo0A}=x during sporulation,

P(sporulation) is the probability of sporulation which can be expressed as the ratio of spores number to the number of total observed cells,

P(P_{spo0A} = x) is the probability of the cell to express a specific value of P_{spo0A}=x.

The way to experimentally evaluate the trend in sporulation probability as a function of P_{spo0A} activity would be therefore to obtain P_{spo0A} values at sporulation for all forespore-forming cells observed in a frame of a time-lapse movie, and then normalize the obtained distribution with the distribution of P_{spo0A} from all cells in the given frame. Figure 4.2A shows a sample frame of the time-lapse fluorescence microscopy movie used for calculation of sporulation probability. The frames were selected to contain a sufficient number of sporulating cells for the analysis, but not yet to be overgrown so that most of the cells would still lie in one plane of focus in a single layer and be available for measurement. The cells were considered sporulating if they expressed a threshold level of P_{spoIIR} fluorescence (at least one standard deviation outside of the mean) (Figure 4.2B, blue window marked by dashed lines). This threshold selection is also taking into account the level of P_{spoIIR} fluorescence associated with the empirical visual observation of phase-

bright spores. After obtaining the distribution of P_{spo0A} expression values in sporulating cells (as defined above) and the corresponding distribution of P_{spo0A} amplitudes in all cells (Figure 4.2C-D), I was able to calculate the conditional probability of spore formation (Figure 4.2E). As expected, it gradually increased with the increased P_{spo0A} activity. Therefore, P_{spo0A} expression provides a measure for the gradual progression to spore formation.

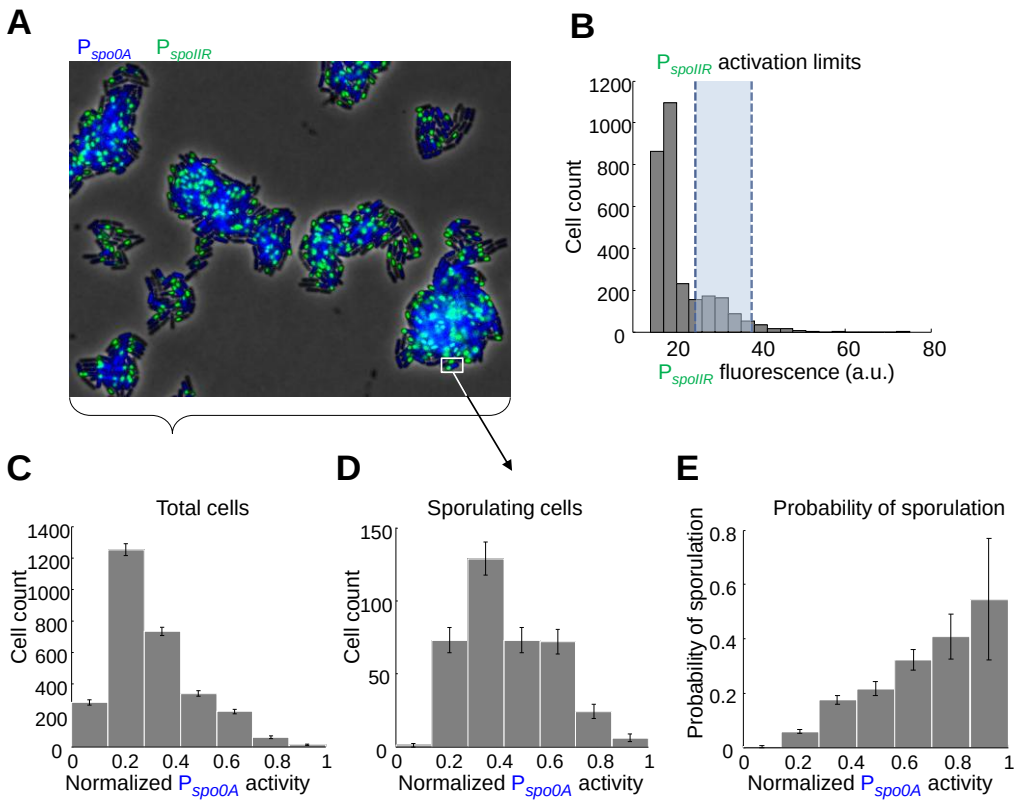

Figure 4.2 (A) A frame from the time-lapse movie of 0A-IIR strain with P_{spo0A}-YFP in blue and P_{spoIIR}-CFP in green illustrating how the total and sporulating cell distributions shown in panels (C) and (D), respectively, were obtained. P_{spo0A} and P_{spoIIR} activity was measured in all cells (n=2900), resulting in the total cell distribution shown in panel (C). P_{spo0A} activities were normalized to the maximum and minimum cell expression level recorded in a given frame, based on an assumption that each analyzed frame contained at least one vegetative cell expressing the baseline P_{spo0A} activity and one cell at the peak of sporulation. P_{spo0A} activities of all cells within the activation limits of P_{spoIIR} fluorescence shown in panel (B) were recorded separately, giving rise to the sporulating cells distribution shown in panel (D). (E) Conditional probability of sporulation is then calculated as the number of sporulating cells observed at specified values of P_{spo0A} expression (number of cells in each bin of sporulating cells distribution) normalized by the number of total cells with the specified P_{spo0A} amplitude (number of cells in the corresponding bin of total cells distribution). Error bars represent counting error.

Initiation of competence is independent from the progression to spore formation

Establishing P_{spo0A} as a reporter for the sporulation progress now allows asking how the probability of the alternate fate of competence is changing as the cells approach spore formation. As a reporter for competence I utilized the expression of promoter for ComG (P_{comG}), one of the operons that contain genes that are crucial for competence development (Chung and Dubnau, 1998). P_{comG} is a well-established competence reporter as it is exclusively regulated transcriptionally by ComK, the master regulator for competence (van Sinderen et al., 1995), with no other direct inputs. Furthermore, the expression of P_{comG} showed perfect correlation with P_{comK} measured in the same cell (Suel et al., 2006). Therefore, by simultaneously measuring P_{spo0A} and P_{comG} expression I was able to track the sporulation and competence master regulators together in the same cell.

Since competence is a transient state, I specifically analyzed the cells that became competent, then exited this state resuming vegetative growth and division, and finally sporulated. The sporulating daughter cell of the initial competent cell to be tracked was chosen arbitrarily, based on the analysis feasibility. Tracking the progeny cells of the formerly competent cell until they sporulated allowed me to establish the peak P_{spo0A} expression at sporulation for this cell line, assuming it to be characteristic for the analyzed lineage. This was necessary to establish a reference point for evaluation of the relative P_{spo0A} value at competence initiation since direct measurement of sporulation peak in this cell is impossible due to the censorship of sporulation fate by competence. A sample resulting trace is shown in Figure 4.3A with the explanation of how the amplitude of P_{spo0A} expression at the initiation of competence was measured. The resulting data from 67 competent cells is plotted in Figure 4.3B. Note that competence was initiated over a

wide range of P_{spo0A} expression amplitudes and at variable times prior to spore formation (Figure 4.3B). These results are consistent with previous studies that indicate a stochastic initiation mechanism for competence (Maamar et al., 2007; Suel et al., 2007).

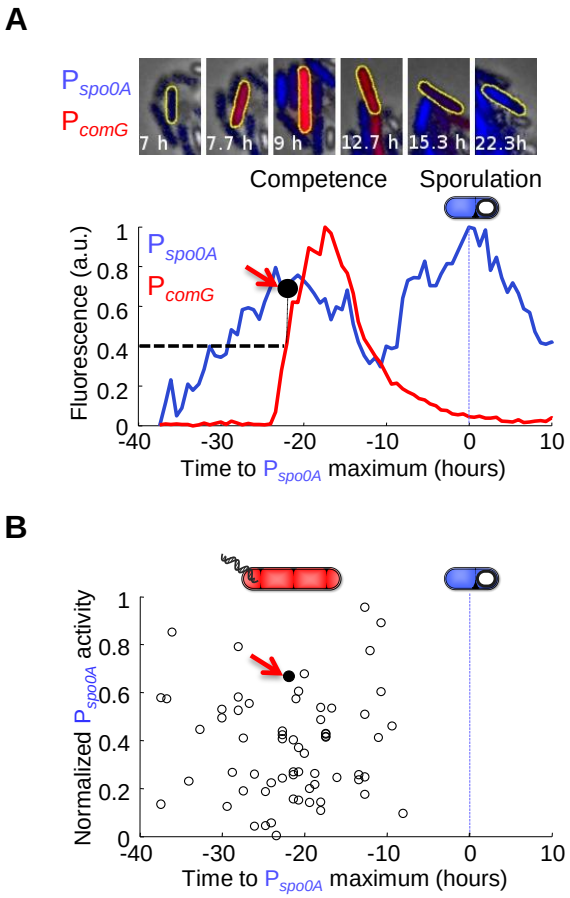

Figure 4.3 (A) Sample quantitative traces illustrating how the activity of sporulation was determined at the initiation of competence. Specifically, the panel shows a single cell (0A-comG strain) undergoing a competence event followed by sporulation. Competence reporter P_{comG} activity is measured by CFP fluorescence intensity (shown in red) and P_{spo0A} activity is measured by YFP fluorescence intensity (in blue). The competence and sporulation events are highlighted by the cartoon and the filmstrip on top. The traces are aligned in time with respect to maximum P_{spo0A} activity at sporulation (set as zero time point). This data is utilized to determine P_{spo0A} activity (black circle highlighted by red arrow) at initiation of competence (defined by >30% P_{comG} activity relative to maximum P_{comG} amplitude at competence). For comparison, both time traces are normalized with respect to amplitude. (B) P_{spo0A} activity (black circles) at initiation of competence measured in single cells, n=67, from 0A-comG strain, as shown in panel (B). The filled circle highlighted by red arrow corresponds to the measurement shown in panel (A). The traces are aligned with respect to maximum P_{spo0A} activity at sporulation as described in panel (A).

Based on this data, I calculated the conditional probability of competence as function of progression to sporulation. The essence of the calculation method is virtually the same as described above for sporulation probability. The straightforward way to experimentally measure competence probability as a function of P_{spo0A} activity would be, in analogy to the calculation above, to obtain P_{spo0A} values at ComK initiation for each competent cell observed in a time-lapse movie, and then normalize the obtained distribution with the distribution of P_{spo0A} from total imaged cells. However, technically it is not feasible to trace all competent cells in a time-lapse movie. To bypass this problem, I analyzed n=48 competent cells from different movies, chosen arbitrarily for the feasibility of tracking over the entire duration of competence and subsequent sporulation. After obtaining this data, I normalized P_{comG} fluorescence traces relative to their respective peak amplitudes at competence and selected a frame for each cell at which its P_{comG} expression crossed over 30% threshold (Figure 4.4A). The P_{spo0A} activities of competent cells at this time point were used to obtain the competence distribution (Figure 4.4B).

Due to presence of other competent cells, I sought the help of Mark Kittisopikul, a graduate student in Gurol Suel lab. We implemented an automatic MATLAB procedure that placed a rectangular ROI around the cell of interest containing the area that corresponded to total frame area divided by number of competent cells in this frame (Figure 4.4A). Assuming the cell density in the frame to be more or less even, the cells inside the ROI would represent the microcolony that would give rise to exactly one competence event. I then calculated the P_{spo0A} levels for every cell inside the ROI and normalized them assuming that each ROI contains at least one sporulating cell (P_{spo0A} =1)

and one vegetative cell or mature spore (P_{spo0A} =0). The resulting data from ROIs for all measured competent cells is shown in Figure 4.4B. To obtain the probability of competence as a function of P_{spo0A} activity, I normalized the number of cells in each bin from competence distribution (Figure 4.4B) by the number of cells in each bin from total cell distribution (Figure 4.4C). The resulting conditional competence probability plot is shown in Figure 4.4D. Surprisingly, the probability of competence initiation remains nearly constant during the progression to spore formation as defined by P_{spo0A} expression (Figure 4.4D). This result indicates that there might be no active cross-regulation between progression to sporulation and initiation of competence.

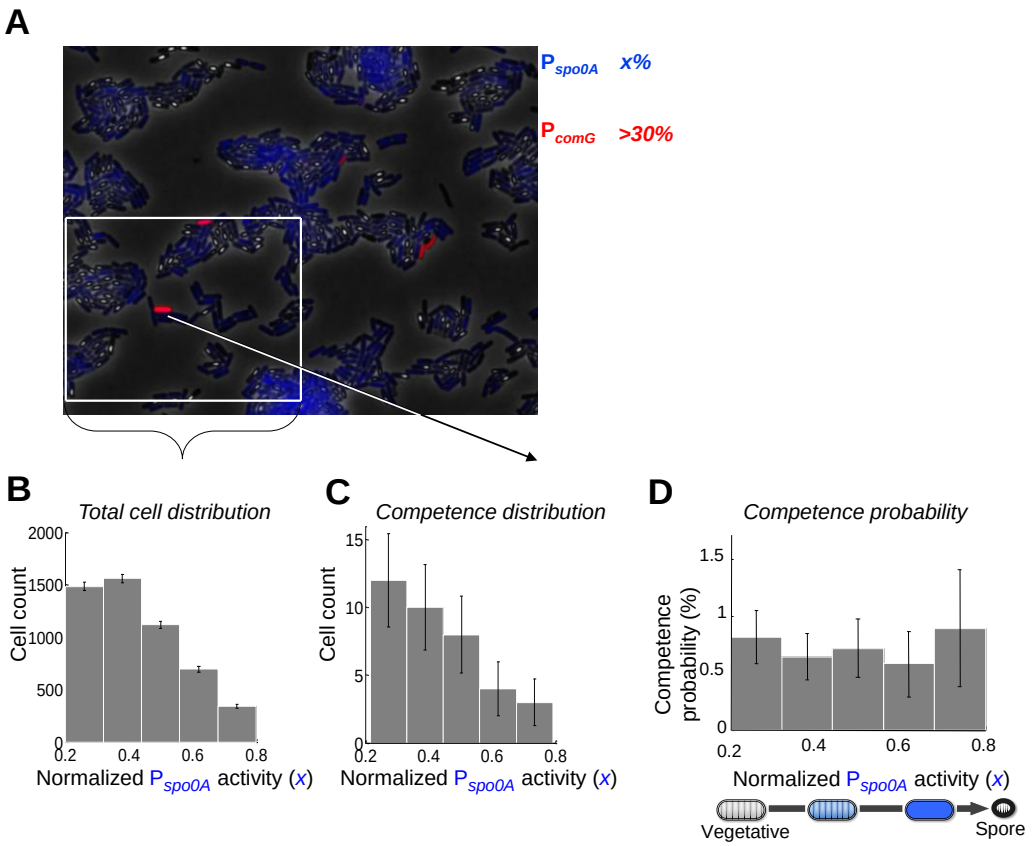

Figure 4.4 (A) A frame corresponding to >30% P_{comG} activity of a cell from the time-lapse movie of 0A-comG strain showing how competence and total cell distributions in panels (B) and (C), respectively, were obtained. P_{comG} (red) and P_{spo0A} (blue) activities were measured as described in Figure 4.3. A competent cell of interest was framed in a rectangular ROI, and the P_{spo0A} activities of all cells inside the ROI were measured. n=54 competent cells were measured in this way, giving rise to competence distribution shown in panel (C), while the P_{spo0A} activities of all cells inside each corresponding ROI were summed for total cell distribution shown in Panel (B). Only data for P_{spo0A} activities between 20% and 80% are shown, because data below 20% is within error and cells above 80% are too close to spore formation (see Figure 4.1). (D) Conditional competence probability distribution, calculated as described in Figure 4.2E. Briefly, the distribution of P_{spo0A} activities for competent cells shown in panel (C) was normalized by the distribution of P_{spo0A} activities for total sporulating cells shown in panel (B). Error bars represent counting error.

Additionally, I measured the conditional probabilities of sporulation and competence as function of the activity of the Spo0F promoter (P_{spo0F}), which is governed by phosphorylated Spo0A (Asayama et al., 1995; Lewandoski et al., 1986). Since P_{spo0A} promoter has more inputs, P_{spo0F}-YFP fluorescence might be a better, more specific reporter for Spo0A~P. By measuring P_{spo0F}-YFP and P_{spo0A}-CFP fluorescence in the same sporulating cells, I found that the activities of these promoters exhibit strong positive correlation (Figure 4.5A, r=0.83). Using the same procedures as described above for the P_{spo0A} reporter, I was able to obtain the sporulation, competence and total distributions of P_{spo0F} values (Figure 4.5B-E). The final resulting trends in probabilities of sporulation and competence as function of either P_{spo0A} or P_{spo0F} activities are shown in Figure 4.6, panels A and B respectively.

In summary, I observed an identical increase in the probability of spore formation as a function of P_{spo0F}, while the probability of competence initiation was also found to be independent of P_{spo0F} expression (Figure 4.6B). This data strengthens the conclusion that sporulation might not exert active cross-regulation to inhibit competence initiation, in other words, the initial temporal progression of these differentiation programs is independent of each other's activities.

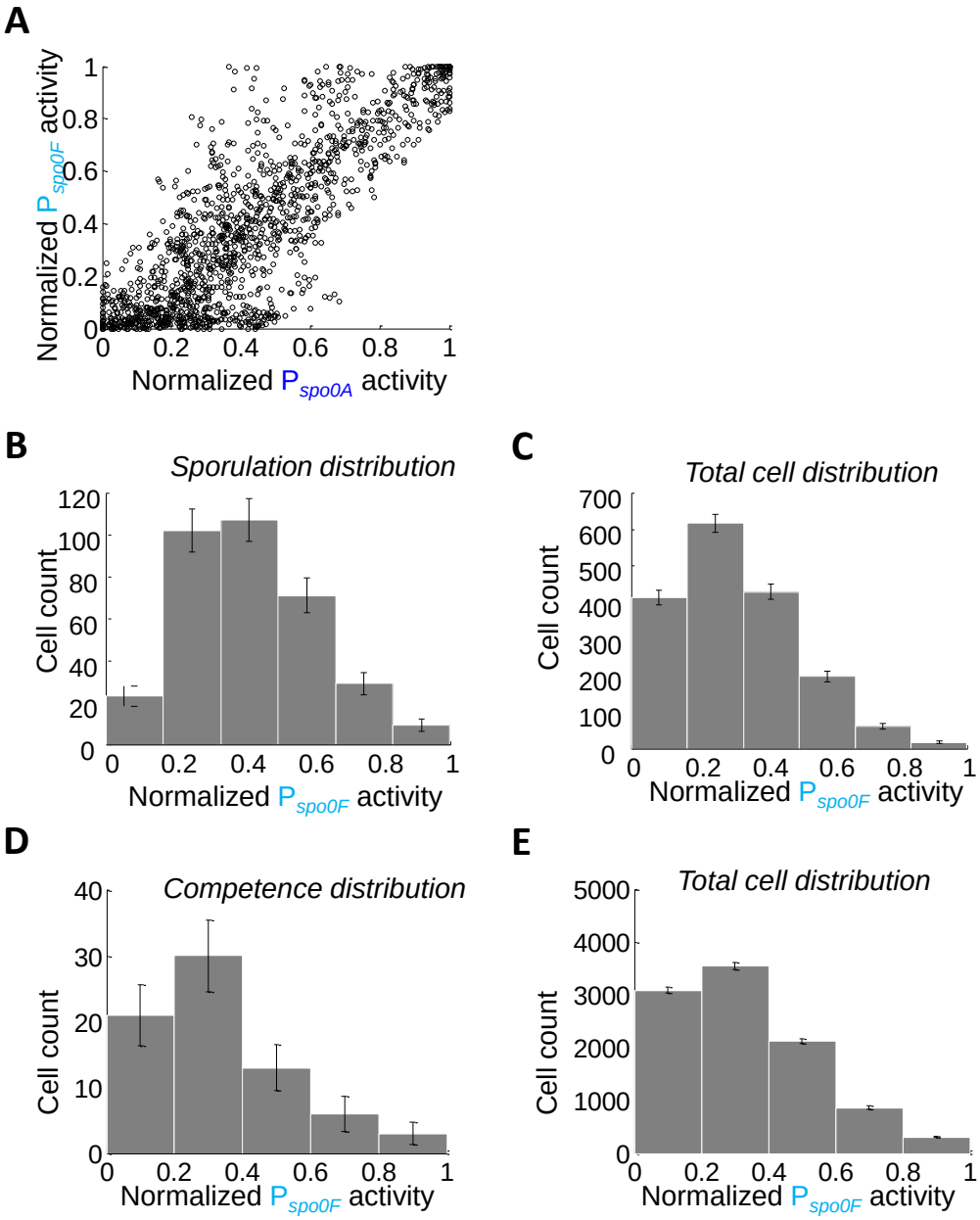

Figure 4.5 (A) Positive correlation between P_{spo0A} and P_{spo0F} expression measured in the same cell (r=0.83). Each dot represents the fluorescence values from one frame of quantitative time traces of sporulating cells simultaneously expressing P_{spo0A}-CFP and P_{spo0F}-YFP, n=20, from strain 0F-0A. Panels (B) and (C) show the sporulation (panel B) and total cell (panel C) distributions of P_{spo0F} activity calculated in the same manner as

described for P_{spo0A} activity in Figure 4.2. Panels (D) and (E) show the show the distributions of P_{spo0F} activities either measured at competence initiation (panel D), or for all cells inside the ROI (panel E), similar to Figure 4.4. For P_{comG}, the activation threshold of 35% was used. Error bars represent counting error.

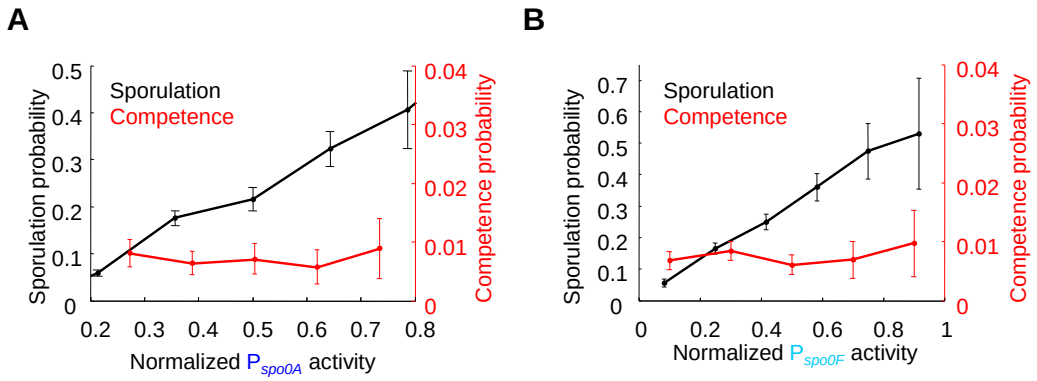

Figure 4.6 Panels (A) and (B) show the conditional probabilities of sporulation and competence as functions of P_{spo0A} and P_{spo0F} activity, respectively. The probability of sporulation was obtained by measuring fluorescence from single cells of a sporulating microcolony of strains 0A-IIR, n=2900 (panel A) and 0F-IIR, n=1836 (panel B) as shown in Figures 4.2 and 4.5, respectively. To obtain the probability of sporulation, the distributions of either P_{spo0A} values (panel A) or P_{spo0F} values (panel B) in cells that have formed a forespore (measured by P_{spoIIR} activation), was normalized by the distributions of corresponding values in total observed cells. Error bars represent counting error. The corresponding conditional probability of competence as function of either P_{spo0A} (panel A) or P_{spo0F} (panel B) expression measured in Figures 4.4 and 4.5, respectively, is plotted with the second y axis (red).

In addition, I took advantage of time-lapse microscopy data to analyze the behavior of sister cells that just before the last cell division shared the same cytoplasm and starting P_{spo0A} expression level. Regardless of the common intracellular concentrations of regulators inherited from the mother cell, I found that sister cells appeared to be able to diverge and commit to alternative cell fates with no more additional divisions after the last common ancestor, even though both of them initially had high level of P_{spo0A} expression (Figure 4.7). Together, these results show that competence can be initiated independently from the progression state of sporulation. This argues against active cross-regulation that can predispose cell fate choice prior to the actual decision point.

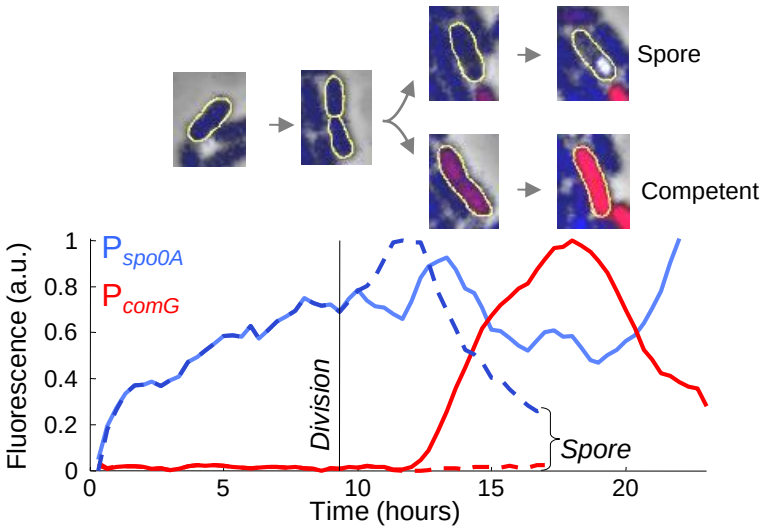

Figure 4.7 Sample quantitative traces of sister cells, one of which is sporulating (dashed traces) while the second becomes competent (solid traces). The division after which the cells split from the common ancestor is indicated as a vertical line. P_{spo0A}-CFP fluorescence is shown in blue and P_{comG}-mCherry fluorescence is in red. Microscopy images with the measured cell outlined are shown on top at corresponding time points for illustration.

Discussion

The results suggest that the probability of initiating ComK expression is independent from the state of the sporulation program at least at the early stages. Since ComK expression above certain threshold is both necessary and sufficient for triggering the differentiation into competence state (Hahn et al., 1996), the results should mean that the initiation of competence is also independent from Spo0A level during early spore formation. The discovered phenomenon of independence between competence initiation probability and the progression state of sporulation program argues against the active suppression of competence genetic circuit by the sporulation-activated cross-regulatory mechanisms. This finding is somewhat alarming since the mutual inhibition through action of multiple cross-regulatory links has been long assumed for sporulation and competence fates (see Chapter 1, Figure 1.1). However, my previous results indicate that progression to sporulation on the single cell level is noisy, resulting in sometimes quite large bursts of sporulation components activity that do not lead to sporulation. It is not surprising then that competence program activation does not depend on the activities of these promoters alone. Otherwise, the critical cell fate decision would be relying on extremely noisy and variable inputs. Therefore, absence of regulatory feedback from early components of the sporulation program to competence might serve to decrease the level of noise in the decision-making between sporulation and competence.

The reasoning behind the belief that competence initiation should depend on sporulation activity was that cross-regulatory suppression was required for these cell fates to be mutually exclusive (Smits et al., 2007). However, no thorough studies to my knowledge have been conducted to test the strict requirements of mutual cross-inhibition

for the exclusiveness of cell fates. Furthermore, decision-making in other systems have been recently discovered to not require such mechanisms. For instance, the choice between apoptosis and slippage upon cell cycle disruption may not require cross-regulation and checkpoints (Huang et al., 2010). In general, how the requirements for mutual exclusiveness for various types of cell fates depend on the dynamics of the competing alternative differentiation programs is a question that warrants further investigation.

CHAPTER FIVE

CROSS-REGULATORY GENES PLAY AN ACTIVE ROLE ONLY AFTER CELL FATE DECISION

Introduction

Despite the identification of several potential cross-regulatory links between sporulation and competence (see Figure 1.1), it is still not known whether these links are active in individual cells prior to, or at the time of cell fate choice. In general, the activity of a gene or protein is rarely characterized in single cells and over time to reveal how it contributes to cellular behavior. Since in the previous chapter competence initiation was suggested to be independent from the progress of sporulation pathway, I wondered if this implied independence of competence and sporulation prior to cell fate choice was reflected in the expression of genes involved in cross-regulation. The activation of cross-regulatory genes prior to the decision point could give rise to a distinct activity pattern just prior to the decision. If such a pattern exists and influences the decision, then I should be able to identify it and predict cell fate outcomes based on the 'signature' gene activity. Therefore, in the present chapter I aim to measure the activities of genes known to be connected both with sporulation and competence development and influence them accordingly. Eventually, I will determine if intricate cross-regulation between programs is required prior to cell fate choice, or if the dynamics of competing differentiation programs can dictate cellular decision-making.

Results

To look for patterns in cross-regulatory genes expression, I again used time-lapse fluorescence microscopy to track the expression of cross-regulatory genes in single *B. subtilis* cells during cell-fate decision-making. For this specific purpose, I had to track the progress of both differentiation programs along with the activity of cross-regulatory gene of interest simultaneously in the same cell. Specifically, I constructed the strains containing three spectrally distinct fluorescent proteins YFP, CFP and mCherry fused to the promoters of either SinI (P_{sinI}) or AbrB (P_{abrB}), along with promoters of Spo0A (P_{spo0A}) and ComG (P_{comG}) respectively. The cross-regulators *abrB* and *sinI* are both regulated by Spo0A (Hahn et al., 1995; Shafikhani et al., 2002; Strauch et al., 1990; Zuber and Losick, 1987). The expression from P_{abrB} is negatively regulated by Spo0A, while P_{sinI} expression, on the contrary, is thought to be activated (Bai et al., 1993). AbrB is a transcription factor that acts on ComK expression in a concentration-dependent manner, permitting higher basal ComK expression at intermediate levels and inhibiting it at low or high levels (Hamoen et al., 2003). SinI is an antagonist of SinR, a transcriptional inducer of ComK, and thus is expected to indirectly repress competence (Bai et al., 1993; Mandic-Mulec et al., 1995; Shafikhani et al., 2002). Therefore, if these cross-regulators play a critical role in making the decision between competence and sporulation, they should exhibit specific and distinct activities prior to the commitment to either fate.

I have separately analysed sporulating and competent cells of the strains containing the combinations of three color reporters described above. The activities of

either P_{sinI} or P_{abrB} were plotted against the activities of P_{spo0A} for sporulating cells and P_{comG} for competent cells, respectively. The resulting differentiation trajectories colored according to time are plotted in Figure 5.1A-D. In addition, averaged time traces of all three measured reporters aligned in time with respect to competence initiation are shown in Figure 5.2. As expected, during sporulation P_{abrB} and P_{spo0A} are anticorrelated, and P_{sinI} and P_{spo0A} are, in contrast, positively correlated (Figures 5.1A and C). The competence trajectories shown in Figure 5.1, panels B and D also include sporulation trajectories, since for the analysis I chose the cells that initiated competence, exited this state and finally sporulated. As explained before in Chapter 4, tracking the sporulation process after competence allows establishing a reference point to evaluate the sporulation program activities at competence initiation. P_{abrB} seems to exhibit weak positive correlation with P_{comG} expression during competence, while P_{sinI} levels generally stay low both before and during competence (Figurse 5.1B-D and 5.2). But more importantly, I was able to measure the activities of P_{abrB} and P_{sinI} both prior to initiation of competence or spore formation, and following the cell fate decision. The analysis of P_{abrB} and P_{sinI} fluorescence just before sporulation or competence revealed no significant differences in absolute expression amplitudes for either gene (Figure 5.1, E and F). Furthermore, no specific pattern of activity predictive of cell fate outcome could be discerned for either regulator (Figure 5.1). Thus, expression of these cross-regulatory genes prior to the decision point is not predictive of cell fate outcomes, favoring the absence of cross-regulation before cell fate choice.

However, I found that the average absolute amplitudes of P_{abrB} and P_{sinI} during the execution of competence or spore formation (after the commitment point) are

markedly distinct (Figure 5.1, E and F). Specifically, P_{abrB} activity was lower in spore forming cells compared to those that have chosen competence, while the opposite was observed for P_{sinI} (Figure 5.1E-F).

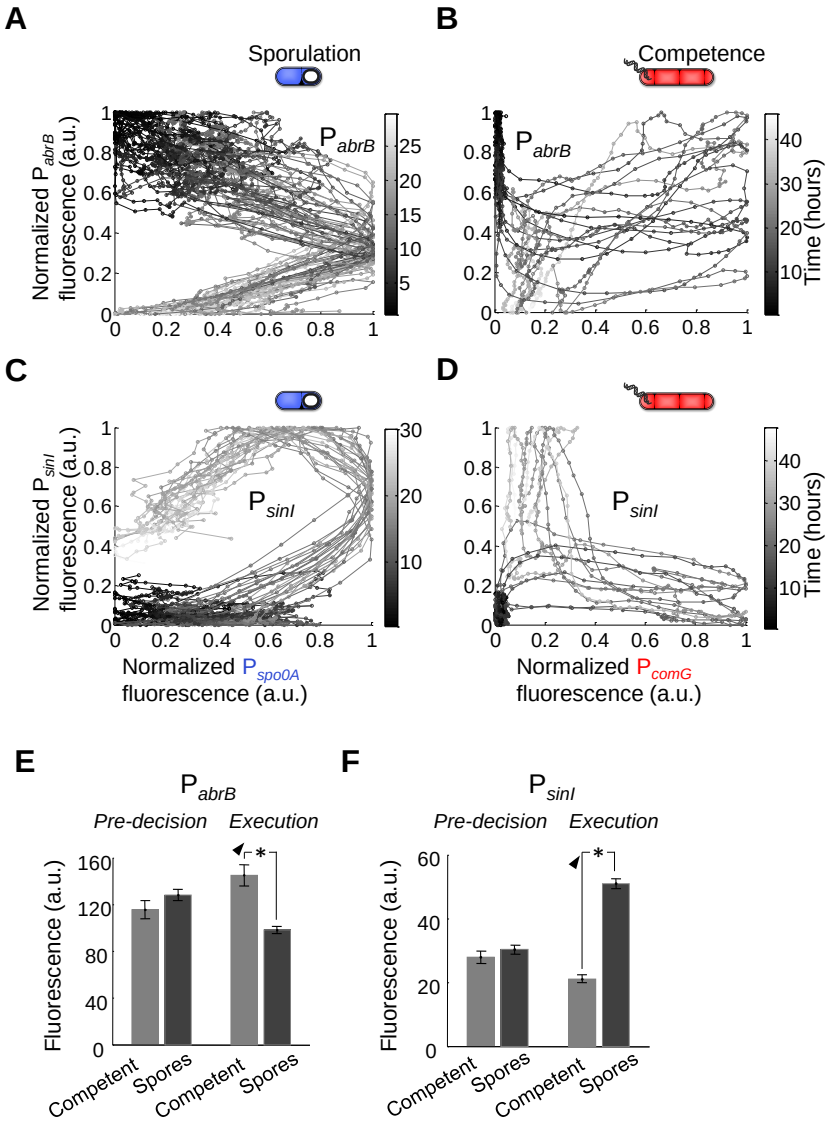

Figure 5.1 Panels (A) through (D) depict normalized single cell fluorescence of either P_{abrB}-YFP (panels A and B, strain 0A-comG-abrB) or P_{sinI}-YFP (panels C and D, strain 0A-comG-sinI) plotted against fluorescence of either P_{spo0A}-CFP (A and C) or P_{comG}-mCherry (B and D) measured in the same cell. Panels A and C show sporulating cells (A, n=40; C, n=25) and panels B and D show competent cells (B, n=10; D, n=10). The traces are colored according to time with darker color corresponding to the beginning of the trace. Panels (E) and (F) show mean P_{abrB}-YFP (E) and P_{sinI}-YFP (F) fluorescence measured in single cells of strains 0A-comG-abrB (n=10 competent and 40 spores), and 0A-comG-sinI (n=10 competent and 25 spores), respectively. The fluorescence

measurements were taken from time points either 40 minutes before initiation of respective cell fate reporter (30% of maximum value for P_{comG}, 90% of maximum value for P_{spo0A}), labeled 'pre-decision', or 40 minutes after the maximum expression of respective cell fate reporter, labeled 'execution'. Error bars represent standard error of the mean (SEM). * $p < 0.001$.

These results suggest that sporulation, as measured by the activities of sporulation-specific genes, appears to be inhibited during competence (Figures 5.1 and 5.2). To investigate this further, I measured P_{spo0A} and P_{spo0F} levels in single competent cells during the period of P_{comG} activation. To establish a reference point for sporulation, as described before, I tracked the progeny of competent cells until sporulation (which is a final resort for virtually all cells in our conditions). Indeed, these measurements showed that average P_{spo0A} activity reached a local minimum during competence (Figure 5.3A). Figure 5.3B shows the difference in distributions of P_{spo0F} activities measured before and during competence. The results indicate that during competence sporulation activity is almost returned to the baseline recorded in the beginning of the time-lapse movie (Figure 5.3). This data suggests that progression to sporulation is inhibited during competence.

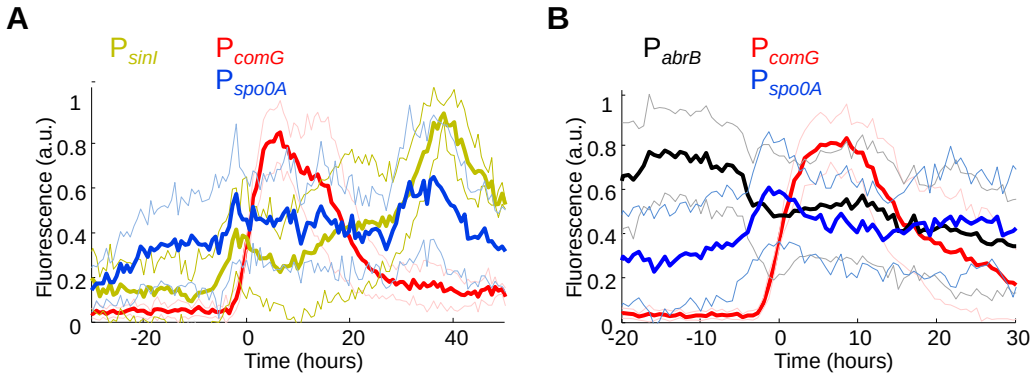

Figure 5.2 Average fluorescence time traces of competent cells from the strains containing combinations of three fluorescent reporters. Individual traces are normalized in amplitude and aligned in time with respect to PcomG initiation (30% of peak activity) prior to averaging. Lighter-colored traces above and below the mean trace indicate standard deviation (SD). (A) Traces from 0A-comG-sinI strain showing Pspo0A-CFP (blue), PsinI-YFP (yellow-green) and PcomG-mCherry (red). (B) Traces from 0A-comG-abrB strain showing Pspo0A-CFP (blue), PabrB-YFP (black) and PcomG-mCherry (red).

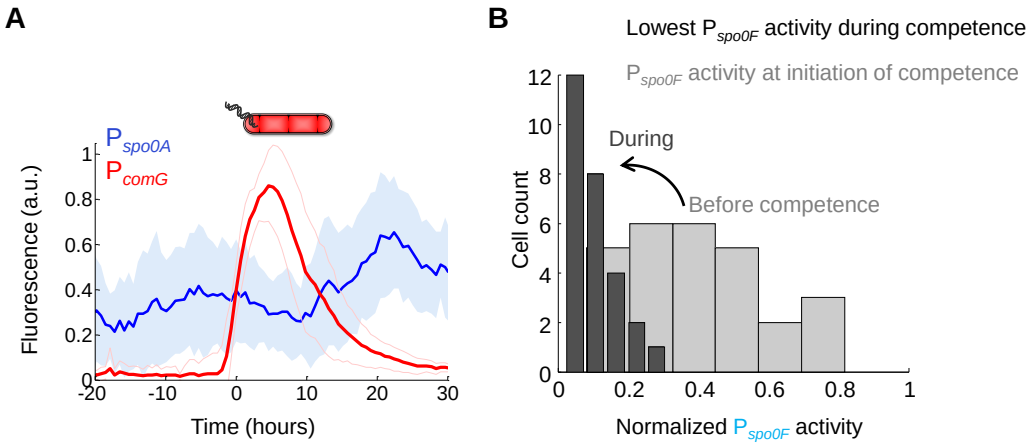

Figure 5.3 (A) Average fluorescence time traces of competent cells from 0A-comG strain showing Pspo0A-YFP (blue) and PcomG-CFP (red). Individual traces (n=67) are normalized in amplitude and aligned in time with respect to PcomG initiation (30% of peak activity) prior to averaging. The blue area and light red curves correspond to standard deviation (SD). (B) Distributions of normalized Pspo0F activities measured in cells of 0F-comG strain undergoing competence. The lowest Pspo0F activities reached by

individual cells during competence are shown in dark grey. Pspo0F activities recorded at initiation of competence (20% of peak activity) are shown in light grey.

Another cross-regulatory gene whose activity is thought to be involved in maintaining mutual cross-regulatory inhibition between *B.subtilis* differentiation pathways is *rok*, repressor of ComK. It was suggested to be regulated by Spo0A, directly bind to the ComK promoter and inhibit it, therefore acting as an inhibitory link from sporulation to competence. It has also been suggested that dependence of ComK expression on SinI and AbrB might be mediated through Rok (Hahn et al., 1995; Hoa et al., 2002). For measuring Rok promoter activity, I constructed a three-color reporter strain expressing P_{rok}-YFP, P_{spo0A}-CFP, and P_{comG}-mCherry as described above. Analysis of competent cells shows that although P_{rok} expression seems to be suppressed during P_{comG} expression, but prior to the decision competence can be initiated even at high Rok levels which do not seem to prevent competence (Figure 5.4). Therefore, presented data enforces the conclusion that while cross-regulatory genes do exhibit specific activity during the execution of competence and spore formation, they play no active role in early decision-making towards these fates.

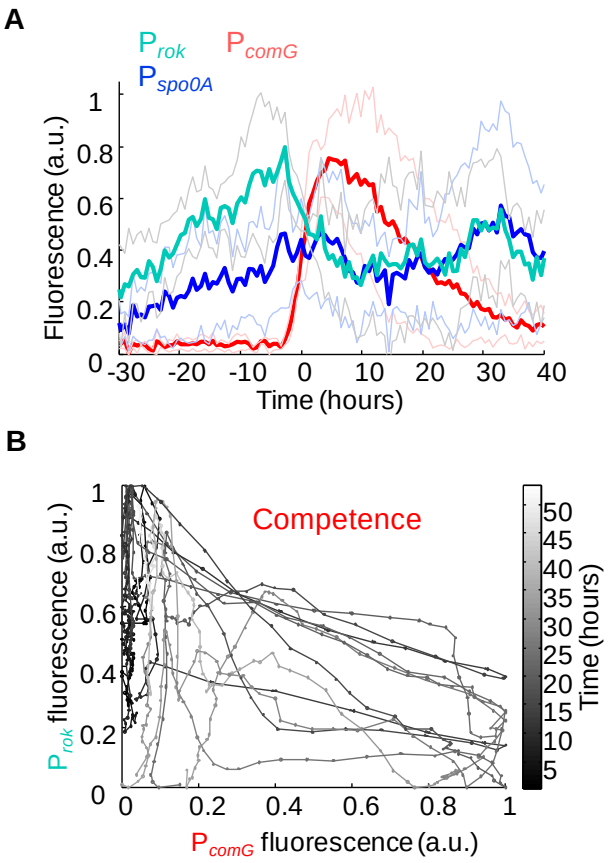

Figure 5.4 Panels (A) and (B) show fluorescence measurements from 0A-comG-rok strain during competence. (A) Average fluorescence time traces of competent cells. P_{spo0A}-CFP fluorescence traces are colored in blue, P_{rok}-YFP is in cyan and P_{comG}-mCherry is in red. Individual traces are normalized in amplitude and aligned in time with respect to P_{comG} initiation (30% of peak activity) prior to averaging. Lighter-colored traces above and below the mean trace indicate standard deviation (SD). (B) Normalized single cell fluorescence of P_{rok}-YFP is plotted against normalized fluorescence of P_{comG}-mCherry measured in the same cell. The traces are colored according to time, as shown in Figure 5.1A-D.

Discussion

The absence of active role for the cross-regulatory genes before the cell fate decision is striking. An important note is that my measurements are not in conflict with the previously established data postulating the activation of the studied regulators in correlation with specific components of sporulation or competence programs (see Chapter 1). I too have found that these genes can be activated, for example, during early accumulation of Spo0A~P. However, this specific activity did not influence the final cell fate choice. In the example of P_{rok} activation profile (see Figure 5.4), many studies have unambiguously described Rok as inhibitor of ComK which was supposed to prevent competence at higher levels of Spo0A. In my data, there is indeed a large increase in P_{rok} expression as Spo0A levels rise, but it is clear that competence can still be initiated even at high P_{rok} amplitudes. Of course, there might be an additional translational level of Rok activity regulation. However, the so-called "opportunity window" for competence development is suggested to close because of inhibition of *rok* by AbrB and Spo0A~P on transcriptional level (Hahn et al., 1995).

Similarly, in my experiments randomly selected competent cells did not appear to favor a specific distinct SinI or AbrB expression level before competence initiation. This argues against the decisive role of cross-regulatory links during cell-fate decision making. Importantly, it also suggests the absence of checkpoints prior to choice between sporulation and competence. Checkpoints during differentiation require a mechanism by which the cell would 1) constantly monitor the state of the progression of differentiation pathway, and 2) terminate or reverse the differentiation in the case of checkpoint activation. In many other differentiation systems, the existence and importance of

checkpoints have been established. One example of a well characterized system that exploits numerous checkpoints is cell cycle progression, which can be halted at specific checkpoints if specific conditions such as DNA replication or chromosome segregation are not met (Truong and Wu, 2011). However, in my bacterial model system I found no evidence that cross-regulator protein-mediated checkpoints regulate the cell fate decision. Specifically, my results suggest that high levels of sporulation program components such as Spo0A~P do not constitute a checkpoint to halt competence development through action of cross-regulatory genes. Rather, these genes exhibit specific activity after the decision, perhaps to help maintain the uninterrupted progression of chosen program. These findings also suggest that the cells might use a different strategy other than checkpoints for guaranteeing the mutual exclusiveness of cell fate outcomes.

CHAPTER SIX

DUAL ACTIVITY CELLS ALLOW MEASUREMENT OF CELL-FATE DECISION-MAKING DYNAMICS

Introduction

It has been long known, and shown in the previous chapter (see Figure 5.3) that competence and sporulation are mutually exclusive cell fates (Grossman, 1995). I wondered how this is reconciled with the discovered apparent absence of cross-regulation prior to the cell-fate decision. Lack of cross-regulation could lead to scenarios of ComK activation almost at any point of sporulation progression, even close to the point of commitment to spore formation, which could potentially disrupt both cell fates. In order to understand better how such conflicts are settled, I specifically searched for cells that initiated ComK expression as the cells were nearing spore formation. Such cells, if identified, could provide a valuable subject for studying the mechanism of cell fate decision between sporulation and competence.

Results

Identification and characterization of conflicted Dual-Activity cells

With the help of Alma Alvarado and Tolga Cagatay in Gürol Süel laboratory, I found a small percentage (0.11±0.04%, N=10561) of previously unobserved cells, referred to here as Dual-Activity (DA) cells, in which ComK expression started just as spores were forming. Cells in this conflicted state, despite ComK expression, proceed directly to form spores (Figure 6.1). Initially, DA cells express P_{comG}, the reporter for the competence master regulator ComK, similarly to those that start regular competence

(Figure 6.1A-B). However, instead of undergoing elongation as seen in competent cells, DA cells immediately begin forespore formation (indicated by the appearance of an asymmetric septum) despite increasing ComK activity (Figure 6.1C-D). Ultimately, similar to all sporulating cells, DA cells progress to lysis of the mother cell and spore release (Figure 6.1C-D). Therefore, DA cells behave exactly like spore forming cells with similar morphological changes and timing (Figures 6.1 and 6.2A), which is very different from typical competence behavior, when cells always exit competence before spore formation (Suel et al., 2006; Suel et al., 2007). The apparently futile expression of ComK seems to be the only difference between DA and regular spore forming cells (Figure 6.2A). The amplitude of ComK expression differs slightly between competent and DA cells, presumably because of the shorter time DA cells spend in the ComK-expressing state before mother cell lysis (Figure 6.1E).

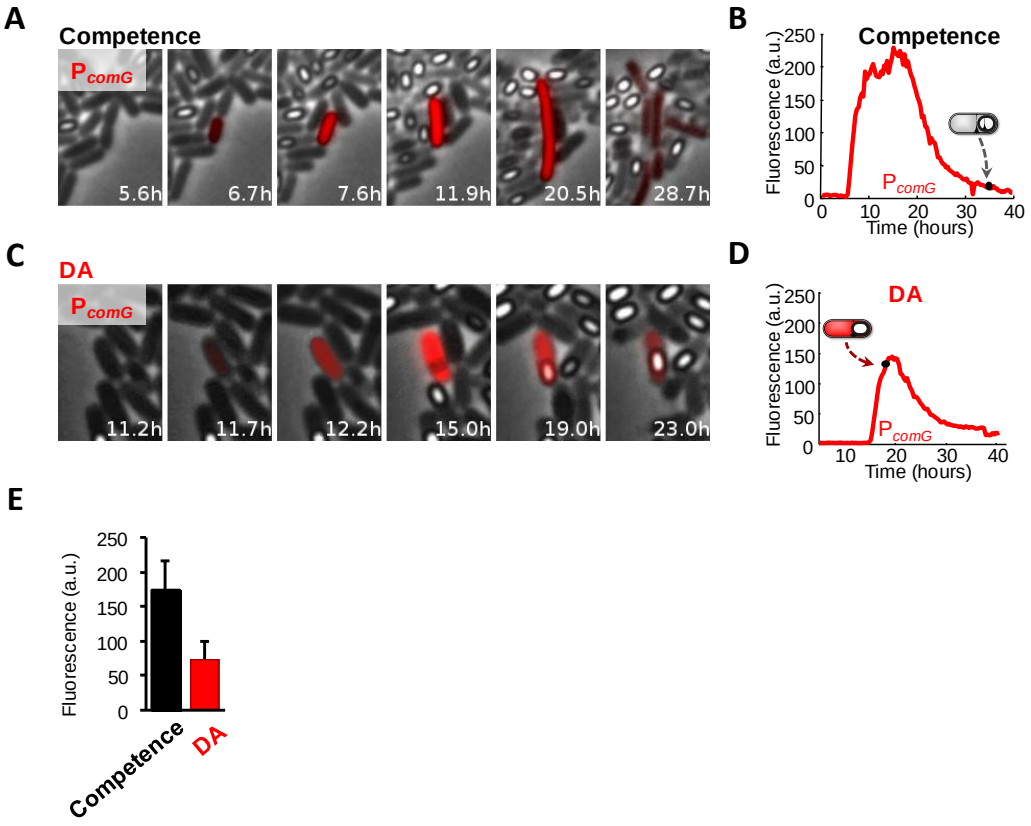

Figure 6.1 Panels (A) and (C) show filmstrip of a representative competent cell (panel A) or DA cell (panel C) visualized by competence reporter PcomG-CFP (red). Panels (B) and (D) show quantitative time traces of the cells shown in Panels (A) and (C), respectively. PcomG activity measured by CFP fluorescence intensity is shown in red. The point of forespore appearance is indicated by an arrow and cell cartoon. (E) Peak fluorescence intensity of PcomG-CFP expression in competent and DA cells. Errorbars indicate standard deviation (SD).

Overall, DA cells seem to be unable to stop sporulation and proceed to competence despite ComK expression. While it is likely that these cells are not experiencing a novel physiological state with a defined biological function, analysis of these conflicted cells might help reveal the timing and dynamics of the cell fate choice. The fact that ComK expression in DA cells is futile means that DA cells mark the point at which the cells have chosen sporulation as their ultimate cell fate. In order to better characterize the dynamics of this point, I further examined the sporulation gene activities in DA cells. In particular, I have constructed reporter strains containing the pair-wise combinations of P_{comG}-CFP with YFP fused to one of the three sporulation promoters described in previous chapters (P_{spo0A}, SpoIIE and P_{spoIIR}) with the addition of the fourth reporter P_{spoIIG}, promoter for SpoIIGA, a protein required for proteolytic cleavage of pro-σ^E (Hofmeister et al., 1995; Stragier et al., 1988; Trempy et al., 1985). Expression dynamics of each reporter pair in single cells obtained by time-lapse fluorescent microscopy were averaged and aligned with respect to P_{comG} activity, which served as a common temporal anchor point (Figure 6.2B). These measurements confirmed that with regard to the overall dynamics of sporulation gene expression DA cells are similar to regular sporulating cells (Figure 6.2B; compare to Figure 3.2D). I was also able to locate the exact timing of P_{comG} expression relative to the measured sporulation steps and thus determine the temporal location of cell-fate decision point since futile P_{comG} expression in DA cells marks the point of competence fate exclusion. The data presented in Figure 6.2B shows that the DA state is observed after P_{spo0A} activation, but before P_{spoIIG} and P_{spoIIR} activation. In particular, the DA state overlaps in time with localization of SpoIIE to the asymmetric septum (Figure 6.2B).

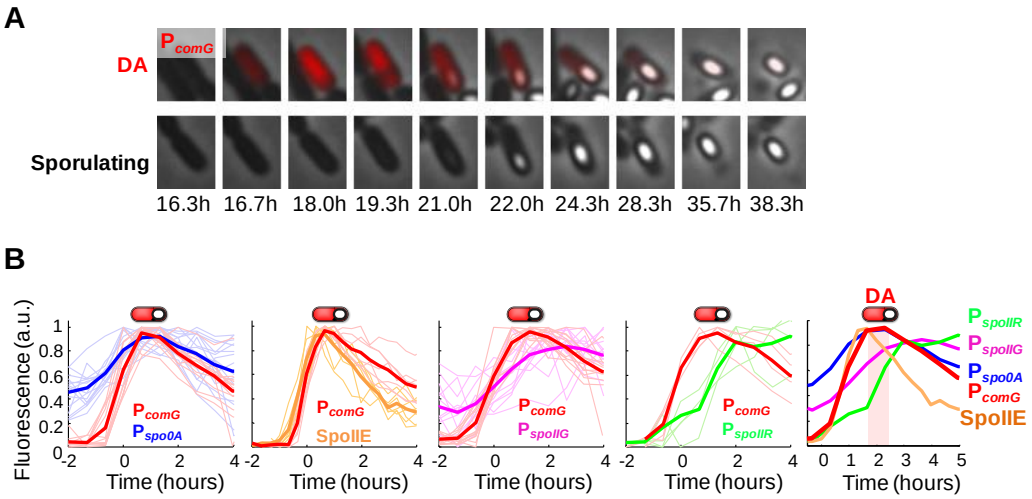

Figure 6.2 (A) Filmstrip of a typical DA cell (upper panel) demonstrating that cells in the DA state form spores with similar dynamics and appearance as normal sporulating cells (lower panel). The DA cell is visualized by competence reporter PcomG-CFP (red). Time in hours is indicated below each frame. (B) Quantitative time traces of single DA cells from strains expressing pair-wise combinations of one of the sporulation reporters Pspo0A (blue, strain 0A-comG, n=15), SpoIIE (orange, strain IIE-comG, n=7), PspoIIG (magenta, strain IIG-comG, n=13) or PspoIIR (green, strain IIR-comG, n=4) and the competence reporter PcomG (red) fused to fluorescent proteins (YFP and CFP respectively) are shown in shaded colors, with mean trace shown on top in bright color. All traces have been normalized in amplitude and aligned in time with respect to PcomG activation (>30% of peak activity) which is set as zero time point. The data from the first four panels (from the left) was combined to produce the fifth panel.

Engineered strain that bypasses the sporulation decision point (NoE) suggests the mechanism of competence exclusion

The established temporal overlap of P_{comG} activation with SpoIIE activity in DA cells was promising because SpoIIE localization to the asymmetric septum marks the first morphological change and the division between mother and forespore compartments during early spore formation (Barak et al., 1996). This step could potentially play a role in the cell-fate decision, and indeed this stage has been suggested to coincide with the point of irreversible commitment to sporulation (Dworkin and Losick, 2005). If SpoIIE localization indeed prevents ComK-expressing DA cells from completing the competence pathway, then a targeted elimination of SpoIIE exactly at this point in time in DA cells could "rescue" the DA cells and allow them to become fully competent.

I investigated this possibility by constructing an engineered NoE strain (for detailed genetic composition see Table 2.1) with disrupted SpoIIE localization specifically in DA cells. In particular, I replaced the native SpoIIE gene with a SpoIIE coding sequence that contained a C-terminal *Escherichia coli* tag (ssrA) targeting it for enzymatic degradation in the presence of the *E. coli* protease factor SspB (Flynn et al., 2001; Gottesman et al., 1998; Griffith and Grossman, 2008; Levchenko et al., 2000). To ensure SpoIIE degradation only during simultaneous expression of ComK, I placed the exogenous SspB protease adaptor protein under the control of the ComK-controlled P_{comG} promoter (Figure 6.3A). In addition, for detection of sporulating and competent cells I introduced the fluorescent proteins YFP and CFP under the control of P_{spo0A} and P_{comG} promoters, respectively. Finally, for the convenience of observation and analysis I increased the fraction of DA cells by ectopically inducing ComK expression from P_{spoIIG}

promoter (see Chapter 7 and Table 7.1). This perturbation, however, was so severe that it disrupted sporulation in cells that simultaneously expressed P_{spo0A} and ComK leading to cell death and completely eliminating DA cells (Figure 6.3D). To allow these prospective DA cells instead to proceed with competence, we added a C-terminal endogenous *B. subtilis* degradation tag (ssrA, or 'XP') to the exogenous SspB protease to destabilize it and reduce its half-life (Wiegert and Schumann, 2001).

The resulting NoE re-wiring did not interfere with sporulation (Figure 6.3C) or successful completion of competence events (Figure 6.3E). Compared to the strain with no NoE modification, expressing only ComK from P_{spoIIG} promoter ([0A-comG] $^{IIG\text{-}K}$), I observed an almost 50% decrease in the fraction of DA cells and a corresponding increase in competence frequency (Figure 6.3B and Table 7.1) indicating that NoE perturbations were able to specifically rescue DA cells allowing them to undergo competence without affecting sporulation. Only partial decrease in the number of DA cells was expected since we used an unstable protease to target SpoIIE for degradation. It should be noted that SpoIIE degradation did not result in an increased frequency of ComK expressing cells, but rather a corresponding redistribution of DA and competence frequencies, indicating that SpoIIE localization by itself did not influence the initial expression of ComK, but played part in ultimate cell fate outcomes.

More detailed measurement of ComK activity in the NoE strain revealed that about 50% of competent cells differed from their wild type counterpart with respect to ComK dynamics. Specifically, I observed consecutive peaks of ComK activity in the competent cells of NoE strain that were distinct from consecutive competence events in cells from the background reporter strain [0A-comG] $^{IIG\text{-}K}$ with respect to time between

peaks, ratio of peak amplitudes and minimum activity between peaks (Figure 6.4A-B). Sample traces of P_{comG} expression in the described subset of NoE cells show that after the initial increase ComK expression immediately drops reaching a low amplitude characteristically observed in DA cells, but then suddenly and rapidly resumes reaching typical competence amplitudes (Figure 6.4C, compare amplitudes with Figure 6.1E). These NoE cells were similar to regular competent cells with respect to cell elongation and also remained in the final high ComK expression state for durations typical for competent cells. This behavior differs from sequential competence events observed in [0A-comG] $^{IIG\text{-}K}$ strain that are separated by at least a minimum time consistent with the refractory period associated with excitable dynamics that underlie competence (Figure 6.4D) (Suel et al., 2006; Suel et al., 2007).

Summarizing the observations, the subset of NoE cells displaying distinct ComK activation pattern shown in Figure 6.4C might represent the reprogrammed DA cells specifically rescued from sporulation following ComK activation. These data suggest that SpoIIE activity and localization to the asymmetric septum is one of the molecular processes that take part in exclusion of competence. Still, it seems that competence is not actively inhibited by SpoIIE localization. Rather, the possibility of competence initiation after SpoIIE localization is eliminated simply because due to the natural sporulation progression the mother cell in which ComK is expressed undergoes cell lysis releasing the spore (Hosoya et al., 2007).

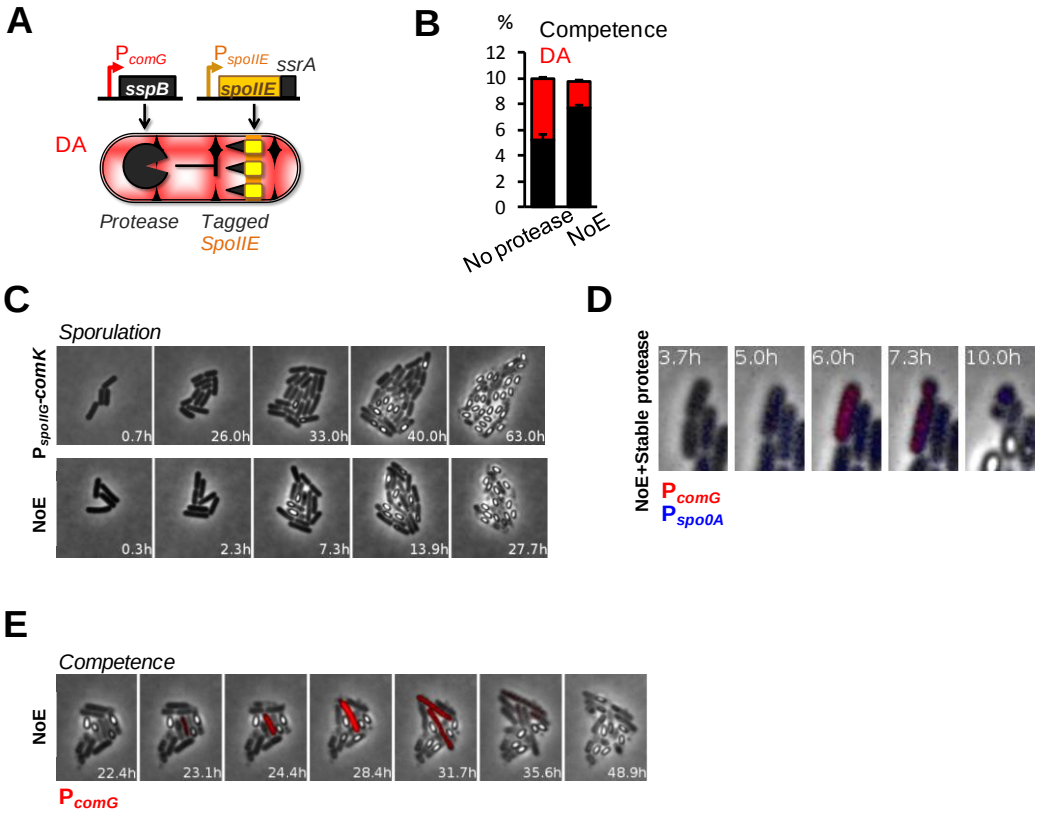

Figure 6.3 (A) The design of the NoE strain. An *E. coli* protease tag ssrA was translationally fused to SpoIIE protein, and a specific *E. coli* protease factor SspB that targets this tag for degradation was expressed from P_{comG} promoter. Simultaneous activation of both differentiation programs, a characteristic of DA state, in engineered NoE cells would result in targeted degradation of SpoIIE. For details, see text. (B) Competent and DA cell frequencies observed in the NoE strain compared to a strain lacking the NoE modification ("No protease"). Black bars show competent cells fraction, while red bars indicate DA cells fraction. Both strains have enhanced background DA frequency for easier analysis as a result of ectopic ComK expression from P_{spoIIG} promoter (see Chapter 7 and Figure 7.4). Error bars represent standard error of the mean (SEM). (C) Filmstrips of a sporulating microcolony from *B. subtilis* strain expressing P_{spoIIG}-comK ([0A-comG] $^{IIG\text{-}K}$) (top panel) and NoE strain (lower panel). Time in hours is indicated on each panel. (D) Filmstrip showing a representative failed sporulation attempt in presence of simultaneous ComK and Spo0A expression in cells of the NoE strain expressing stable *E. coli* SspB protease factor (see text). P_{comG}–CFP is shown in red and P_{spo0A}-YFP is in blue. Time in hours is indicated on each panel. (E) Filmstrip showing a typical competence event visualized by CFP expressed from P_{comG} promoter (in red) followed by sporulation in NoE strain. Time in hours is indicated on each panel.

.

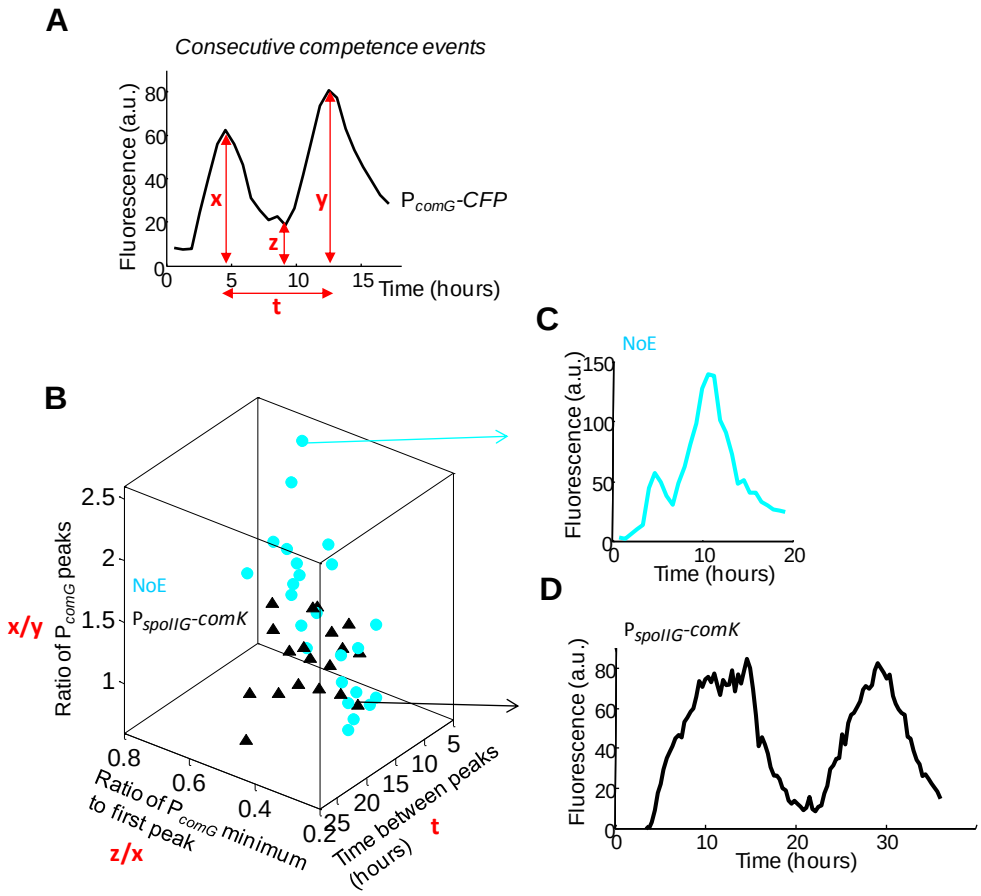

Figure 6.4 (A) A sample quantitative trace of P_{comG}–CFP fluorescence in a cell of NoE strain undergoing two consecutive ComK activation events. The parameters measured to generate the distributions shown in panel (B) are shown in red. *x* and *y*, peak P_{comG}–CFP expression during the first and the second round of ComK activation, respectively; *z*, minimum P_{comG} activity between peaks of ComK activation; *t*, time between consecutive peaks of P_{comG} activity. (B) Distribution of properties of consecutive ComK activation events measured as described in panel A in cells of strain expressing P_{spoIIG}-comK ([0A-comG] $^{IIG\text{-}K}$) (black triangles) and cells of NoE strain (cyan circles). The plotted parameters are as indicated. Each data point corresponds to the measurement of one cell. Note the distinct distributions of data points for strain expressing P_{spoIIG}-comK ([0A-comG] $^{IIG\text{-}K}$) and for the NoE strain. Panels (C) and (D) show time traces of P_{comG} activation from NoE (panel C, in cyan) and the strain expressing P_{spoIIG}-comK ([0A-comG] $^{IIG\text{-}K}$) (panel D, in black) corresponding to the data points in panel (B) indicated by arrows.

The dynamics of gene expression in DA cells help reveal the mechanism of cell-fate decision

The similarity of DA cells to sporulating cells is further supported by measurements of cross-regulatory gene activities (discussed in Chapter 5) in DA cells. In particular, I measured the activities of P_{abrB}-YFP and P_{sinI}-YFP specifically in single DA cells of the three-color reporter strains also containing P_{spo0A}-CFP and P_{comG}-mCherry. I found that the activities of these cross-regulators both prior and following the P_{spo0A} activation are identical between DA cells and regular sporulating cells (Figure 6.5A,B). Additionally, in contrast to competent cells (see Chapter 5, Figure 5.1B,D), DA cells display the same P_{abrB} and P_{sinI} activity patterns as sporulating cells (Figure 6.5C,D, compare to Chapter 5, Figure 5.1A,C). The combined average time traces of P_{abrB}, P_{rok} and P_{sinI} aligned to the expression of P_{spo0A} as a common anchor constitute a relative temporal profile of cross-regulatory genes' activities in sporulating and DA cells, respectively (Figure 6.6A,B). The only difference observed between these profiles is the stochastic expression of P_{comG} in DA cells that by itself is not preceded or followed by any changes in regulatory gene expression. These findings further demonstrate that active cross-regulation or checkpoints do not play a critical role prior to cell fate choice. Furthermore, the very existence of cells in this DA state argues that expression of the competence master regulator ComK is not inhibited by the progression to sporulation, and vice versa, that sporulation is not inhibited by expression of ComK.

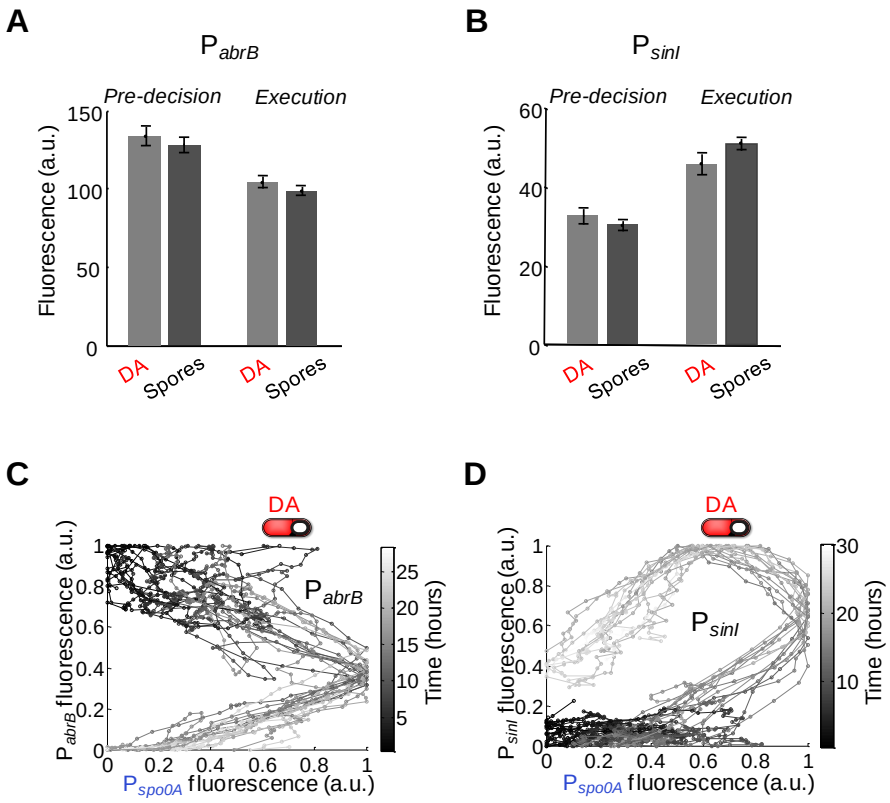

Figure 6.5 Panels (A) and (B) show mean P_{abrB}-YFP (A) and P_{sinI}-YFP (B) fluorescence measured in single cells of strains 0A-comG-abrB (n=17 DA and 40 spores), and 0A-comG-sinI (n=16 DA and 25 spores), respectively. The fluorescence measurements were taken from the time point either 40 minutes before initiation of P_{spo0A} (90% of maximum value), labeled 'pre-decision', or 40 minutes after the maximum expression of P_{spo0A}, labeled 'execution'. Error bars represent standard error of the mean (SEM). Panels (C) and (D) depict normalized single cell fluorescence of either P_{abrB}-YFP (panel C, strain 0A-comG-abrB, n=17) or P_{sinI}-YFP (panel D, strain 0A-comG-sinI, n=16) plotted against fluorescence of P_{spo0A}-CFP measured in the same DA cell. The traces are colored according to time with darker color corresponding to the beginning of the trace.

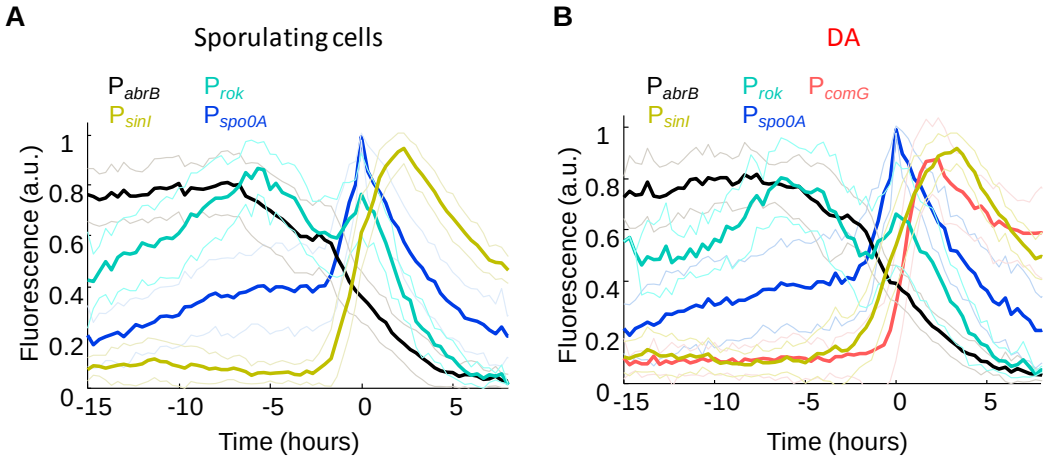

Figure 6.6 Average fluorescence time traces of sporulating (panel A) or DA cells (panel B) from the strains containing combinations of Pspo0A (blue, strain 0A-comG), PabrB (black, strain AbrB-comG), PsinI (brown, strain SinI-comG) or Prok (cyan, strain Rok-comG) and the competence reporter PcomG (red) fused to fluorescent proteins (YFP and CFP respectively). Individual traces are normalized in amplitude and aligned in time with respect to Pspo0A maximum prior to averaging. Lighter-colored traces above and below the mean trace indicate standard deviation (SD).

The hallmark of DA cells is simultaneous expression of both the sporulation and competence master regulators Spo0A and ComK, respectively. However, in these cells competence is censored while spore formation proceeds uninterruptedly. Therefore, the quantitative measurements of the timing of competence (PcomG) relative to sporulation (Pspo0A) reporters in DA cells allowed me to determine the precise location of the competence censorship point with respect to time and sporulation progression. Specifically, I plotted the amplitude of Pspo0A expression at the initiation of PcomG expression in DA cells as shown in Figure 6.7A (see also Chapter 4, Figure 4.3 for the similar analysis of competent cells). In contrast to regular competent cells shown for reference, PcomG expression in DA cells was restricted to a narrow time window just before spore formation at which the amplitude of Pspo0A activity was high and less

variable (Figure 6.7B). These findings further support the role of DA cells as uncovering the reference point of cell fate choice that is taking place in a very sharp and deterministic fashion very close in time to the morphological spore formation, when Pspo0A activity is highest.

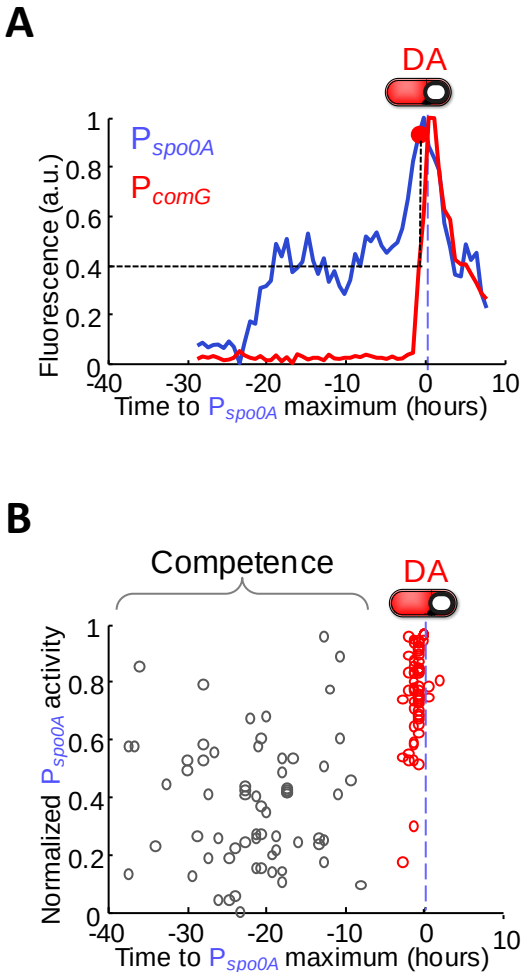

Figure 6.7 (A) Sample time traces illustrating how the activity of sporulation was determined specifically in DA cells. The panel shows a single DA cell (0A-comG strain), in which P_{comG} activity is measured by CFP fluorescence intensity (shown in red) and P_{spo0A} activity is measured by YFP fluorescence intensity (in blue). The traces are aligned in time with respect to maximum P_{spo0A} activity at sporulation (set as zero time point). This data is utilized to determine P_{spo0A} activity (red circle) at initiation of P_{comG} expression in DA cells (defined by >30% P_{comG} activity relative to maximum observed P_{comG} amplitude), similar to Figure 4.3. For comparison, both time traces are normalized with respect to amplitude. (B) P_{spo0A} activity measured in single DA cells (red circles), n=67. The data was combined from measurements of 0A-comG, $[0A\text{-}comG]^{0A\text{-}K}$, $[0A\text{-}comG]^{IIG\text{-}K}$ strains (see Chapter 7). The traces are aligned with respect to maximum P_{spo0A} activity at sporulation as described in panel (A). P_{spo0A} activity at the onset of competence (black circles) determined in Figure 4.3 is shown for comparison.

Discussion

The identification of cells in the conflicted DA state, where both sporulation and competence differentiation programs are simultaneously active, demonstrates the absence of cross-regulation and checkpoints during *B. subtilis* cell fate decision-making. This state, while possibly not corresponding to a novel physiological phenotype, identifies cells captured in the exact moment of making a cell fate decision, specifically, excluding the possibility of competence and thereby choosing sporulation as the only available cell fate. This point of view is supported by measurements of gene expression profile specifically in DA cells that shows that brief pulse of ComK expression by itself does not alter the dynamics of sporulation components activation. Additionally, in agreement with the conclusions of the previous chapter, the activities of cross-regulatory genes such as AbrB, SinI and Rok are also 'oblivious' to the ComK expression in DA cells. On the other hand, ComK expression in DA cells is initiated at the peak of sporulation-specific gene expression, when according to the "competence window" model it should be turned off (see also next chapter). This finding emphasizes the absence of active cross-regulation between competence and sporulation circuits, at least on the initiation level.

Measurements of gene expression profiles in DA cells also permit to precisely identify the temporal location of competence exclusion point which was found to coincide with the step of SpoIIE localization to the asymmetric septum. Intriguingly, targeted degradation of SpoIIE allowed to specifically rescue at least ~50% of DA cells from competence exclusion, or, in other words, to change the cell fate decision. Interestingly, I previously found that the step of SpoIIE localization to the polar septum was still subject to spontaneous reversibility in ~2% of sporulating cells (see Chapter 3).

In other words, at this step the cells seem to have excluded competence possibility, but still have not fully committed to sporulation either, since the ultimate sporulation commitment point is coinciding with P_{spoIIR} activation reporting σ^F activity in the forespore compartment (see Chapter 3). Even though the time between SpoIIE and P_{spoIIR} peaks according to my measurements is very short (~1 hour; see Figure 3.2), these observations could still suggest an intriguing possibility that the points of alternative cell fate exclusion and irreversible commitment to sporulation fate are separate in time for *B. subtilis* cells. This adds complexity to the definition of cell-fate commitment point since the former is about the choice between alternative fates rather than the latter that represents the choice between waiting or proceeding to differentiation. Passing the point of cell fate exclusion does not automatically mean that the cell cannot reverse its chosen fate, it rather simply indicates that some of the alternatives are not available any longer. The possible temporal separation between the decision points suggest the time window when the cell have 'chosen' a fate among other possibilities, but have not irreversibly committed to it yet. This temporal separation may serve a biological purpose, since it provides the system additional time to respond to environmental cues while ensuring no interference from the alternative programs.

The significant role of asymmetric septum formation in DA cell fate choice could provide a hint for the mechanism of competence cell fate exclusion. In DA cells, polar septation takes place concurrently with ComK expression which in competent cells is supposed to block cell division indirectly by the action of ComGA (Haijema et al., 2001). This multi-purpose protein which is also an important component of DNA uptake machinery (Briley et al., 2011), inhibits FtsZ ring formation in competent cells, but

apparently not growth in our conditions (resulting in the elongated phenotype shown in Figure 6.1A). Importantly, FtsZ rings assembly is also a critical step in asymmetric septum formation (Ben-Yehuda and Losick, 2002). According to this reasoning, my findings indicate that ComK expression in DA cells is truly futile because apparently it not only fails to influence sporulation, but also does not lead to the development of traits characteristic for competent state. Therefore, the data suggests that true competent state in fact might not be even reached in DA cells, regardless of ComK expression, because otherwise the cells would not be able to build the asymmetric septum. I conclude that polar septation in DA cells by itself seems to be the factor that plays an important role in competence exclusion.

CHAPTER SEVEN

TEMPORAL COMPETITION BETWEEN SPORULATION AND COMPETENCE DETERMINES CELL FATE CHOICE

Introduction

Analysis of the DA state in the previous chapter revealed that competence exclusion coincides with polar septation. The fact that DA cells are able to build a functional septum and divide asymmetrically, as explained above, suggests that true competence state is never reached in DA cells despite ComK expression. However, ComK expression normally is sufficient to trigger functional competence state. If competence is somehow excluded without active inhibition of ComK, then there must be another physical mechanism by which functional competence development is prevented. A feasible explanation of why DA cells never reach competent state would be lack of time before polar septation takes place. Indeed, if the ComK-induced downstream competence proteins fail to get expressed and assembled before the sporulation septum formation, the asymmetric division and associated morphological changes could physically block further development of competence. How much time then does competence need after initiation of ComK expression to become able to suppress sporulation activities? This question is still open, although there is a hint that the process of functional competence development could be fairly slow since the duration of competence state as measured by high ComK levels in my experimental conditions ranges from ~8 hours all the way up to 40 hours (Cagatay et al., 2009; Suel et al., 2007). It is also unknown when exactly the cell becomes functionally competent, i.e., becomes

able to bind and uptake extracellular DNA. Ultimately, polar septation and functional competence development seem to be competing processes, the relative timings of which could define the cell fate decision.

Results

Relative timing between sporulation and competence programs appears to determine cell fate

I examined if DA cells had sufficient time to develop functional competence before mother cell lysis during spore formation. As competence is functionally defined by the ability to take up extracellular DNA, I traced the assembly of the ATP-dependent complex required for the DNA uptake at the cell pole. Specifically, I visualized the cell pole localization of the membrane protein ComGA which is a critical part of the competence DNA uptake complex (Briley et al., 2011). Utilizing single-cell fluorescence time-lapse microscopy as previously described, I observed multiple bright ComGA-YFP foci formation in 78% of cells with activated ComK (measured by P_{comG} expression amplitude) (Figure 7.1A and C). The highly mobile foci, consistent with the literature (Chung et al., 1998; Hahn et al., 2005), mostly localized to the cell poles, but could also be observed at the midpoint of the cell, although less common (Figure 7.1A). In stark contrast, none of the observed DA cells from multiple movies exhibited similar ComGA-YFP foci (Figure 7.1B and C). This finding indicates that DA cells fail to assemble the critical downstream ComGA machinery required for the biological function of competence.

In order to investigate the possible reason for the lack of DNA uptake complexes in DA cells, I determined how much time on average the cells need to build and localize these complexes after the initiation of competence program. During typical competence events, ComGA localization occurred on average 4 hours after initiation of ComK expression (Figure 7.1D,F). However, in DA cells asymmetric septum formation proceeded immediately after the initiation of ComK expression, followed by mother cell lysis. Indeed, measurement of the timing of SpoIIE localization in DA cells revealed that the asymmetric septation occurred on average only 40 minutes after initiation of ComK expression in these cells (Figure 7.1E,F). In summary, DA cells reach SpoIIE localization and consequent spore formation in less time than is needed for the assembly of the DNA uptake machinery during competence (Figure 7.1F). The lack of time can also explain the lack of ComGA foci formation in DA cells. It thus appears that when the cells pass the SpoIIE localization stage, they are destined to proceed with sporulation by default. Even if competence gene expression happens to be initiated, competence simply runs out of time, leaving spore formation as the only possible outcome.

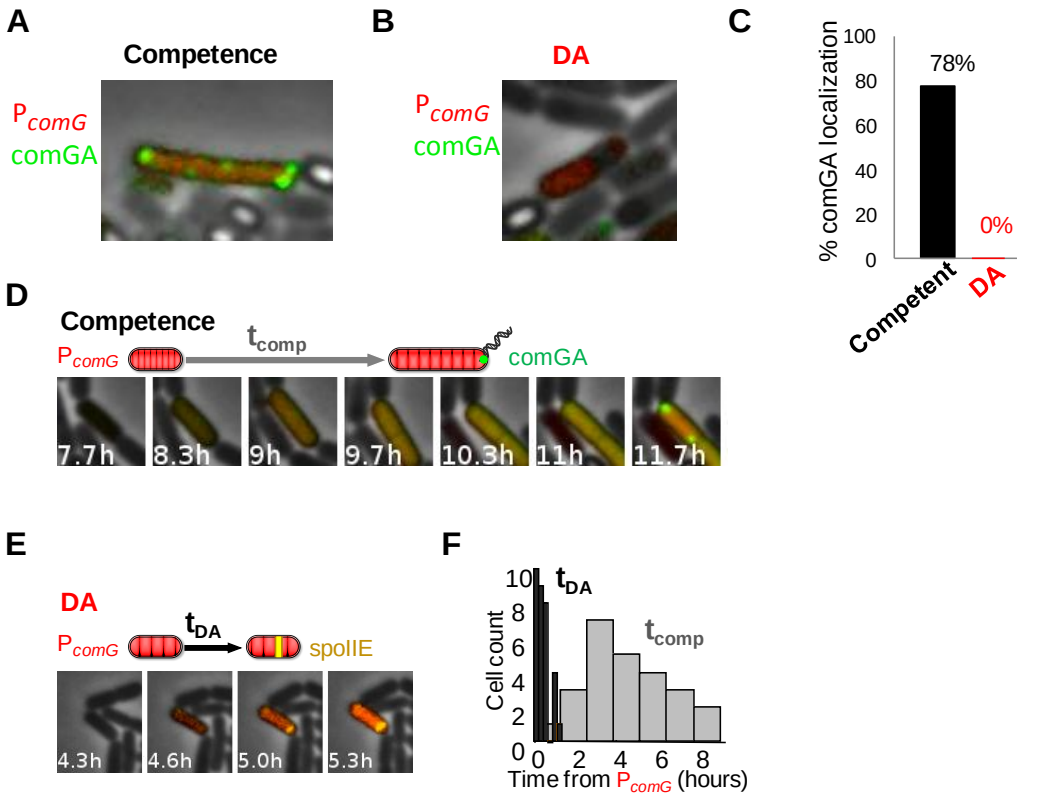

Figure 7.1 Panels (A) and (B) show a representative competent (panel A) and DA cell (panel B) from the strain [comG-comGA]IIG-K expressing PcomG-CFP (red) and ComGA-YFP (green). Note the appearance of ComGA loci in competent, but not in DA cell. (C) Frequency of ComGA loci appearance in competent (n = 107) and DA cells (n=77). (D) Filmstrip showing a typical competent cell from the [comG-comGA]IIG-K strain. Time between PcomG initiation (>30% maximum) and ComGA localization to cell poles (11.7h) is indicated as tcomp. (E) Filmstrip of a representative DA cell visualized by PcomG-CFP (red) and SpoIIE-YFP (orange). Time between PcomG initiation (>30% maximum) and SpoIIE localization to asymmetric septum (>40% maximum, 5.3h) is indicated as tDA. (F) Histogram of time between PcomG initiation (set as zero time point) and either ComGA localization to cell poles in competent cells (tcomp, n=27), or SpoIIE localization to asymmetric septum in DA cells (tDA, n=32) measured in single cells as described in panels (D) and (E).

Based on these observations, I hypothesized that the choice between the sporulation and competence programs is mediated by a simple molecular race mechanism (Figure 7.2). Per this hypothesis, the relative timing of competing differentiation programs is a critical determinant of cellular decision-making in *B. subtilis* (Figure 7.2). Since competence is initiated when ComK expression stochastically exceeds a certain threshold (Maamar et al., 2007; Suel et al., 2006), and the probability of this event remains independent of sporulation progression as shown in Chapter 4, then ComK expression can be initiated even at the later steps of sporulation, such as immediately before SpoIIE localization. Even though normally the cells that reach the state of functional competence are able to suppress further sporulation development (see Figure 5.3), in this case, the cells lack sufficient time to develop this state, therefore competence state is censored giving rise to the 'conflicted' DA state that results in spore formation (Figure 7.2). In contrast, competence is possible and sporulation is censored if ComK expression occurs much earlier than SpoIIE localization, allowing ample time for the functional competence development (Figure 7.2). Such temporal competition can ensure mutually exclusive cell fates, even if both programs were initiated at the same time, since only one of them has sufficient time to differentiate into its functional state.

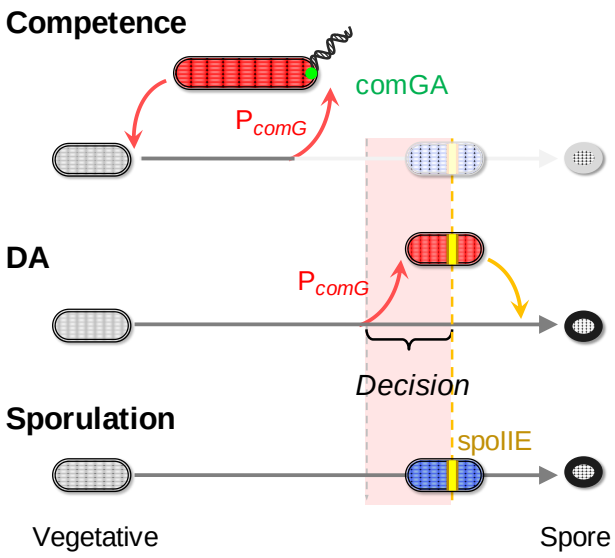

Figure 7.2 Diagram of the "molecular race" hypothesis. Competence (top panel) occurs if ComK expression begins early enough to give sufficient time for ComGA localization (green dot) before SpoIIE (yellow line). However, functional competence cannot develop if ComK is expressed within the critical time window (termed "Decision" and shown in pink) close to SpoIIE localization, resulting in DA state where sporulation takes over (middle panel). Sporulation is shown in the bottom panel for reference.

DA cell frequency can be accurately predicted under the temporal race hypothesis

In light of the temporal race hypothesis, the small percentage of cells captured in the DA state is not surprising and can be predicted from the data (Figure 7.3A). So far, I have determined that the probability of ComK initiation is independent from progression to spore formation even at high levels of Spo0A and Spo0F expression (Chapter 4). I also determined that in DA cells ComK expression is restricted within a narrow time window between the localization of SpoIIE and expression of SpoIIR, which coincides with the commitment point for spore formation (see Chapter 6, Figure 6.2B). Therefore, under the temporal race hypothesis, the DA state is defined by the simultaneous occurrence of two low probability events in the same cell: 1) stochastic initiation of ComK expression, and 2) close temporal proximity to the decision towards spore formation. Since our conclusions (Chapter 4) indicate that these events are independent, the probability of observing DA cells should correspond to the product of the frequency of competence initiation (measured to be ~2%, see Table 7.1) and the probability of a cell to reside in the time window between the localization of SpoIIE and expression of SpoIIR. From the data shown in Figure 6.2B, this time window was measured to be ~1 hour long, while the average time for a cell to reach spore formation under our movie conditions was found to be ~17 hours (Figure 7.3B). Thus, the expected frequency of DA cells under our conditions is 2% times 6%, or ~0.1%, which is in fact very similar to the experimentally observed frequency of 0.11% ± 0.04% (see Table 7.1). The fact that the frequency of DA cells can be predicted using the collected data under the assumption of independence between sporulation progression and competence initiation further supports the temporal race hypothesis.

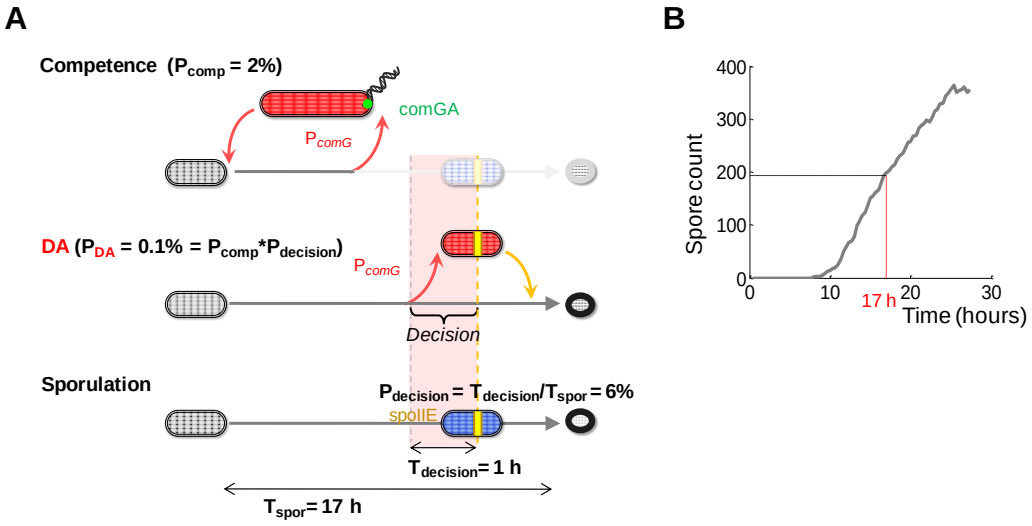

Figure 7.3 (A) Calculation of DA cell frequency under the temporal competition hypothesis. Briefly, the probability of observing a DA cell equals to the product of probability of ComK activation (Pcomp, measured to be ~2%) and the probability of this event to occur in the "decision" time window (Pdecision). This "decision" time window was measured to be ~1 hour (see Figure 6.2B, shaded pink area), while the mean sporulation time was estimated to be take 17 hours (panel B). Therefore, Pdecision is ~6%, and DA frequency is expected to be ~0.1% which is very close to experimental value (see Table 7.1). (B) Estimation of the time it takes the cells to reach phase-bright spore formation. Phase-bright spores were counted in each frame of a typical time-lapse movie of sporulating B. subtilis microcolony (strain 0F-comG). Under our imaging conditions, ~50% of observed cells reach sporulation in 17 hours.

Engineered strains with perturbed relative timing between initiation of competence and sporulation support the molecular race hypothesis

According to the molecular race hypothesis, the timing of ComK expression relative to the sporulation program is a major determinant of the cell fate outcome. I tested this prediction by using the native sporulation promoters whose expression is turned on at different stages of progression to sporulation to drive ComK expression (see Figures 3.2D and 6.2B). To make the engineered strains, I ectopically expressed a copy of *comK* from each of the previously characterized sporulation promoters P_{spo0A}, P_{spoIIG} and P_{spoIIR} (for their activation temporal profile, see Figures 3.2D and 6.2B). I also expressed in the same strains each of the three sporulation reporters described previously (P_{spo0A}-YFP, P_{spoIIG}-YFP and P_{spoIIR}-YFP) in combination with P_{comG}-CFP (Figure 7.4A). As expected, the dynamics of sporulation reporters' activation remained unchanged in the DA cells of strains with ectopic *comK* expression (Figure 7.4B-D). This finding confirms that ectopic expression of an extra *comK* copy does not interfere with the mechanism and dynamics of the normal decision-making process.

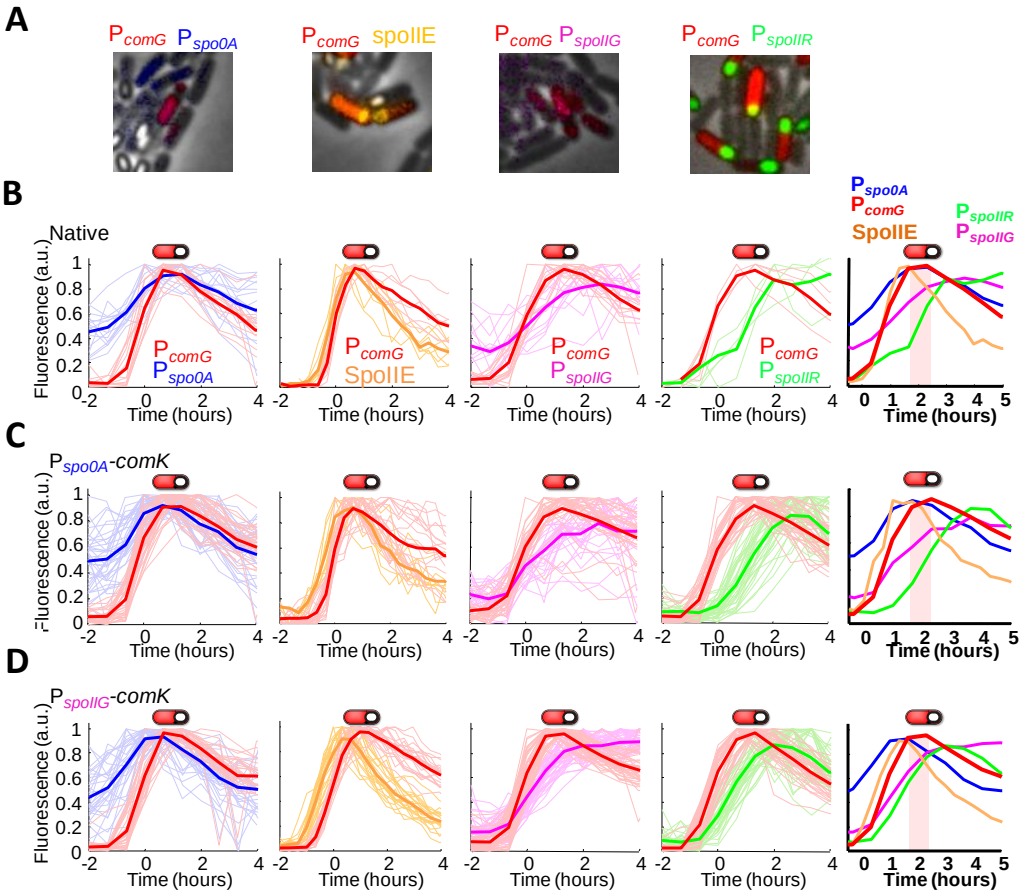

Figure 7.4 (A) DA cells from strains, left to right: [0A-comG]IIGK, [IIE-comG] IIGK, [IIG-comG] IIGK, [IIR-comG] IIGK, expressing pair-wise combinations of one of the sporulation reporters Pspo0A (blue), SpoIIE (orange), PspoIIG (magenta) or PspoIIR (green) and the competence reporter PcomG (red) fused to fluorescent proteins (YFP and CFP respectively). In panels (B) through (D) time traces of single DA are shown in shaded colors, with mean trace shown on top in bright color. All traces have been normalized in amplitude and aligned in time with respect to PcomG activation (>30% of peak activity) which is set as zero time point. The data from the first four panels (from the left) in panels (B) through (D) was combined to produce the fifth panel, as in Figure 6.2B. (B) Strains with no ectopic ComK expression shown here for reference, left to right: 0A-comG, n=15; IIE-comG, n=7; IIG-comG, n=13; IIR-comG, n=4. (C) Strains in which ComK is expressed from the Pspo0A promoter, from left to right: [0A-comG]0A-K, n=36; [IIE-comG]0A-K, n=27; [IIG-comG]0A-K, n=29; [IIR-comG]0A-K, n=39. (D) Strains in which ComK is expressed from the PspoIIG promoter, from left to right: [0A-comG]IIG-K, n=33. [IIE-comG]IIG-K, n =21. [IIG-comG]IIG-K, n=48. [IIR-comG]IIG-K, n=38).

Next, in order to test the molecular race hypothesis, I measured the frequencies of cell fate outcomes in the engineered strains and plotted them against each other in Figure 7.5B, where each dot represents an engineered strain in the "cell fate outcome space" and arrows point out the direction of change introduced by the modifications. As expected, *comK* expression from P_{spoIIR}, which is activated after the decision point (Figure 7.5A, upper panel, see also Figure 6.2B), did not alter cell fate choice relative to the strain with no ectopic *comK* expression, referred to in this experiment as "wild type" (Figure 7.5B). On the other hand, *comK* expression from the early sporulation promoter P_{spo0A} resulted in the marked increase of both competent and DA cells frequencies. Comparing the outcomes, cell fate choice in the P_{spo0A}-comK expressing strain is biased towards competence, with competence frequency increase almost 7-fold from 2% (SD=0.3%) to 13.9% (SD=1.9%) (Figure 7.5B, red arrows). The corresponding slight increase in DA frequency is anticipated, since P_{spo0A} activation curve is broad and not limited to the early stages of sporulation (see Figure 3.2). In contrast, *comK* expression from the later sporulation promoter P_{spoIIG} only slightly increased competence frequency to 5.2% (SD=0.7%), while DA cell frequency rose dramatically from 0.11% (SD=0.04%) to 4.8% (SD=0.2%), a 60-fold increase over the "wild type" (Figure 7.5B, red arrows). The detailed frequencies of cell fate outcomes in the engineered strains are presented in Table 7.1. These results are consistent with our temporal race hypothesis according to which ComK expression during the "decision window" coinciding with SpoIIE and P_{spoIIG} activation should lead to the DA outcome (see Figures 7.2 and 6.2B). Together, the data demonstrate how the differences in timing of ComK expression relative to the sporulation program can influence cellular decision-making.

Expression of *comK* from various sporulation-specific promoters affects not only timing, but the strength of comK expression. It could be argued that the amount of ComK expressed in our experiments during some of the later stages was simply insufficient to drive competence, as opposed to the DA phenotype. Therefore, I investigated the contribution of the strength of ectopic ComK expression by introducing a respective second copy of ComK expression to each strain, expressed from the second copy of the same respective promoter (Figure 7.5A, middle panel). In cells with two copies of P_{spo0A}-*comK*, the frequency of competence relative to the DA outcome increased compared to its single copy counterpart. Specifically, I observed fewer DA cells and more competent cells, leading to the increase of the ratio of competence to DA cells from 5.5 to 29.3 with the addition of the second copy of P_{spo0A}-*comK* (Figure 7.5B, green arrows). On the other hand, in the cells with two copies of P_{spoIIG}-*comK* the DA frequency rose 5 fold relative to their single copy counterpart, reaching 23.6% (SD=2.3%), which is a 300 fold increase relative to the "wild type" strain. However, doubling of P_{spoIIG}-*comK* only increased competence frequency by less than 3-fold (Figure 7.5B, green arrows). These data confirms that doubling the amount of *comK* at the same stage of sporulation development does not change the outcome preference. In other words, the timing dependent bias for either competence or DA outcome remains even when ectopic ComK expression is doubled. Although additional ComK expression did increase the overall frequency of cells expressing ComK, as expected, overall, it is the timing of ComK expression that appears to dictate cell fate choice.

So far, I successfully manipulated the timing of ComK expression relative to the sporulation program. However, another way of altering the cell fate outcomes as

predicted by the temporal competition hypothesis would be slowing down sporulation. In particular, delaying sporulation progress during ComK expression would favor competence. To test this prediction, we ectopically expressed *yneA* from the previously used sporulation stage specific promoters (Figure 7.5A, bottom panel). The *yneA* gene expression is triggered by cellular stress, DNA damage and also, importantly, competence. The product of this gene YneA has been shown to delay growth and suppress cell division by delaying FtsZ ring formation, which is in turn required for both symmetric and asymmetric septation (Haijema et al., 1996; Kawai et al., 2003). Interestingly, asymmetric septum formation by FtsZ, as mentioned above, is a necessary step during sporulation since it triggers SpoIIE localization (Ben-Yehuda and Losick, 2002). As follows, the expression of *yneA* is expected to delay progression to spore formation (Kawai et al., 2003). I confirmed the expected delay by performing single cell measurements of P_{spo0A} and P_{spoIIG} activities in sporulating cells of strains ectopically expressing *yneA* from each of the these promoters. In particular, I found prolonged periods of high P_{spo0A} and P_{spoIIG} expression in some sporulating cells with ectopic *yneA* expression, that were not observed in cells lacking P_{spoIIG}-yneA (Figure 7.6). Therefore, I could utilize ectopic yneA expression driven by sporulation stage-specific promoters to study the effect of sporulation delay on cell fate outcomes.

In accordance to this logic, I ectopically expressed *yneA* in strains described above in addition to ectopic *comK* expression (Figure 7.5A, bottom panel). To synchronize the delay of sporulation and activation of *comK* expression, *yneA* and *comK* were expressed each from a separate copy of the same sporulation-specific promoter. This strategy should allow precise control of the timing between the two differentiation

programs. The data presented in Figure 7.5B shows that *comK* expression and delay of sporulation by *yneA* expression have markedly different effects on cell fate choice. Both at early and late sporulation stages, ectopic expression of *yneA* from either P_{spo0A} or P_{spoIIG} promoters, respectively, increased competence, but not DA cell frequency (Figure 7.5B, blue arrows). On the contrary, DA cell frequency in *yneA*-expressing strains dropped. These data indicate that yneA-mediated shift of sporulation progression relative to ComK expression could also influence cell fate outcomes. In particular, the data shows that a delay of sporulation at either stage favors competence events by giving competence development extra time. These findings further support the molecular race hypothesis.

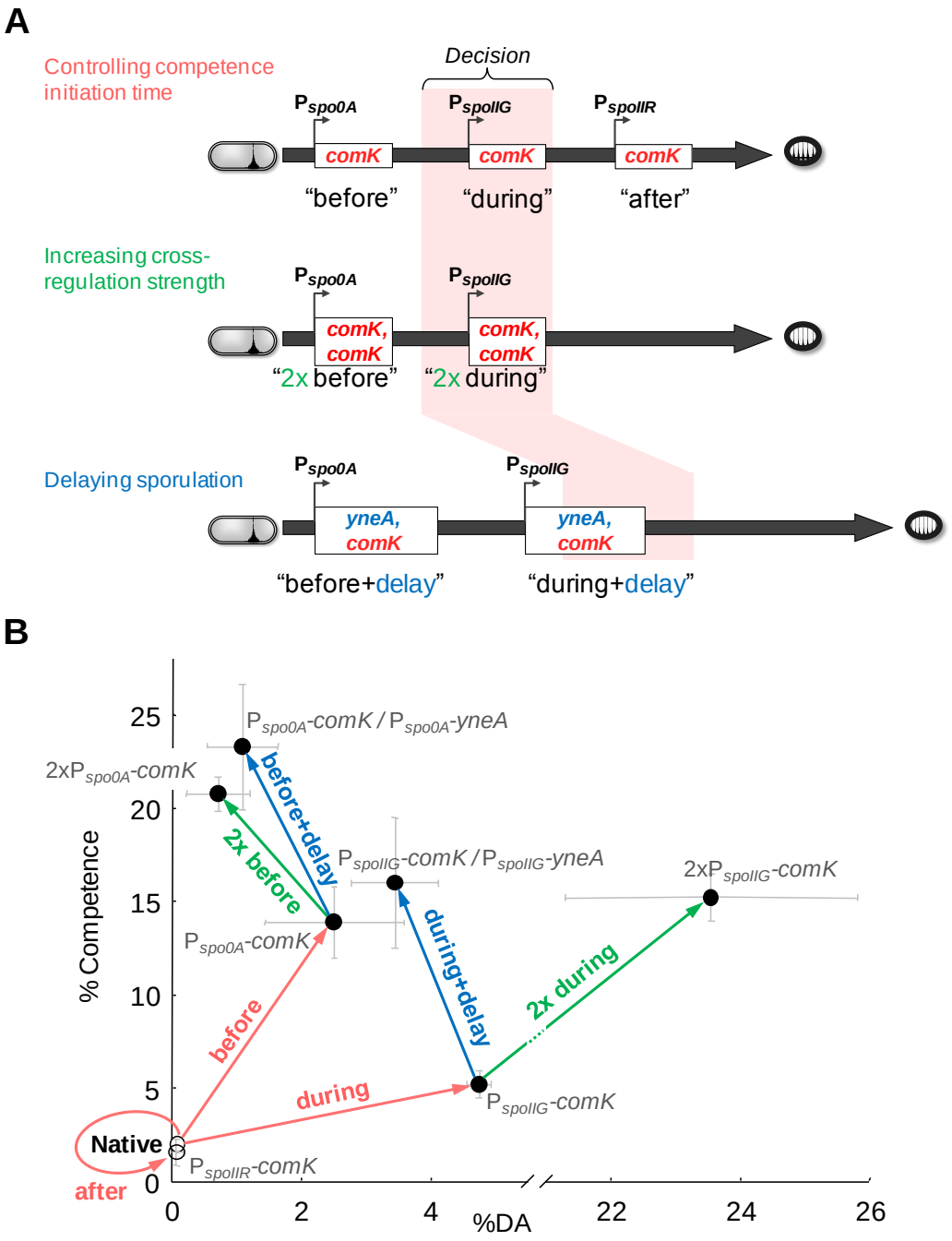

Figure 7.5 (A) Engineered cross-regulatory links between sporulation and competence circuits designed to test the "molecular race" hypothesis. Top panel, comK is ectopically expressed either from the early stage of sporulation (Pspo0A promoter) before the

decision time window discussed in Figure 7.4 (“Decision”, pink area), the later stage close in time to decision (PspoIIG promoter) or past the decision window (PspoIIR promoter). Middle panel, two independent copies of comK gene are ectopically expressed from the indicated promoters (Pspo0A and PspoIIG). Bottom panel, yneA is ectopically expressed together with comK from either early (Pspo0A) or later (PspoIIG) stage of sporulation. (B) Competence and DA fractions measured in the strains expressing yneA and/or comK from early and late stage-specific sporulation promoters as described in panel (A). All strains are also expressing PcomG-CFP to report ComK activity. Each dot indicates the labeled specific strain. ‘Native’ denotes the PY79 B. Subtilis strain expressing only the PcomG reporter. ‘Before’ and ‘During’ expression corresponds to ectopic expression from Pspo0A and PspoIIG promoters, respectively, as shown in panel (A). Red arrows indicate comK expression. Green arrows point to strains expressing two copies of Pspo0A-comK (‘2x before’) and PspoIIG-comK (‘2x during’) denoted ‘2xPspo0A-comK’ and ‘2xPspoIIG-comK’, respectively. Blue arrows show yneA expression from either Pspo0A or PspoIIG promoter, termed ‘before + delay’ and ‘during + delay’, respectively. Detailed statistics for all strains can be found in Table 7.1. Error bars represent standard deviation.

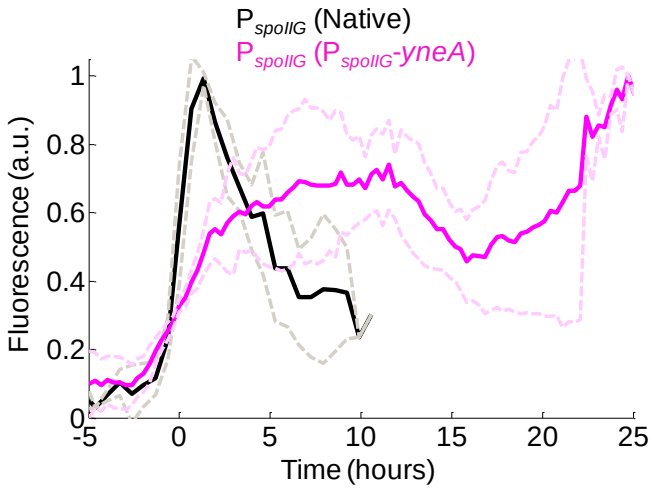

Figure 7.6 Averaged P_{spoIIG}-YFP time traces from single cells of 0A-IIG strain (black, n=5) and strain $[IIG]^{IIG\text{-}yneA}$ in which *yneA* is ectopically expressed from the P_{spoIIG} promoter (magenta, n=5). For $[IIG]^{IIG\text{-}yneA}$ strain, representative cells that express P_{spoIIG} for extended period of time have been selected. For 0A-IIG strain, sample sporulating cells are shown for comparison. The time traces are normalized with respect to maximum and aligned at P_{spoIIG} initiation (>30% of maximum activity). Dashed traces represent standard deviation.

	Native		P_{spo0A}-*comK*		P_{spoIIG}-*comK*		P_{spoIIR}-comK	
	Competent	DA	Competent	DA	Competent	DA	Competent	DA
Mean	**1.98**	**0.08**	**13.87**	**2.51**	**5.20**	**4.75**	**1.55**	**0.06**
STD	0.29	0.10	1.92	1.07	0.70	0.19	0.69	0.13

	2xP_{spoIIG}-comK		2xP_{spo0A}-comK		P_{spoIIG}-*yneA*		P_{spoIIG}-*comK*/P_{spoIIG}-*yneA*	
	Competent	DA	Competent	DA	Competent	DA	Competent	DA
Mean	**15.21**	**23.55**	**20.78**	**0.71**	**0.91**	**0.08**	**16.00**	**3.45**
STD	1.23	2.26	0.91	0.49	0.49	0.14	3.49	0.68

	P_{spo0A}-*yneA*		P_{spo0A}-*comK*/P_{spo0A}-*yneA*		NoE	
	Competent	DA	Competent	DA	Competent	DA
Mean	**2.57**	**0.00**	**23.29**	**1.09**	**7.67**	**2.09**
STD	0.29	0.00	3.36	0.55	0.59	0.26

Table 7.1 Percent fractions of competent and DA cells measured for indicated strains. The frequencies were counted as numbers of ComK initiations per total number of cells observed in a defined time-lapse movie frame (visualized as activity of P_{comG} reporter). A minimum of three measurements was made for each strain. STD, standard deviation.

DISCUSSION

By measuring the timing of two competing morphological processes: polar septation during sporulation and DNA uptake during competence, I found that a mutually exclusive cell fate outcome in DA cells is reached through temporal competition between competence and sporulation. The temporal competition cell-fate decision mechanism suggests that the timing of ComK expression relative to the sporulation program determines the ultimate cell fate outcome. Indeed, a simple calculation based on this hypothesis assuming that ComK activation probability is independent of sporulation progression (as shown in Chapter 4) gives a very precise estimate of DA cell frequency in the population. This finding emphasizes that DA cells are not simply some "broken" cells in which the decision-making process has gone awry, but an expected and normal consequence of the specific chosen decision-making strategy.

Specifically, in these cells ComK has been randomly activated too close in time to polar septation. Regardless of ComK expression, once the sporulation process reaches the step of asymmetric septum formation and the associated localization of SpoIIE, there is insufficient time for such cells to reach the functional state of competence. Cell-fate decision making by this temporal competition mechanism does not prevent ComK expression per se even if competence cell fate is already unreachable. From the cost and benefit perspective, the futile expression of competence-associated genes in DA cells is energetically unfavorable. However, only a small percentage of cells initiate competence and an even smaller fraction ever access the DA state. Therefore, the futile gene expression cost associated with this temporal race only burdens a tiny fraction of the population. On the other hand, if the cells instead employed the checkpoint strategy by maintaining a complex network of cross-regulation that would constantly monitor the state of sporulation, such network would have to be active in all cells. Therefore, in my model organism when one of the cell fates is only activated in a fraction of cell population, the discovered temporary competition mechanism might be beneficial. In the more general case however, different cell fate choice strategies may be favorable depending on whether cells exhibit a frequency bias in adopting alternative cell fates.

A straightforward test for the influence of timing of ComK expression on the ultimate cell fate outcome could be performed by controlling the time of *ComK* expression. One way of implementing this strategy would be coupling of ComK expression to externally inducible promoters. However, sporulation process is highly heterogeneous in time across cells, thereby not permitting exact control over the timing of ComK expression in every individual cell. Instead, I used the native cell intrinsic timing

of the progression to sporulation by coupling ComK expression to the sporulation stage-specific promoters whose activation I measured in Chapter 3. This approach bypasses the need to synchronize cell to cell variability within the population and allows me to test the temporal race prediction in the *B. subtilis* cells sporulating naturally and exhibiting the normal heterogeneity in sporulation timing. Importantly, I could precisely force ComK expression either before, after or during the "decision" time window identified in Figure 6.2B. The unchanged dynamics of decision-making in DA cells of strains with ectopic expression of *comK* emphasize the lack of cross-regulation between competence and sporulation, since an extra copy of *comK* does not seem to influence any sporulation gene expression regardless of *comK* expression strength and timing (Figure 7.4). Nevertheless, the cell fate outcome is drastically changed by manipulating the ComK expression time. The relative contribution of timing versus strength of ComK expression has also been tested, as well as the simultaneous delay of sporulation program (Figure 7.5). The resulting data shows that relative timing between competing differentiation programs is a major determinant of cell fate outcome in my model system.

Importantly, the sole manipulation of relative timing between sporulation and competence allowed the system to experience almost any ratio of cell-fate outcomes. This approach to altering cell fates frequency could allow for subtler fine-tuning of the outcomes, suggesting a possible alternative to more traditional straightforward manipulations such as gene knockouts and overexpression. Perhaps a similar approach could be considered to manipulate the cell fate outcomes in other decision-making systems.

CHAPTER EIGHT

GENERAL DISCUSSION AND FUTURE DIRECTIONS

How cell fate decisions are being made on the level of a single cell is generally poorly understood for most multipotent differentiation systems from microbes to mammalian cells. Over the last few years, an important role of stochasticity has been uncovered in making cell fate decisions. Instead of always following a fixed developmental path determined by hard-wired genetic networks, the cells might accommodate a varying degree of randomness during cell fate decision making (Balazsi et al., 2011; Huang et al., 2010; Maamar et al., 2007; Quesenberry et al., 2005). This may result in heterogeneity, or noise in the process of decision-making. The major source of intracellular noise on a molecular level is believed to be the fluctuating intracellular concentrations of signaling molecules as the result of low molecule numbers and bursts in transcription and translation (Blake et al., 2006). Notably, competence in *B. subtilis* is initiated as a result of noisy expression of the key regulator ComK in a random fraction of cells (Suel et al., 2006).

However, in the same conditions an alternative cell fate of sporulation can become active and compete with competence. Many studies including current work have shown that the development of sporulation genetic program is very heterogeneous even among cells originating from the same single mother cell, suggesting that noise is also a major factor in spore formation (Chastanet et al., 2010; de Jong et al., 2010). Unlike competence, sporulation, once started, seems to be halted or even reversed in a subpopulation of cells, contributing to the overall heterogeneity (see Chapter 3). Given

two competing processes with distinct dynamics, but generally noisy behavior, what would be the best way to relate them to generate mutually exclusive cell fates?

My results suggest that until some later point in the development of either program, there is no cross-talk between them. Rather, the cell fate outcome is determined by temporal competition between competing programs (Chapter 7). Such strategy at first would seem counter-intuitive and even dangerous, since activation of both programs at once could potentially have disastrous consequences. However, as noted before, this strategy seems to be suitable for *B. subtilis*, probably because of the specific properties of both competing programs. For the temporal competition to provide a robust and reliable cell-fate decision mechanism, specific requirements could be in place for the dynamics and durations of competing differentiation programs. For example, sporulation is slow, stepwise and reversible at initial stages, while competence is relatively fast and excitable (Chapter 3). The difference in the dynamics of these processes might enhance the efficiency of the temporal race mechanism.

The cell fate decision-making mechanism based on a similar temporal competition has been described in several other systems. For example, the decision between cell death and slippage in mammalian cells during mitotic arrest appears to be determined by a stochastic kinetic competition between two uncoupled pathways (Huang et al., 2010). In their study the authors either blocked, or accelerated each of the two alternative cell fates and measured the kinetic properties of the remaining one. By comparison of the properties of each cell fate in presence or absence of the competitor, they made the conclusion that the fates are mechanistically independent, with mathematical simulation to support their model. Correlation between times towards

respective fates has also been used for the B-cell fate selection after activation, shown to be mediated by an intracellular stochastic competition (Duffy and Hodgkin, 2012; Duffy et al., 2012). It would be interesting to compare the relative dynamics of these differentiation programs to better understand what are the specific requirements for the temporal competition to provide a robust and reliable cell-fate decision mechanism.

Another interesting feature of decision-making between competence and sporulation is provided by the transient nature of competence cell fate. I have shown that many cells are able to initiate competence at early sporulation stages and complete sporulation after exiting the competent state (see Figures 4.3, 5.2 and 5.3 as example). However, it is unknown whether the cells 'remember' their sporulation progress during competence, or rather lose that information and start the sporulation process anew after completing competence. Depending on the answer, competence can be viewed either as complete 'censorship' of sporulation cell fate or mere 'interruption' of sporulation process. While both scenarios offer potentially interesting implications for decision-making, in the light of my finding suggesting the lack of cross-regulation between sporulation and competence, the corresponding lack of correlation between post-competence sporulation dynamics and pre-competence sporulation activity would be expected. In such case, competence could be also regarded as a temporary relief from the obligation to either grow vegetatively or make the decision to sporulate under the harsh conditions. In other words, the differentiation of a small fraction of cells into competence, in addition to enriching the genetic repertoire of the population, could also provide a 'fresh' pool of cells that would have 'forgotten' their past sporulation activity and would be ready to start this process anew upon exit from competence, somewhat like the

dormant and un-replicating *E. coli* persister cells. Such scenario would fit nicely into the overall theme that seems to be true for *Bacillus subtilis* differentiation strategy: control is good but too much control (and memory) seems to be too big of a burden.

APPENDIX A

A1. MATHEMATICAL MODELING

Population models of sporulation progression

In order to examine the potential advantages of reversible progression to cell fate choice, we compared the response of three simplified models of cellular decision-making to a variable-stress environment. These models describe the dynamics of a population of cells progressing toward sporulation under stress, in terms of the number of cells existing at any given time in a given state along the progression, beginning with the vegetative state and ending in the spore state. The dynamics of cell populations in all these states is given by a set of coupled ordinary differential equations that are linear, and thus can be solved exactly (see below). The three models, shown schematically in Fig. A1.1, involve either a purely irreversible/all-or-none, purely reversible/gradual, or a hybrid process that take cells from their initial vegetative state to their final spore state. In the irreversible-only scheme, cells decide in a single step whether or not to sporulate, and the decision is irreversible. The reversible-only model takes cells gradually toward sporulation through multiple reversible intermediate states, without any real decision taking place along the process. Only the ultimate transition to the spore state, taking place after the decision, is irreversible. Finally, the third model features the actual sporulation dynamics identified here for *B. subtilis* that combines a gradual progression through reversible intermediate states with an irreversible all-or-none decision prior to the spore transition.

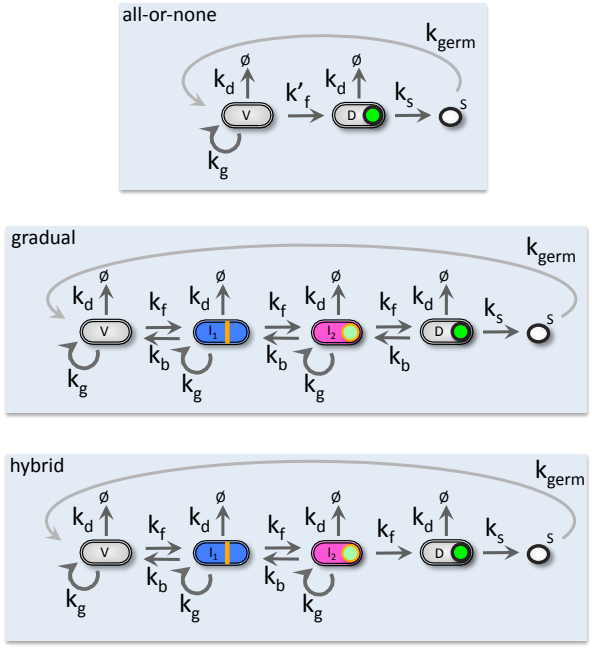

Figure A1.1: Three alternative models of sporulation progression.

Model description

The population dynamics of the cell population as it progresses towards sporulation is given by the following linear dynamical equations:

$$\frac{d\mathbf{n}}{dt} = \mathsf{A}\mathbf{n} \tag{A1.1}$$

where $\mathbf{n}$ is the state vector of the system giving the number of cells in the different states, and A is the matrix that contains the transition rates between cell populations (in what follows we represent vectors by boldface lowercase letters and matrices by uppercase letters). As described above, we consider three different schemes of sporulation progression, shown in Fig. A1.1. For each scheme, the structures of $\mathbf{n}$ and A are different, as we now describe.

- In the *irreversible-only* model, cells decide in a single step whether or not to sporulate. The model comprises three distinct cellular states: vegetative (V), decided (D), and spore (S). The corresponding state vector is thus three dimensional, $\mathbf{n} = (v, d, s)^T$ (with the superindex 'T' indicating transposition of the vector). The transition matrix has the form:

$$\mathsf{A} = \begin{pmatrix} -k'_f - k_d + k_g + k_{\text{germ}} & 0 & 0 \\ k'_f & -k_d - k_s & 0 \\ 0 & k_s & -k_{\text{germ}} \end{pmatrix}$$

  Note that the rank of A is 2, because the spore dynamics does not affect the other two variables. The number of spores is merely a readout of the cell population in the presence of sustained stress. The transition rates on which A depends are defined in Fig. A1.1.

- In the *reversible-only model*, the transition from vegetative cells to spores occurs in a multi-step manner. Here we assume two distinct intermediate states (I_1 and I_2). Note that there is no all-or-none decision in this case, because the final transition to the decided state (D) is reversible. In this scenario, cells simply "leak" towards sporulation while they are in the so-called decided state. The state vector is now five-dimensional, $\mathbf{n} = (v, i_1, i_2, d, s)^T$. The transition matrix has the form:

$$\mathsf{A} = \begin{pmatrix} -k_f - k_d + k_g + k_{\text{germ}} & k_b & 0 & 0 & 0 \\ k_f & k_g - k_d - k_b - k_f & k_b & 0 & 0 \\ 0 & k_f & k_g - k_d - k_b - k_f & k_b & 0 \\ 0 & 0 & k_f & -k_s - k_d - k_b & 0 \\ 0 & 0 & 0 & k_s & -k_{\text{germ}} \end{pmatrix}$$

- The *hybrid model* combines characteristics of both the irreversible-only and reversible-

only models described above. On the one hand, the model is irreversible because the transition towards the decided state is all-or-none. On the other other, the model progresses gradually towards that decision via intermediate steps. The state vector is again five-dimensional, $\mathbf{n} = (v, i_1, i_2, d, s)^T$, and the transition matrix now takes the form:

$$\mathsf{A} = \begin{pmatrix} -k_f - k_d + k_g + k_{\text{germ}} & k_b & 0 & 0 & 0 \\ k_f & k_g - k_d - k_b - k_f & k_b & 0 & 0 \\ 0 & k_f & k_g - k_d - k_b - k_f & 0 & 0 \\ 0 & 0 & k_f & -k_s - k_d & 0 \\ 0 & 0 & 0 & k_s & -k_{\text{germ}} \end{pmatrix}$$

Temporal evolution in a constant environment

Since Eq. (A1.1) is linear, it can be solved in a straightforward way in the case of a constant environment (i.e. for constant reaction rates). The solution is simply

$$\mathbf{n}(t) = \sum_{i=1}^{d} c_i \mathbf{v_i} \exp(\lambda_i t)\,, \tag{A1.2}$$

where d denotes the dimension of the square matrix A, whose eigenvalues are represented by λ_i and the eigenvectors by $\mathbf{v_i}$. The scalars c_i are integration constants that depend on the initial condition of the trajectory. This solution can be expressed in a more compact form by defining the $d \times d$ matrix of eigenvectors V (whose columns are the eigenvectors of A), the $d \times d$ matrix of eigenvalues Λ (a diagonal matrix whose diagonal elements are the eigenvalues of A), and the d-dimensional vector $\mathbf{c}$ of integration constants. With those

definitions, the solution (A1.2) can be written as

$$\mathbf{n}(t) = \mathsf{V} \exp(\Lambda t)\, \mathbf{c} \tag{A1.3}$$

The expression that gives the values of the integration constants in terms of the initial conditions is simply

$$\mathbf{n}(0) = \mathsf{V}\mathbf{c} \quad \Longrightarrow \quad \mathbf{c} = \mathsf{V}^{-1}\mathbf{n}(0)$$

Thus the final expression for the system's dynamics is simply:

$$\mathbf{n}(t) = \mathsf{V} \exp(\Lambda t)\, \mathsf{V}^{-1}\mathbf{n}(0) \tag{A1.4}$$

Temporal evolution under dichotomic stress cycles

In order to examine the response of each of the three models described above to a varying environment, we now consider a random dichotomic variation of the stress as shown in the main text. In this scenario, the stress fluctuates randomly between two values, with the low-stress (rich) and high-stress (poor) phases lasting a time that follows an exponentially decreasing distribution corresponding to a random Poisson process.

The two phases have distinct values of the reaction parameters defined in Fig. A1.1. For instance, we assume that during the low-stress phase there is no progression towards sporulation ($k_f = k_s = 0$) and the death rate is very small in comparison with the growth rate. Oppositely, during the high-stress phase we consider that there is no possibility to reverse the sporulation progression ($k_b = 0$), while the growth rate is greatly diminished with re-

spect to the rich-medium condition. The specific parameter values used in this paper are given in Table A1.1. We note that k_f and k'_f are chosen such that the average time to the decision (from V to D) is the same in all models (i.e. $k'_f = k_f/3$).

rate	value (rich phase)	value (poor phase)
k_f	0	0.6
k'_f	0	0.2
k_b	20	0
k_g	1	0.1
k_d	0.1	1
k_s	0	0.2
k_{germ}	0.1	0

Table A1.1: Parameter values in the rich and poor phases.

Let T be the total duration of the environmental cycle, and t_p and t_r the durations of the poor and rich phases, respectively (see Fig. A1.2). After the poor phase of the first cycle,

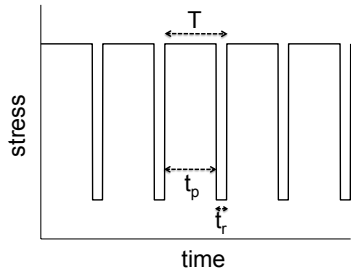

Figure A1.2: Stress modulation.

the population is, according to Eq. (A1.4),

$$\mathbf{n}(t_p) = \mathsf{V}_\mathsf{p} \exp\left(\Lambda_\mathsf{p} t_p\right) \mathsf{V}_\mathsf{p}^{-1} \mathbf{n}(0) \tag{A1.5}$$

This value is now used as initial condition of the following rich phase, after which the population is:

$$\mathbf{n}_1 = \mathsf{V}_\mathsf{r} \exp\left(\Lambda_\mathsf{r} t_r\right) \mathsf{V}_\mathsf{r}^{-1} \mathsf{V}_\mathsf{p} \exp\left(\Lambda_\mathsf{p} t_p\right) \mathsf{V}_\mathsf{p}^{-1} \mathbf{n}_0 \,, \tag{A1.6}$$

where the subindex in **n** denotes now the cycle. After q cycles, the population is thus

$$\mathbf{n}_q = \left(\mathsf{V}_\mathsf{r} \exp\left(\Lambda_\mathsf{r} t_r\right) \mathsf{V}_\mathsf{r}^{-1} \mathsf{V}_\mathsf{p} \exp\left(\Lambda_\mathsf{p} t_p\right) \mathsf{V}_\mathsf{p}^{-1}\right)^q \mathbf{n}_0 \,. \tag{A1.7}$$

BIBLIOGRAPHY

Amati, G., Bisicchia, P., and Galizzi, A. (2004). DegU-P represses expression of the motility fla-che operon in Bacillus subtilis. Journal of bacteriology 186, 6003-6014.

Arigoni, F., Duncan, L., Alper, S., Losick, R., and Stragier, P. (1996). SpoIIE governs the phosphorylation state of a protein regulating transcription factor sigma F during sporulation in Bacillus subtilis. Proceedings of the National Academy of Sciences of the United States of America 93, 3238-3242.

Asai, K., Kawamura, F., Yoshikawa, H., and Takahashi, H. (1995). Expression of kinA and accumulation of sigma H at the onset of sporulation in Bacillus subtilis. Journal of bacteriology 177, 6679-6683.

Asayama, M., and Kobayashi, Y. (1993). Signal transduction and sporulation in Bacillus subtilis: heterologous phosphorylation of Spo0A, a sporulation initiation gene product. Journal of biochemistry 114, 385-388.

Asayama, M., Yamamoto, A., and Kobayashi, Y. (1995). Dimer form of phosphorylated Spo0A, a transcriptional regulator, stimulates the spo0F transcription at the initiation of sporulation in Bacillus subtilis. Journal of molecular biology 250, 11-23.

Bai, U., Mandic-Mulec, I., and Smith, I. (1993). SinI modulates the activity of SinR, a developmental switch protein of Bacillus subtilis, by protein-protein interaction. Genes & development 7, 139-148.

Balaban, N.Q., Merrin, J., Chait, R., Kowalik, L., and Leibler, S. (2004). Bacterial persistence as a phenotypic switch. Science 305, 1622-1625.

Balazsi, G., van Oudenaarden, A., and Collins, J.J. (2011). Cellular decision making and biological noise: from microbes to mammals. Cell 144, 910-925.

Barak, I., Behari, J., Olmedo, G., Guzman, P., Brown, D.P., Castro, E., Walker, D., Westpheling, J., and Youngman, P. (1996). Structure and function of the Bacillus SpoIIE protein and its localization to sites of sporulation septum assembly. Molecular microbiology 19, 1047-1060.

Ben-Yehuda, S., and Losick, R. (2002). Asymmetric cell division in B. subtilis involves a spiral-like intermediate of the cytokinetic protein FtsZ. Cell 109, 257-266.

Berka, R.M., Hahn, J., Albano, M., Draskovic, I., Persuh, M., Cui, X., Sloma, A., Widner, W., and Dubnau, D. (2002). Microarray analysis of the Bacillus subtilis K-state: genome-wide expression changes dependent on ComK. Molecular microbiology 43, 1331-1345.

Bertrand, J.Y., and Traver, D. (2009). Hematopoietic cell development in the zebrafish embryo. Curr Opin Hematol 16, 243-248.

Black, F., and Myron, S. (1973). The Pricing of Options and Corporate Liabilities. The Journal of Political Economy 81, 637-654.

Blake, W.J., Balazsi, G., Kohanski, M.A., Isaacs, F.J., Murphy, K.F., Kuang, Y., Cantor, C.R., Walt, D.R., and Collins, J.J. (2006). Phenotypic consequences of promoter-mediated transcriptional noise. Mol Cell 24, 853-865.

Bongiorni, C., Ishikawa, S., Stephenson, S., Ogasawara, N., and Perego, M. (2005). Synergistic regulation of competence development in Bacillus subtilis by two Rap-Phr systems. Journal of bacteriology 187, 4353-4361.

Briley, K., Jr., Dorsey-Oresto, A., Prepiak, P., Dias, M.J., Mann, J.M., and Dubnau, D. (2011). The secretion ATPase ComGA is required for the binding and transport of transforming DNA. Molecular microbiology 81, 818-830.

Britton, R.A., Eichenberger, P., Gonzalez-Pastor, J.E., Fawcett, P., Monson, R., Losick, R., and Grossman, A.D. (2002). Genome-wide analysis of the stationary-phase sigma factor (sigma-H) regulon of Bacillus subtilis. Journal of bacteriology 184, 4881-4890.

Burbulys, D., Trach, K.A., and Hoch, J.A. (1991). Initiation of sporulation in B. subtilis is controlled by a multicomponent phosphorelay. Cell 64, 545-552.

Cagatay, T., Turcotte, M., Elowitz, M.B., Garcia-Ojalvo, J., and Suel, G.M. (2009). Architecture-dependent noise discriminates functionally analogous differentiation circuits. Cell 139, 512-522.

Campo, N., Marquis, K.A., and Rudner, D.Z. (2008). SpoIIQ anchors membrane proteins on both sides of the sporulation septum in Bacillus subtilis. The Journal of biological chemistry 283, 4975-4982.

Cervin, M.A., Lewis, R.J., Brannigan, J.A., and Spiegelman, G.B. (1998). The Bacillus subtilis regulator SinR inhibits spoIIG promoter transcription in vitro without displacing RNA polymerase. Nucleic acids research 26, 3806-3812.

Chastanet, A., Vitkup, D., Yuan, G.C., Norman, T.M., Liu, J.S., and Losick, R.M. (2010). Broadly heterogeneous activation of the master regulator for sporulation in Bacillus subtilis. Proceedings of the National Academy of Sciences of the United States of America.

Choi, H.S., Han, S., Yokota, H., and Cho, K.H. (2007). Coupled positive feedbacks provoke slow induction plus fast switching in apoptosis. FEBS Lett 581, 2684-2690.

Chung, J.D., Stephanopoulos, G., Ireton, K., and Grossman, A.D. (1994). Gene expression in single cells of Bacillus subtilis: evidence that a threshold mechanism controls the initiation of sporulation. Journal of bacteriology 176, 1977-1984.

Chung, Y.S., Breidt, F., and Dubnau, D. (1998). Cell surface localization and processing of the ComG proteins, required for DNA binding during transformation of Bacillus subtilis. Molecular microbiology 29, 905-913.

Chung, Y.S., and Dubnau, D. (1998). All seven comG open reading frames are required for DNA binding during transformation of competent Bacillus subtilis. Journal of bacteriology 180, 41-45.

Comella, N., and Grossman, A.D. (2005). Conservation of genes and processes controlled by the quorum response in bacteria: characterization of genes controlled by the quorum-sensing transcription factor ComA in Bacillus subtilis. Molecular microbiology 57, 1159-1174.

Core, L., and Perego, M. (2003). TPR-mediated interaction of RapC with ComA inhibits response regulator-DNA binding for competence development in Bacillus subtilis. Molecular microbiology 49, 1509-1522.

Dahl, M.K., Msadek, T., Kunst, F., and Rapoport, G. (1992). The phosphorylation state of the DegU response regulator acts as a molecular switch allowing either degradative enzyme synthesis or expression of genetic competence in Bacillus subtilis. The Journal of biological chemistry 267, 14509-14514.

de Jong, I.G., Veening, J.W., and Kuipers, O.P. (2010). Heterochronic phosphorelay gene expression as a source of heterogeneity in Bacillus subtilis spore formation. Journal of bacteriology 192, 2053-2067.

Dubnau, D. (1991a). Genetic competence in Bacillus subtilis. Microbiological reviews 55, 395-424.

Dubnau, D. (1991b). The regulation of genetic competence in Bacillus subtilis. Molecular microbiology 5, 11-18.

Dubnau, D. (1999). DNA uptake in bacteria. Annu Rev Microbiol 53, 217-244.

Dubnau, D., Hahn, J., Roggiani, M., Piazza, F., and Weinrauch, Y. (1994). Two-component regulators and genetic competence in Bacillus subtilis. Research in microbiology 145, 403-411.

Dubnau, D., and Losick, R. (2006). Bistability in bacteria. Molecular microbiology 61, 564-572.

Duffy, K.R., and Hodgkin, P.D. (2012). Intracellular competition for fates in the immune system. Trends in cell biology 22, 457-464.

Duffy, K.R., Wellard, C.J., Markham, J.F., Zhou, J.H., Holmberg, R., Hawkins, E.D., Hasbold, J., Dowling, M.R., and Hodgkin, P.D. (2012). Activation-induced B cell fates are selected by intracellular stochastic competition. Science 335, 338-341.

Dworkin, J., and Losick, R. (2005). Developmental commitment in a bacterium. Cell 121, 401-409.

Errington, J. (1993). Bacillus subtilis sporulation: regulation of gene expression and control of morphogenesis. Microbiological reviews 57, 1-33.

Errington, J. (2003). Regulation of endospore formation in Bacillus subtilis. Nature reviews Microbiology 1, 117-126.

Eswaramoorthy, P., Duan, D., Dinh, J., Dravis, A., Devi, S.N., and Fujita, M. (2010). The threshold level of the sensor histidine kinase KinA governs entry into sporulation in Bacillus subtilis. Journal of bacteriology 192, 3870-3882.

Ferrell, J.E., Jr., and Machleder, E.M. (1998). The biochemical basis of an all-or-none cell fate switch in Xenopus oocytes. Science 280, 895-898.

Flynn, J.M., Levchenko, I., Seidel, M., Wickner, S.H., Sauer, R.T., and Baker, T.A. (2001). Overlapping recognition determinants within the ssrA degradation tag allow modulation of proteolysis. Proceedings of the National Academy of Sciences of the United States of America 98, 10584-10589.

Frandsen, N., and Stragier, P. (1995). Identification and characterization of the Bacillus subtilis spoIIP locus. Journal of bacteriology 177, 716-722.

Fujita, M., Gonzalez-Pastor, J.E., and Losick, R. (2005). High- and low-threshold genes in the Spo0A regulon of Bacillus subtilis. Journal of bacteriology 187, 1357-1368.

Fujita, M., and Losick, R. (2002). An investigation into the compartmentalization of the sporulation transcription factor sigmaE in Bacillus subtilis. Molecular microbiology 43, 27-38.

Fujita, M., and Losick, R. (2005). Evidence that entry into sporulation in Bacillus subtilis is governed by a gradual increase in the level and activity of the master regulator Spo0A. Genes & development 19, 2236-2244.

Fujita, M., and Sadaie, Y. (1998). Feedback loops involving Spo0A and AbrB in in vitro transcription of the genes involved in the initiation of sporulation in Bacillus subtilis. Journal of biochemistry 124, 98-104.

Gottesman, S., Roche, E., Zhou, Y., and Sauer, R.T. (1998). The ClpXP and ClpAP proteases degrade proteins with carboxy-terminal peptide tails added by the SsrA-tagging system. Genes & development 12, 1338-1347.

Griffith, K.L., and Grossman, A.D. (2008). Inducible protein degradation in Bacillus subtilis using heterologous peptide tags and adaptor proteins to

target substrates to the protease ClpXP. Molecular microbiology 70, 1012-1025.

Grossman, A.D. (1995). Genetic networks controlling the initiation of sporulation and the development of genetic competence in Bacillus subtilis. Annu Rev Genet 29, 477-508.

Hahn, J., Luttinger, A., and Dubnau, D. (1996). Regulatory inputs for the synthesis of ComK, the competence transcription factor of Bacillus subtilis. Molecular microbiology 21, 763-775.

Hahn, J., Maier, B., Haijema, B.J., Sheetz, M., and Dubnau, D. (2005). Transformation proteins and DNA uptake localize to the cell poles in Bacillus subtilis. Cell 122, 59-71.

Hahn, J., Roggiani, M., and Dubnau, D. (1995). The major role of Spo0A in genetic competence is to downregulate abrB, an essential competence gene. Journal of bacteriology 177, 3601-3605.

Haijema, B.J., Hahn, J., Haynes, J., and Dubnau, D. (2001). A ComGA-dependent checkpoint limits growth during the escape from competence. Molecular microbiology 40, 52-64.

Haijema, B.J., van Sinderen, D., Winterling, K., Kooistra, J., Venema, G., and Hamoen, L.W. (1996). Regulated expression of the dinR and recA genes during competence development and SOS induction in Bacillus subtilis. Molecular microbiology 22, 75-85.

Haima, P., Bron, S., and Venema, G. (1987). The effect of restriction on shotgun cloning and plasmid stability in Bacillus subtilis Marburg. Mol Gen Genet 209, 335-342.

Hamoen, L.W., Kausche, D., Marahiel, M.A., van Sinderen, D., Venema, G., and Serror, P. (2003). The Bacillus subtilis transition state regulator AbrB binds to the -35 promoter region of comK. FEMS Microbiol Lett 218, 299-304.

Hamoen, L.W., Van Werkhoven, A.F., Venema, G., and Dubnau, D. (2000). The pleiotropic response regulator DegU functions as a priming protein in competence development in Bacillus subtilis. Proceedings of the National Academy of Sciences of the United States of America 97, 9246-9251.

Hilbert, D.W., and Piggot, P.J. (2004). Compartmentalization of gene expression during Bacillus subtilis spore formation. Microbiol Mol Biol Rev 68, 234-262.

Hoa, T.T., Tortosa, P., Albano, M., and Dubnau, D. (2002). Rok (YkuW) regulates genetic competence in Bacillus subtilis by directly repressing comK. Molecular microbiology 43, 15-26.

Hoch, J.A. (1976). Genetics of bacterial sporulation. Adv Genet 18, 69-98.

Hoch, J.A. (1993a). The phosphorelay signal transduction pathway in the initiation of Bacillus subtilis sporulation. J Cell Biochem 51, 55-61.

Hoch, J.A. (1993b). Regulation of the phosphorelay and the initiation of sporulation in Bacillus subtilis. Annu Rev Microbiol 47, 441-465.

Hofmeister, A.E., Londono-Vallejo, A., Harry, E., Stragier, P., and Losick, R. (1995). Extracellular signal protein triggering the proteolytic activation of a developmental transcription factor in B. subtilis. Cell 83, 219-226.

Horneck, G., Moeller, R., Cadet, J., Douki, T., Mancinelli, R.L., Nicholson, W.L., Panitz, C., Rabbow, E., Rettberg, P., Spry, A., et al. (2012). Resistance of bacterial endospores to outer space for planetary protection purposes--experiment PROTECT of the EXPOSE-E mission. Astrobiology 12, 445-456.

Hosoya, S., Lu, Z., Ozaki, Y., Takeuchi, M., and Sato, T. (2007). Cytological analysis of the mother cell death process during sporulation in Bacillus subtilis. Journal of bacteriology 189, 2561-2565.

Hosoya, T., Maillard, I., and Engel, J.D. (2010). From the cradle to the grave: activities of GATA-3 throughout T-cell development and differentiation. Immunol Rev 238, 110-125.

Huang, H.C., Mitchison, T.J., and Shi, J. (2010). Stochastic competition between mechanistically independent slippage and death pathways determines cell fate during mitotic arrest. PLoS One 5, e15724.

Huang, H.C., Shi, J., Orth, J.D., and Mitchison, T.J. (2009). Evidence that mitotic exit is a better cancer therapeutic target than spindle assembly. Cancer Cell 16, 347-358.

Itano, A., and Neill, J. (1919). Influence of Temperature and Hydrogen Ion Concentration Upon the Spore Cycle of Bacillus Subtilis. The Journal of general physiology 1, 421-428.

Jiang, M., Shao, W., Perego, M., and Hoch, J.A. (2000). Multiple histidine kinases regulate entry into stationary phase and sporulation in Bacillus subtilis. Molecular microbiology 38, 535-542.

Karow, M.L., Glaser, P., and Piggot, P.J. (1995). Identification of a gene, spoIIR, that links the activation of sigma E to the transcriptional activity of sigma F during sporulation in Bacillus subtilis. Proceedings of the National Academy of Sciences of the United States of America 92, 2012-2016.

Kawai, Y., Moriya, S., and Ogasawara, N. (2003). Identification of a protein, YneA, responsible for cell division suppression during the SOS response in Bacillus subtilis. Molecular microbiology 47, 1113-1122.

Keeble, J.A., and Gilmore, A.P. (2007). Apoptosis commitment--translating survival signals into decisions on mitochondria. Cell research 17, 976-984.

Kerney, K.R., and Schuerger, A.C. (2011). Survival of Bacillus subtilis endospores on ultraviolet-irradiated rover wheels and Mars regolith under simulated Martian conditions. Astrobiology 11, 477-485.

Khvorova, A., Chary, V.K., Hilbert, D.W., and Piggot, P.J. (2000). The chromosomal location of the Bacillus subtilis sporulation gene spoIIR is important for its function. Journal of bacteriology 182, 4425-4429.

Khvorova, A., Zhang, L., Higgins, M.L., and Piggot, P.J. (1998). The spoIIE locus is involved in the Spo0A-dependent switch in the location of FtsZ rings in Bacillus subtilis. Journal of bacteriology 180, 1256-1260.

Klein, L., and Jovanovic, K. (2011). Regulatory T cell lineage commitment in the thymus. Seminars in immunology 23, 401-409.

Kobayashi, K. (2007). Gradual activation of the response regulator DegU controls serial expression of genes for flagellum formation and biofilm formation in Bacillus subtilis. Molecular microbiology 66, 395-409.

Kruger, N.J., and Stingl, K. (2011). Two steps away from novelty--principles of bacterial DNA uptake. Molecular microbiology 80, 860-867.

Kunst, F., Msadek, T., Bignon, J., and Rapoport, G. (1994). The DegS/DegU and ComP/ComA two-component systems are part of a network controlling degradative enzyme synthesis and competence in Bacillus subtilis. Research in microbiology 145, 393-402.

Kussell, E., and Leibler, S. (2005). Phenotypic diversity, population growth, and information in fluctuating environments. Science 309, 2075-2078.

Lazazzera, B.A. (2000). Quorum sensing and starvation: signals for entry into stationary phase. Current opinion in microbiology 3, 177-182.

Levchenko, I., Seidel, M., Sauer, R.T., and Baker, T.A. (2000). A specificity-enhancing factor for the ClpXP degradation machine. Science 289, 2354-2356.

Lewandoski, M., Dubnau, E., and Smith, I. (1986). Transcriptional regulation of the spo0F gene of Bacillus subtilis. Journal of bacteriology 168, 870-877.

Lewis, P.J., Wu, L.J., and Errington, J. (1998). Establishment of prespore-specific gene expression in Bacillus subtilis: localization of SpoIIE phosphatase and initiation of compartment-specific proteolysis. Journal of bacteriology 180, 3276-3284.

Londono-Vallejo, J.A., Frehel, C., and Stragier, P. (1997). SpoIIQ, a forespore-expressed gene required for engulfment in Bacillus subtilis. Molecular microbiology 24, 29-39.

Lopez, D., Vlamakis, H., and Kolter, R. (2009). Generation of multiple cell types in Bacillus subtilis. FEMS microbiology reviews 33, 152-163.

Maamar, H., Raj, A., and Dubnau, D. (2007). Noise in gene expression determines cell fate in Bacillus subtilis. Science 317, 526-529.

Magnuson, R., Solomon, J., and Grossman, A.D. (1994). Biochemical and genetic characterization of a competence pheromone from B. subtilis. Cell 77, 207-216.

Malhotra, S., and Kincade, P.W. (2009). Wnt-related molecules and signaling pathway equilibrium in hematopoiesis. Cell Stem Cell 4, 27-36.

Malleshaiah, M.K., Shahrezaei, V., Swain, P.S., and Michnick, S.W. (2010). The scaffold protein Ste5 directly controls a switch-like mating decision in yeast. Nature.

Mandic-Mulec, I., Doukhan, L., and Smith, I. (1995). The Bacillus subtilis SinR protein is a repressor of the key sporulation gene spo0A. Journal of bacteriology 177, 4619-4627.

Middleton, R., and Hofmeister, A. (2004). New shuttle vectors for ectopic insertion of genes into Bacillus subtilis. Plasmid 51, 238-245.

Mirouze, N., Desai, Y., Raj, A., and Dubnau, D. (2012). Spo0A~P imposes a temporal gate for the bimodal expression of competence in Bacillus subtilis. PLoS genetics 8, e1002586.

Moir, A. (2006). How do spores germinate? Journal of applied microbiology 101, 526-530.

Moldovan, N.I. (2005). Functional adaptation: the key to plasticity of cardiovascular "stem" cells? Stem Cells Dev 14, 111-121.

Molle, V., Fujita, M., Jensen, S.T., Eichenberger, P., Gonzalez-Pastor, J.E., Liu, J.S., and Losick, R. (2003). The Spo0A regulon of Bacillus subtilis. Molecular microbiology 50, 1683-1701.

Ogura, M., Liu, L., Lacelle, M., Nakano, M.M., and Zuber, P. (1999). Mutational analysis of ComS: evidence for the interaction of ComS and MecA in the regulation of competence development in Bacillus subtilis. Molecular microbiology 32, 799-812.

Ohlsen, K.L., Grimsley, J.K., and Hoch, J.A. (1994). Deactivation of the sporulation transcription factor Spo0A by the Spo0E protein phosphatase. Proceedings of the National Academy of Sciences of the United States of America 91, 1756-1760.

Parker, G.F., Daniel, R.A., and Errington, J. (1996). Timing and genetic regulation of commitment to sporulation in Bacillus subtilis. Microbiology 142 (Pt 12), 3445-3452.

Parra, M. (2009). Epigenetic events during B lymphocyte development. Epigenetics 4, 462-468.

Perego, M. (2001). A new family of aspartyl phosphate phosphatases targeting the sporulation transcription factor Spo0A of Bacillus subtilis. Molecular microbiology 42, 133-143.

Perego, M., and Hoch, J.A. (1991). Negative regulation of Bacillus subtilis sporulation by the spo0E gene product. Journal of bacteriology 173, 2514-2520.

Perkins, T.J., and Swain, P.S. (2009). Strategies for cellular decision-making. Mol Syst Biol 5, 326.

Pfeuty, B. (2012). Dynamical principles of cell-cycle arrest: reversible, irreversible, and mixed strategies. Physical review E, Statistical, nonlinear, and soft matter physics 86, 021917.

Phillips, Z.E., and Strauch, M.A. (2002). Bacillus subtilis sporulation and stationary phase gene expression. Cell Mol Life Sci 59, 392-402.

Piggot, P.J., and Hilbert, D.W. (2004). Sporulation of Bacillus subtilis. Current opinion in microbiology 7, 579-586.

Pottathil, M., and Lazazzera, B.A. (2003). The extracellular Phr peptide-Rap phosphatase signaling circuit of Bacillus subtilis. Frontiers in bioscience : a journal and virtual library 8, d32-45.

Prindull, G.A., and Fibach, E. (2007). Are postnatal hemangioblasts generated by dedifferentiation from committed hematopoietic stem cells? Exp Hematol 35, 691-701.

Quesenberry, P., Abedi, M., Dooner, M., Colvin, G., Sanchez-Guijo, F.M., Aliotta, J., Pimentel, J., Dooner, G., Greer, D., Demers, D., et al. (2005). The marrow cell continuum: stochastic determinism. Folia Histochem Cytobiol 43, 187-190.

Quesenberry, P.J., and Aliotta, J.M. (2008). The paradoxical dynamism of marrow stem cells: considerations of stem cells, niches, and microvesicles. Stem Cell Rev 4, 137-147.

Roberts, J.L., White, W.C., and Ojerholm, E. (1938). Influence of Osmotic Pressure on Sporulation by Bacillus Subtilis. Plant physiology 13, 649-653.

Rosenfeld, N., Young, J.W., Alon, U., Swain, P.S., and Elowitz, M.B. (2005). Gene regulation at the single-cell level. Science 307, 1962-1965.

Sanosaka, T., Namihira, M., and Nakashima, K. (2009). Epigenetic mechanisms in sequential differentiation of neural stem cells. Epigenetics 4, 89-92.

Schlothauer, T., Mogk, A., Dougan, D.A., Bukau, B., and Turgay, K. (2003). MecA, an adaptor protein necessary for ClpC chaperone activity. Proceedings of the National Academy of Sciences of the United States of America 100, 2306-2311.

Schultz, D., Wolynes, P.G., Ben Jacob, E., and Onuchic, J.N. (2009). Deciding fate in adverse times: sporulation and competence in Bacillus subtilis. Proceedings of the National Academy of Sciences of the United States of America 106, 21027-21034.

Serror, P., and Sonenshein, A.L. (1996a). CodY is required for nutritional repression of Bacillus subtilis genetic competence. Journal of bacteriology 178, 5910-5915.

Serror, P., and Sonenshein, A.L. (1996b). Interaction of CodY, a novel Bacillus subtilis DNA-binding protein, with the dpp promoter region. Molecular microbiology 20, 843-852.

Setlow, P. (2006). Spores of Bacillus subtilis: their resistance to and killing by radiation, heat and chemicals. Journal of applied microbiology 101, 514-525.

Shafikhani, S.H., Mandic-Mulec, I., Strauch, M.A., Smith, I., and Leighton, T. (2002). Postexponential regulation of sin operon expression in Bacillus subtilis. Journal of bacteriology 184, 564-571.

Smits, W.K., Bongiorni, C., Veening, J.W., Hamoen, L.W., Kuipers, O.P., and Perego, M. (2007). Temporal separation of distinct differentiation pathways by a dual specificity Rap-Phr system in Bacillus subtilis. Molecular microbiology 65, 103-120.

Sonenshein, A.L. (2005). CodY, a global regulator of stationary phase and virulence in Gram-positive bacteria. Current opinion in microbiology 8, 203-207.

Sterlini, J.M., and Mandelstam, J. (1969). Commitment to sporulation in Bacillus subtilis and its relationship to development of actinomycin resistance. Biochem J 113, 29-37.

Stragier, P., Bonamy, C., and Karmazyn-Campelli, C. (1988). Processing of a sporulation sigma factor in Bacillus subtilis: how morphological structure could control gene expression. Cell 52, 697-704.

Stragier, P., and Losick, R. (1996). Molecular genetics of sporulation in Bacillus subtilis. Annu Rev Genet 30, 297-241.

Strauch, M., Webb, V., Spiegelman, G., and Hoch, J.A. (1990). The SpoOA protein of Bacillus subtilis is a repressor of the abrB gene. Proceedings of the National Academy of Sciences of the United States of America 87, 1801-1805.

Strauch, M.A., Trach, K.A., Day, J., and Hoch, J.A. (1992). Spo0A activates and represses its own synthesis by binding at its dual promoters. Biochimie 74, 619-626.

Strauch, M.A., Wu, J.J., Jonas, R.H., and Hoch, J.A. (1993). A positive feedback loop controls transcription of the spoOF gene, a component of the sporulation phosphorelay in Bacillus subtilis. Molecular microbiology 7, 967-974.

Suel, G.M., Garcia-Ojalvo, J., Liberman, L.M., and Elowitz, M.B. (2006). An excitable gene regulatory circuit induces transient cellular differentiation. Nature 440, 545-550.

Suel, G.M., Kulkarni, R.P., Dworkin, J., Garcia-Ojalvo, J., and Elowitz, M.B. (2007). Tunability and noise dependence in differentiation dynamics. Science 315, 1716-1719.

Thattai, M., and van Oudenaarden, A. (2004). Stochastic gene expression in fluctuating environments. Genetics 167, 523-530.

Trach, K.A., and Hoch, J.A. (1993). Multisensory activation of the phosphorelay initiating sporulation in Bacillus subtilis: identification and sequence of the protein kinase of the alternate pathway. Molecular microbiology 8, 69-79.

Trempy, J.E., Bonamy, C., Szulmajster, J., and Haldenwang, W.G. (1985). Bacillus subtilis sigma factor sigma 29 is the product of the sporulation-essential gene spoIIG. Proceedings of the National Academy of Sciences of the United States of America 82, 4189-4192.

Truong, L.N., and Wu, X. (2011). Prevention of DNA re-replication in eukaryotic cells. J Mol Cell Biol 3, 13-22.

Turgay, K., Hahn, J., Burghoorn, J., and Dubnau, D. (1998). Competence in Bacillus subtilis is controlled by regulated proteolysis of a transcription factor. The EMBO journal 17, 6730-6738.

van Sinderen, D., Luttinger, A., Kong, L., Dubnau, D., Venema, G., and Hamoen, L. (1995). comK encodes the competence transcription factor, the key regulatory protein for competence development in Bacillus subtilis. Molecular microbiology 15, 455-462.

Veening, J.W., Hamoen, L.W., and Kuipers, O.P. (2005). Phosphatases modulate the bistable sporulation gene expression pattern in Bacillus subtilis. Molecular microbiology 56, 1481-1494.

Veening, J.W., Smits, W.K., Hamoen, L.W., and Kuipers, O.P. (2006). Single cell analysis of gene expression patterns of competence development and initiation of sporulation in Bacillus subtilis grown on chemically defined media. Journal of applied microbiology 101, 531-541.

Verhamme, D.T., Kiley, T.B., and Stanley-Wall, N.R. (2007). DegU co-ordinates multicellular behaviour exhibited by Bacillus subtilis. Molecular microbiology 65, 554-568.

Weir, J., Predich, M., Dubnau, E., Nair, G., and Smith, I. (1991). Regulation of spo0H, a gene coding for the Bacillus subtilis sigma H factor. Journal of bacteriology 173, 521-529.

Welinder, E., Ahsberg, J., and Sigvardsson, M. (2011). B-lymphocyte commitment: identifying the point of no return. Seminars in immunology 23, 335-340.

Wiegert, T., and Schumann, W. (2001). SsrA-mediated tagging in Bacillus subtilis. Journal of bacteriology 183, 3885-3889.

Wolf, D.M., Vazirani, V.V., and Arkin, A.P. (2005a). Diversity in times of adversity: probabilistic strategies in microbial survival games. J Theor Biol 234, 227-253.

Wolf, D.M., Vazirani, V.V., and Arkin, A.P. (2005b). A microbial modified prisoner's dilemma game: how frequency-dependent selection can lead to random phase variation. J Theor Biol 234, 255-262.

Wu, L.J., Feucht, A., and Errington, J. (1998). Prespore-specific gene expression in Bacillus subtilis is driven by sequestration of SpoIIE phosphatase to the prespore side of the asymmetric septum. Genes & development 12, 1371-1380.

Young, J.W., Locke, J.C., Altinok, A., Rosenfeld, N., Bacarian, T., Swain, P.S., Mjolsness, E., and Elowitz, M.B. (2012). Measuring single-cell gene expression dynamics in bacteria using fluorescence time-lapse microscopy. Nature protocols 7, 80-88.

Zeng, L., Skinner, S.O., Zong, C., Sippy, J., Feiss, M., and Golding, I. (2010). Decision making at a subcellular level determines the outcome of bacteriophage infection. Cell 141, 682-691.

Zuber, P., and Losick, R. (1987). Role of AbrB in Spo0A- and Spo0B-dependent utilization of a sporulation promoter in Bacillus subtilis. Journal of bacteriology 169, 2223-2230.